AD____________________

Award Number: W81XWH-05-1-0431

TITLE: Synergistic inhibition of Her2/neu and p53-MDM2 pathways

PRINCIPAL INVESTIGATOR: Nouri Neamati, Ph.D

CONTRACTING ORGANIZATION: University of Southern California
Los Angeles, CA 90033

REPORT DATE: September 2007

TYPE OF REPORT: Addendum to Final

PREPARED FOR: U.S. Army Medical Research and Materiel Command
Fort Detrick, Maryland 21702-5012

DISTRIBUTION STATEMENT: Approved for Public Release;
Distribution Unlimited

The views, opinions and/or findings contained in this report are those of the author(s) and should not be construed as an official Department of the Army position, policy or decision unless so designated by other documentation.

REPORT DOCUMENTATION PAGE

Form Approved
OMB No. 0704-0188

Public reporting burden for this collection of information is estimated to average 1 hour per response, including the time for reviewing instructions, searching existing data sources, gathering and maintaining the data needed, and completing and reviewing this collection of information. Send comments regarding this burden estimate or any other aspect of this collection of information, including suggestions for reducing this burden to Department of Defense, Washington Headquarters Services, Directorate for Information Operations and Reports (0704-0188), 1215 Jefferson Davis Highway, Suite 1204, Arlington, VA 22202-4302. Respondents should be aware that notwithstanding any other provision of law, no person shall be subject to any penalty for failing to comply with a collection of information if it does not display a currently valid OMB control number. **PLEASE DO NOT RETURN YOUR FORM TO THE ABOVE ADDRESS.**

1. REPORT DATE *(DD-MM-YYYY)* 01-09-2007	**2. REPORT TYPE** Addendum to Final	**3. DATES COVERED** *(From - To)* 1 SEP 2006 - 31 AUG 2007

4. TITLE AND SUBTITLE

Synergistic inhibition of Her2/neu and p53-MDM2 pathways

5a. CONTRACT NUMBER

5b. GRANT NUMBER
W81XWH-05-1-0431

5c. PROGRAM ELEMENT NUMBER

6. AUTHOR(S)
Nouri Neamati, Ph.D.

E-Mail: neamati@usc.edu

5d. PROJECT NUMBER

5e. TASK NUMBER

5f. WORK UNIT NUMBER

7. PERFORMING ORGANIZATION NAME(S) AND ADDRESS(ES)

University of Southern California
Los Angeles, CA 90033

8. PERFORMING ORGANIZATION REPORT NUMBER

9. SPONSORING / MONITORING AGENCY NAME(S) AND ADDRESS(ES)
U.S. Army Medical Research and Materiel Command
Fort Detrick, Maryland 21702-5012

10. SPONSOR/MONITOR'S ACRONYM(S)

11. SPONSOR/MONITOR'S REPORT NUMBER(S)

12. DISTRIBUTION / AVAILABILITY STATEMENT
Approved for Public Release; Distribution Unlimited

13. SUPPLEMENTARY NOTES

14. ABSTRACT
Overexpression of HER2/neu, as well as the overexpression of MDM2 has been known to be significant markers in malignancy of breast cancer in different ways. Activating the p53 pathway (a tumor suppressor protein) by inhibiting MDM2 activity while inactivating HER2/neu (a tumor activating protein) is a unique strategy to restore both wild type p53 function and inhibit poor breast cancer cell receptor function. Therefore, combination of drugs targeting HER2/neu and MDM2 pathways will allow for a two-pronged attack on breast cancer. The overall objective of our proposal is to determine if small molecule drugs designed to inhibit HER2/neu can be applied in combination with drugs designed to inhibit p53-MDM2 activity. This will enable us to ascertain if there is a synergistic effect as well as allow us to develop an understanding of the critical players in the overall cell signaling cascade. Initially, our objectives will be to design novel therapeutic agents based on pharmacophore and docking studies able to inhibit either the HER2/neu pathway or the p53-MDM2 pathway. Subsequently, designed small molecule drugs able to strongly induce apoptosis in breast cancer cell lines by inhibiting either pathway will be used in combination studies in vitro and in vivo to assess synergistic effects.

15. SUBJECT TERMS
p53-MDM2 interaction, HER2/neu, inhibitor design, synergy, pharmacophore, docking studies

16. SECURITY CLASSIFICATION OF:			**17. LIMITATION OF ABSTRACT**	**18. NUMBER OF PAGES**	**19a. NAME OF RESPONSIBLE PERSON** USAMRMC
a. REPORT U	**b. ABSTRACT** U	**c. THIS PAGE** U	UU	127	**19b. TELEPHONE NUMBER** *(include area code)*

Standard Form 298 (Rev. 8-98)
Prescribed by ANSI Std. Z39.18

Table of Contents

Page

Introduction………………………………………………………………….……..…… 3

Body………………………………………………………………………………….. 4

Key Research Accomplishments………………………………………….……….. 11

Reportable Outcomes……………………………………………………………… 12

Conclusion…………………………………………………………………….……. 13

References……………………………………………………………………….…. 14

Appendices…………………………………………………………………………… 15

INTRODUCTION

Of recent interest in breast cancer therapy is blocking the activity of HER2/neu (a member of the EGFR family), known to be overexpressed in 20-30% of breast cancers correlating with poor prognosis. Another major concern in breast cancer is the status of p53-MDM2 where MDM2 (a protein known to downregulate p53) is overexpressed in 68% of malignant breast cancers partly due to overexpression of the estrogen receptor. Both the HER2/neu and MDM2 pathways are regarded separately, but it is possible in the plethora of cellular signaling cascades that one can have an effect on the other and vice versa. It is evident that protein-protein interactions are important in all signaling cascades. These interactions are very specific, selective, and evolutionarily optimized. Thus, a selective interruption of protein-protein interactions by small molecule drugs targeting to HER2/neu and MDM2 may be an innovative approach to cancer therapy. We are developing small-molecule drugs against both targets and hypothesize that such drugs are synergistic when used in combination.

BODY

Our main task was to employ computational methods to identify small molecules able to fit into the hydrophobic cleft of MDM2 and to evaluate in vitro activity of these compounds in p53 wild-type and mutated cell lines. In this work, we performed pharmacophore model studies including the substructure concept and the explicit shape constrains to the active conformation of Nutlin and the p53 fragment that binds to MDM2. Database screening using these models resulted in a series of structurally novel compounds. Ninety representative hits were selected for initial cytotoxicity assay against a panel of breast cancer cell lines as well as HCT116 $p53^{+/+}$ and $p53^{-/-}$ cell lines. Eight of the compounds showed desirable activities in these cell lines.

Functional Feature Pharmacophore Model. Functional feature pharmacophore model studies were extensively performed on both Nutlin and the p53 side chain of the conserved triad motif, F19, W23, L26 by Catalyst software package. The conformation of Nutlin and p53 was taken from the x-ray structures and modeled conformation. For Nutlin pharmacophore model development, we first mapped H-bond donor, H-bond acceptor, hydrophobic and aromatic ring features to the active conformation. We then assigned geometrical constraints to each feature, i.e., coordinate and size of the feature. Finally, all the selected features were merged into one pharmacophore model. Following a similar procedure, a pharmacophore model of the p53 triad motif, F19, W23, L26, was also derived.

Shape-merged single compound pharmacophore query. Catalyst software package was used to generate the explicit shape constraint of Nutlin or p53 side chain ligand (Figures 1 and 2). First, the active conformation of the template molecule (Nutlin and p53 fragment of amino acid residues from 19-26) was mapped to the corresponding feature model, respectively. Then the explicit shape constraint was generated. Finally, the shape was merged with the feature model as a single query in Catalyst, that we referred to as the shape-merged pharmacophore model. The similarity tolerance of shape is an important parameter to adjust the percentage of hits yielded from database screening. The values of 0.5-1 was used as default value in the shape-merged p53 side chain model, but for the shape-merged Nutlin feature model, we relaxed the shape similarity to values of 0.45-1.

Docking studies. The docking studies were carried out by the GOLD (version 1.2 Genetic Optimization for Ligand Docking) software package running on our multi-processor linux PC and a 24-processor Silicon Graphics Onyx workstation as described. We used the crystal structure of Nutlin bound MDM2 complex (pdb code 1RV1) as the template target, and the ligand, Nutlin, was subsequently removed to keep the binding pocket available. Hydrogen atoms were added to both protein and ligand according to the protonation state at pH 7.0 during the docking studies.

The docking area was defined as a sphere with the radius of 15 Å at the central coordinate position (47.47, 12.31, 35.24) of the Nutlin molecule as observed in the crystal structure of MDM2 binding pocket. The ligand was placed within the active site using a least-squares fitting procedure. All docking runs were performed using standard default settings with a population size of 100, a maximum number of 100,000 operations, a mutation and crossover rate of 95. The scoring function was contributed basically from H-bond interaction, van der Waals interactions within the complex, and the ligand internal energy, which was summarized by ligand steric and torsional energies. Explicit electrostatic interaction was ignored but was modeled into the H-bond interactions.

Nutlin-based pharmacophore model. Referring to the interactions between Nutlin and the target protein, MDM2, determined in the X-ray structure (1RV1), only hydrophobic features (P1-P6) were considered in the pharmacophore model (Figure 1a). The features P1, P2, and P4 were mapped by the benzene ring and P3 by aliphatic methane group, which was observed to interact with MDM2 by its Van der Waals contacts. Additionally, P5 and P6 were recognized by the bromine substitutes. We generated explicit shape of Nutlin in its active orientation, as shown in Figure 1b. Apparently, both feature model (Figure 1a) and shape constraint itself (Figure 1b) can be used independently as searching query to screen small molecule database. In this work however, we combined the shape constraint onto the feature model to generate a shape-merged pharmacophore model, labeled as SM1 (Figure 1b), in order to comprehensively describe the chemical characteristics of Nutlin. Consequently, the shaped-merged model, SM1, was applied to screen our in-house database and 705 compounds were identified to fulfill this query. We selected structurally diverse compounds for further cell-based studies.

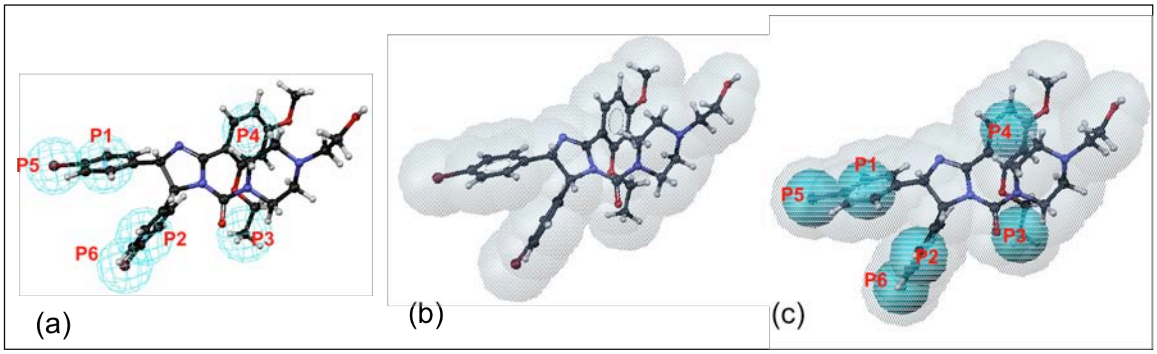

Figure 1. Pharmacophore models generated from active conformation of Nutlin. (a) Mapping Nutlin onto the feature pharmacophore model. (b) Mapping Nutlin to the shape-only query. (c) Mapping Nutlin onto shape-merged pharmacophore model.

p53 side chain-based pharmacophore model

Since the p53-MDM2 fragment was resolved by x-ray technique, several peptide libraries were previously designed to compete with the p53 binding. The first published putative p53-based pharmacophore model addressed the hydrophobic features recognized by the side chain of F19, W23 and L26, and H-bond donor mapped by the W23 indole side chain. Its application to screen the NCI database resulted in a series of non-peptide sulfonamide inhibitors. In this work, however, we extended the pharmacophore studies by taking into account explicit shape of the active conformation of the p53 fragment, determined by the x-ray structure. Two shape-merged pharmacophore models were systematically generated as shown in Figure 2. Figure 2a shows the model with the consideration of only three hydrophobic features, but enhanced by shape constraint, referred to as SM2. Figure 2b shows the shape-merged model, referred to as SM3, that keeps additional hydrogen-bond feature. Therefore, SM2 and SM3 were treated as independent queries to virtually screen our in-house database.

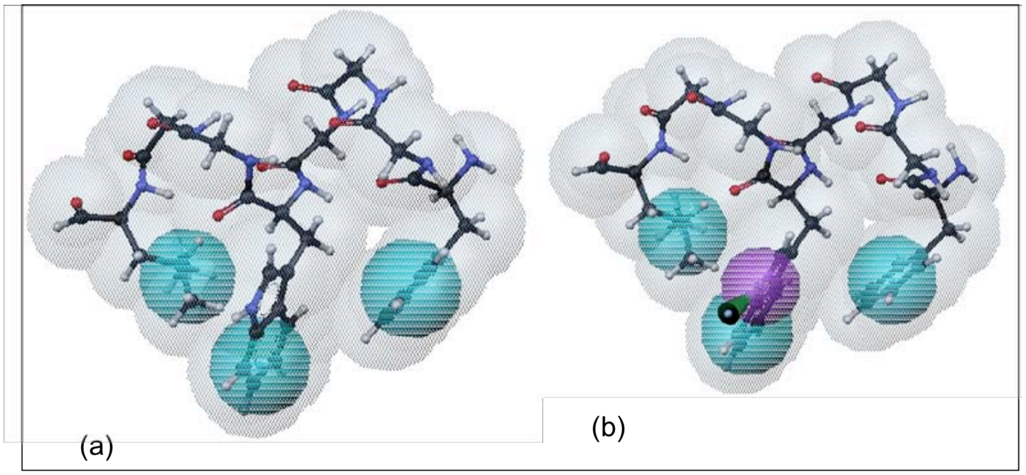

Figure 2. Pharmacophore models derived from the side chains of p53 fragment interacting with MDM2 p53 binding domain. (a) p53 fragment (amino acide residue 19-26) mapping onto the 3-hydrophobic feature pharmacophore model. (b) p53 fragment (amino acide residue 19-26) mapping onto the hetero-feature pharmacophore model.

Database search. Substructure queries, and the shape-merged pharmacophore models derived from either the Nutlin or the side chain of p53 fragment in their active conformation, respectively, were applied to screen our in-house database by Catalyst. For each model we identified anywhere from 700 to 900 hits. Testing selected compounds from two of the searches generated novel compounds with significant activities in two different cytotoxicity assays. Among the tested compounds, MP15, MP17, MP22, and MP31 showed superior activity against cells with wild-type p53 expression. The IC_{50} values range from 1-10 μM using MTT assay and 0.5-5 μM using colony formation assay. The docked structures of selected compounds are shown in Figure 3.

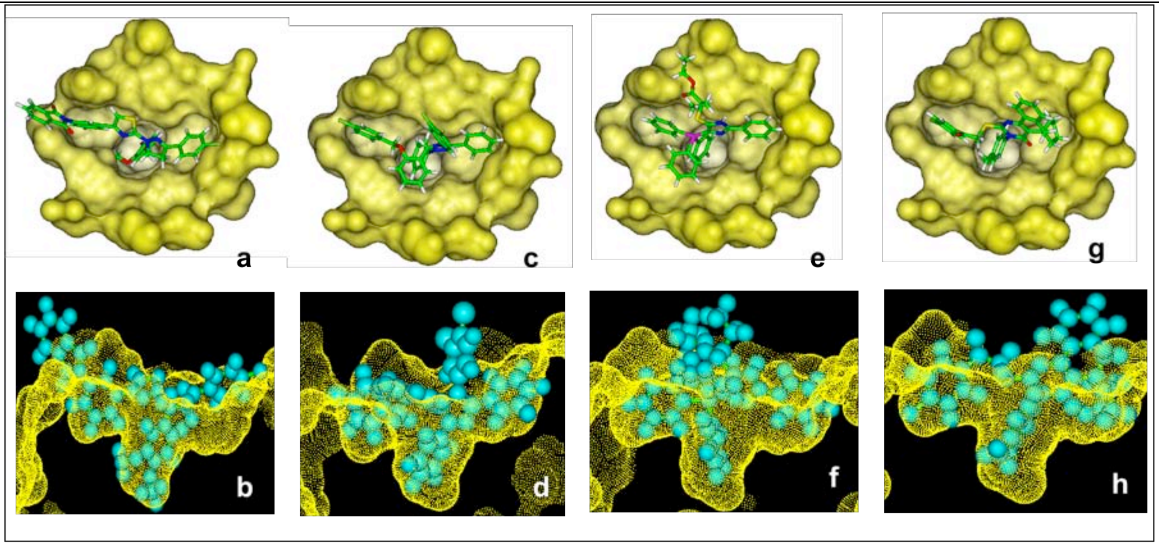

Figure 3. Predicted binding mode analysis of active compounds. MDM2 binding surface is displayed in yellow (dot or solid) surface, and ligand is rendered as stick or ball-stick. (a) and (b) show the MP15 binding into the MDM2 pocket, (a is for top view and b for side view). (c) and (d) show the MP17 binding into the MDM2 pocket. (e) and (f) show the MP22 binding into the MDM2 pocket. (g) and (h) show the MP31 binding into the MDM2 pocket.

Novel inhibitors of HER2/neu

For HER2/neu part of the project we identified several novel compounds by screening a subset of our in-house collection of 1,000 structurally diverse compounds. Four compounds Lnz 10, 18, 25, and 28 that showed significant inhibition of HER2/neu kinase activity were tested against SKBR3 cells using MTT (not shown) and colony formation assay (Figures 4 and 5).

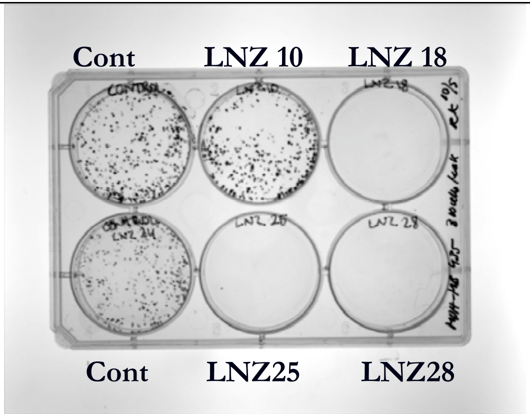

Figure 4. Activity of a selected HER2/neu inhibitors (LNZ 10, 18, 25, and 28) in SKBR3 breast cancer cells using colony formation assay.

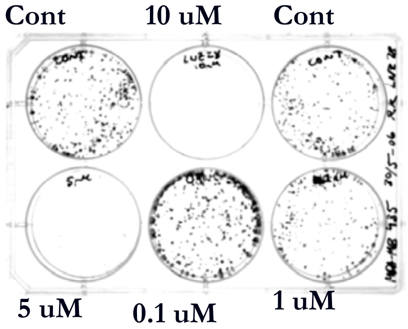

Figure 5. Activity of LNZ 28 in SKBR3 breast cancer cells using colony formation assay.

LNZ28 Treatment Induces a G_0/G_1-Phase Arrest. Cell cycle perturbations induced by Lnz 28 were examined in SKBR3 cells. The analysis of DNA profiles by flow cytometry indicated that Lnz 28 induced G_0/G_1-phase arrest. As shown in Figure 6, nearly 81% of the cells were still retained in G_0/G_1-phase after 48 hours of treatment with Lnz 28 (5 μM). Similar effects were obtained on asynchronus MDA-MB-435 cancer cell lines (data not shown).

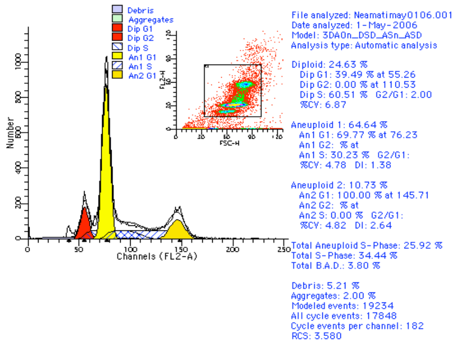

```
File analyzed: Neamatimay0106.001
Date analyzed: 1-May-2006
Model: 3DA0n_DSD_ASn_ASD
Analysis type: Automatic analysis

Diploid: 24.63 %
  Dip G1: 39.49 % at 55.26
  Dip G2: 0.00 % at 110.53
  Dip S: 60.51 %   G2/G1: 2.00
  %CV: 6.87

Aneuploid 1: 64.64 %
  An1 G1: 69.77 % at 76.23
  An1 G2:  % at
  An1 S: 30.23 %   G2/G1:
  %CV: 4.78   DI: 1.38

Aneuploid 2: 10.73 %
  An2 G1: 100.00 % at 145.71
  An2 G2:  % at
  An2 S: 0.00 %   G2/G1:
  %CV: 4.82   DI: 2.64

Total Aneuploid S-Phase: 25.92 %
Total S-Phase: 34.44 %
Total B.A.D.: 3.80 %

Debris: 5.21 %
Aggregates: 2.00 %
Modeled events: 19234
All cycle events: 17848
Cycle events per channel: 182
RCS: 3.580
```

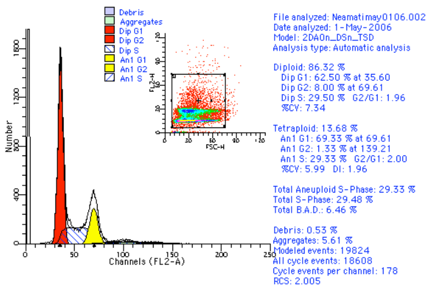

```
File analyzed: Neamatimay0106.002
Date analyzed: 1-May-2006
Model: 2DA0n_DSn_TSD
Analysis type: Automatic analysis

Diploid: 86.32 %
  Dip G1: 62.50 % at 35.60
  Dip G2: 8.00 % at 69.61
  Dip S: 29.50 %   G2/G1: 1.96
  %CV: 7.34

Tetraploid: 13.68 %
  An1 G1: 69.33 % at 69.61
  An1 G2: 1.33 % at 139.21
  An1 S: 29.33 %   G2/G1: 2.00
  %CV: 5.99   DI: 1.96

Total Aneuploid S-Phase: 29.33 %
Total S-Phase: 29.48 %
Total B.A.D.: 6.46 %

Debris: 0.53 %
Aggregates: 5.61 %
Modeled events: 19824
All cycle events: 18608
Cycle events per channel: 178
RCS: 2.005
```

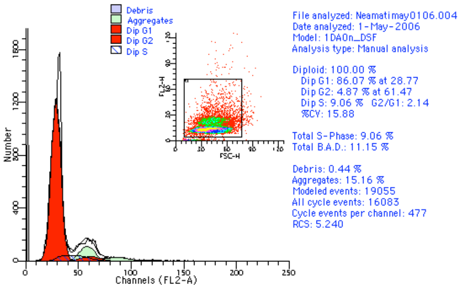

```
File analyzed: Neamatimay0106.004
Date analyzed: 1-May-2006
Model: 1DA0n_DSF
Analysis type: Manual analysis

Diploid: 100.00 %
  Dip G1: 86.07 % at 28.77
  Dip G2: 4.87 % at 61.47
  Dip S: 9.06 %  G2/G1: 2.14
  %CV: 15.88

Total S-Phase: 9.06 %
Total B.A.D.: 11.15 %

Debris: 0.44 %
Aggregates: 15.16 %
Modeled events: 19055
All cycle events: 16083
Cycle events per channel: 477
RCS: 5.240
```

	Contro	12 hr	48 hr
G0/G1	58%	67 %	81%
S	19%	14%	4%
G2/M	23%	19%	15%

Figure 6. Cell cycle profile of cells treated with 5 μM of Lnz 28.

In collaboration with Ya-Qiu Long we have prepared 500 mg of Lnz 28 for our proposed animal studies. These studies will be performed in 2008 through different funding mechanism.

In parallel we have performed computational search of our 5,000,000 compounds and identified additional novel HER2 antagonist. The full disclosure of this study is attached in the appendix. This paper was communicated to the Journal of Medicinal Chemistry and was recently accepted with minor revision. Please see appendix.

KEY RESEARCH ACCOMPLISHMENTS

Three highly robust pharmacophore models were developed based on p53 peptide fragment, Nutlin structure, and MDM2 pocket. These pharmacophore models were validated against a database of all patented MDM2 antagonists. This allowed us to write the most comprehensive review of inhibitors of p53-MDM2 interaction, which was recently published in Expert Opinions in Therapeutics Patents.

Several small-molecule inhibitor of p53-MDM2 interaction were identified. One example belongs to an entirely novel class of anticancer drugs. We filed a provisional patent on these molecules.

To the best of our knowledge, the application of shape merged with pharmacohporic feature and its use to MDM2 as a target has never been previously attempted. This could potentially be a very useful tool for other studies targeting protein-protein interaction.

We also screened a subset of our in-house collection of small-molecule compounds against HER2/neu. A series of novel compounds were identified and subsequently tested in cell-based assays. We also wrote a very comprehensive review of inhibitors of HER2/neu, which was recently submitted to Expert Opinions in Therapeutics Patents.

At least four lead molecules targeting HER2-neu activity were identified. Structure-optimization in collaboration with Dr. Ya-Qiu Long was initiated and we have prepared 500 mg of our most potent compound LNZ-28 for in vivo studies.

We also performed more robust computational studies and identified a series of novel HER2 antagonists. Account of this study is summarized in our recent paper, which has been accepted by the Journal of Medicinal Chemistry with minor revision.

REPORTABLE OUTCOMES

Patent Application
Neamati, N. and J. Deng, Structure-based anticancer drug design targeting p53-MDM2 interactions (2005).

Peer-reviewed publications
Deng, J.; Dayam, R.; Neamati, N., Patented small molecule inhibitors of p53-MDM2 interaction. *Expert Opin Ther Patents* **2006,** 16, (3), 165-188.

Dayam R, Grande, F.; Al-Mawsawi, L-Q., Neamati, N. Recent advances in the design and discovery of small-molecule therapeutics targeting HER2/neu. *Expert Opin Ther Patents* **2007,** 17, (1), 83-102**.**

Gundla, R.; kazemi, R.; Sanam, R.; Muttineni, R.; Dayam, R.; Jagarlapudi, ARP,; Neamati, N. Discovery of novel small-molecule inhibitors of HER2/neu: Combined ligand-based and target-based approach. J. Med. Chem. (Accepted with minor revision).

Deng, J.; Taheri, L.; and Neamati, N. Design and discovery of novel small-molecule compounds targeting p53-MDM2 interaction (Under preparation)

CONCLUSIONS

We have successfully discovered a series of novel inhibitors of both p53-MDM2 interaction as well as HER2/neu kinase activity. This success attests to your unique approach in structure-based drug design. Our compounds show significant cytotoxicity against breast cancer cell lines. Our animal studies will be performed in the 2008 under different funding mechanism. Thus far, we have filed one patent application and published three papers and an additional manuscript is under preparation. This is a major project in our laboratory and our goal is to use these preliminary results to apply for a bigger grant.

REFERENCES
N/A

APPENDICES

Expert Opinion

1. Introduction
2. Discovery of small molecule inhibitors of p53–MDM2 interaction
3. Discovery of small molecule ubiquitin ligase inhibitors
4. Small molecule activators of mutant p53
5. Expert opinion

For reprint orders, please contact: reprints@ashley-pub.com

Ashley Publications
www.ashley-pub.com

Patented small molecule inhibitors of p53–MDM2 interaction

Jinxia Deng, Raveendra Dayam & Nouri Neamati†
Department of Pharmaceutical Sciences, School of Pharmacy, University of Southern California, 1985 Zonal Avenue, PSC304A, Los Angeles, California 90089, USA

The interaction between p53 and murine double minute 2 (MDM2) provides an attractive drug target in oncology. Small molecule inhibitors of this interaction have not only provided strong evidence for blocking the protein–protein interaction, but are also extremely useful as biological probes and ultimately as novel therapeutics. Here, a comprehensive review of the patented small molecule inhibitors of the p53–MDM2 interaction are provided. These inhibitors are divided into eight classes of compounds that include *cis*-imidazolines, benzodiazepines, fused indoles, substituted piperazines, substituted piperidines, aryl boronic acids, spiro-indoles, and α-helix mimetic compounds. The best documented class of compounds, *cis*-imidazolines (e.g., Nutlins) are selective and potent inhibitors of the p53–MDM2 interaction, and selected examples exhibit potency in the nanomolar range. Nutlins induce apoptosis in p53 wild-type cells and show *in vivo* efficacy in mice xenograft models. Additional strategies briefly discussed in this review, and which are under current exploration in targeting the p53 pathway, include the inhibition of MDM2-mediated p53 ubiquitylation and restoration of DNA-binding activity of mutant p53 protein using small molecules.

Keywords: anticancer drug, MDM2, mutant p53, p53–MDM2 interaction, protein–protein interaction, ubiquitin ligase inhibitor

*Expert Opin. Ther. Patents (2006) **16**(2):165-188*

Copyright ... ions. Printing and distribution strictly prohibited

1. Introduction

1.1 MDM2

Murine double minute 2 (MDM2) is an oncogene originally isolated from a mouse fibroblast cell line that underwent a spontaneous transformation [1]. Later this gene was rediscovered as a p53 binding protein in several rat fibroblast cell lines [2]. The human homologue has since shown to be overexpressed in 8% of various sarcomas, up to 68% in angiosarcomas and ~ 30% in soft tissue sarcomas [3-7]. A large number of cancers with MDM2 overexpression harbour wild-type p53. In some cancers, MDM2 overexpression can be correlated with accelerated cancer progression and poor response rate [8-13]. Several studies suggest that MDM2 overexpression is associated with increased metastasis, although the function and mechanism of MDM2 in cancer metastasis demands more studies [10,14,15]. Three-dimensional structural information is not yet available for the full-length MDM2 protein. The domain compositions of p53 and MDM2 are shown in **Figure 1**. However, biological mapping has shown that the human *MDM2* gene encodes for a protein containing 491 amino acids with multiple domains and consensus sequences. These include a p53-binding domain, a nuclear localisation signal (NLS), a nuclear export signal (NES), an acidic region, a zinc-finger and a ring-finger domain (**Figure 1A**) [6,16,17]. MDM2 is largely considered a major negative regulator of p53 tumour suppressor gene [18,19].

1.2 p53

p53 contains 393 amino acid residues. The protein is a transcription factor that regulates the expression of proteins that mediate distinct cellular responses such as

10.1517/13543776.16.2.165 © 2006 Ashley Publications ISSN 1354-3776

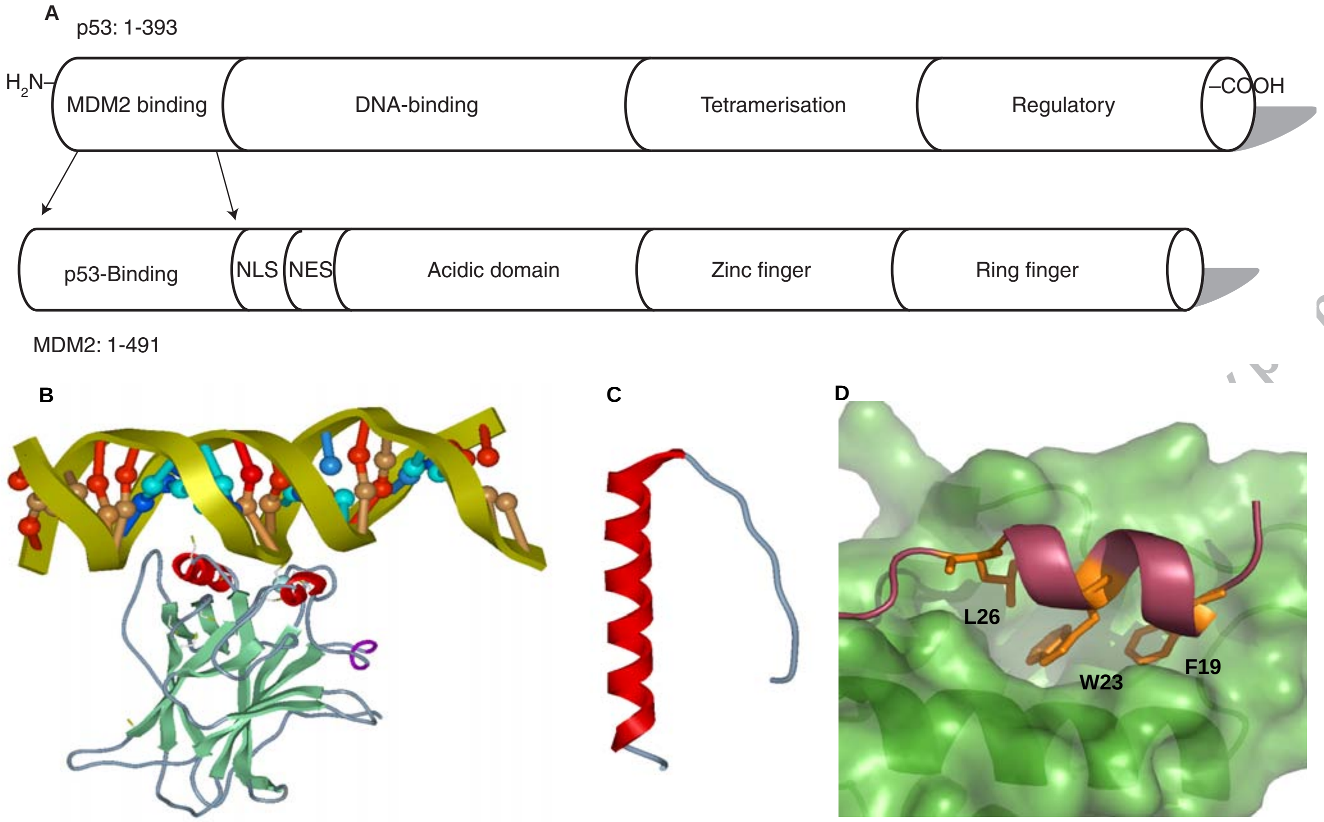

Figure 1. Schematic representations of the functional domains of p53 and MDM2. A) Domain composition of p53 and MDM2. **B)** Core domain of p53 complexed with the DNA (PDB 1TSR [26]). Image generated by Molsoft ICM-Browser. **C)** Tetramerisation domain of p53 (PDB 1C26 [31]). Image generated by Molsoft ICM-Browser. **D)** p53 peptide bound MDM2 (PDB 1YCR [35]). Green surface represents MDM2. Helix in red represents p53 peptide bound to MDM2, and the side chains in orange show triad motif: L26, W23, F19. Image generated by PyMOL. Colour figure available online at www.ashley-pub.com.

NES: Nuclear export signal; NLS: Nuclear localisation signal.

Copyright of Ashley Publications.

apoptosis and cell growth arrest [20,21]. Not surprisingly, p53 is the most frequently inactivated protein in human cancers [22]. Over 50% of human cancers contain p53 mutations that inactivate its transcription regulation activity [23]. Most cancer-associated p53 mutations occur within the DNA-binding domain, rendering p53 unable to act as a sequence-specific DNA binding transcription factor [24]. The fact that mutational inactivation of p53 is observed as one of the most common cancer genetic events indicates that p53 plays a critical role in suppressing the tumour growth. Structural studies have shown that p53 is made up of at least four functional domains that regulate its transcriptional activities: i) an N-terminal transactivation domain, which is required for the interaction with transcriptional protein machinery as well as a proline-rich domain; ii) a central conserved DNA-binding core domain; iii) a tetramerisation domain assisting in sequence-specific DNA binding; and iv) a C-terminal negative regulatory domain, which when phosphorylated, primes the latent sequence-specific DNA-binding function of p53 for activation [6]. The N-terminal transactivation domain contains the binding pocket where most of the important negative cellular regulators of p53 bind, that is MDM2 oncoprotein (**Figure 1A**) [25]. The structures of the DNA binding, tetramerisation and the C-terminal regulatory domains of human p53 have been determined by NMR or crystallography (**Figures 1B** and **C**) [26-34]. Currently, there is no such structural information available on the entire human p53 N-terminal domain. However, the crystal structure of a p53 peptide that contains residues 15 – 29 in complex with MDM2 has been resolved (**Figure 1D**) [35].

1.3 P53–MDM2 interaction

MDM2 regulates p53 protein activity in at least three different ways [36]. Briefly, i) it binds to the p53 transactivation domain, thereby blocking the transcriptional activity; ii) subsequent to p53-binding, it induces nuclear export; and iii) it stimulates the degradation of p53 by catalysing ubiquitylation of the protein through the ubiquitin/proteasome pathway (for recent reviews, see [37,38]). Transcription of the *MDM2* gene itself is regulated by p53 in response to cellular stress, indicating that p53 and MDM2 form an autoregulatory feedback

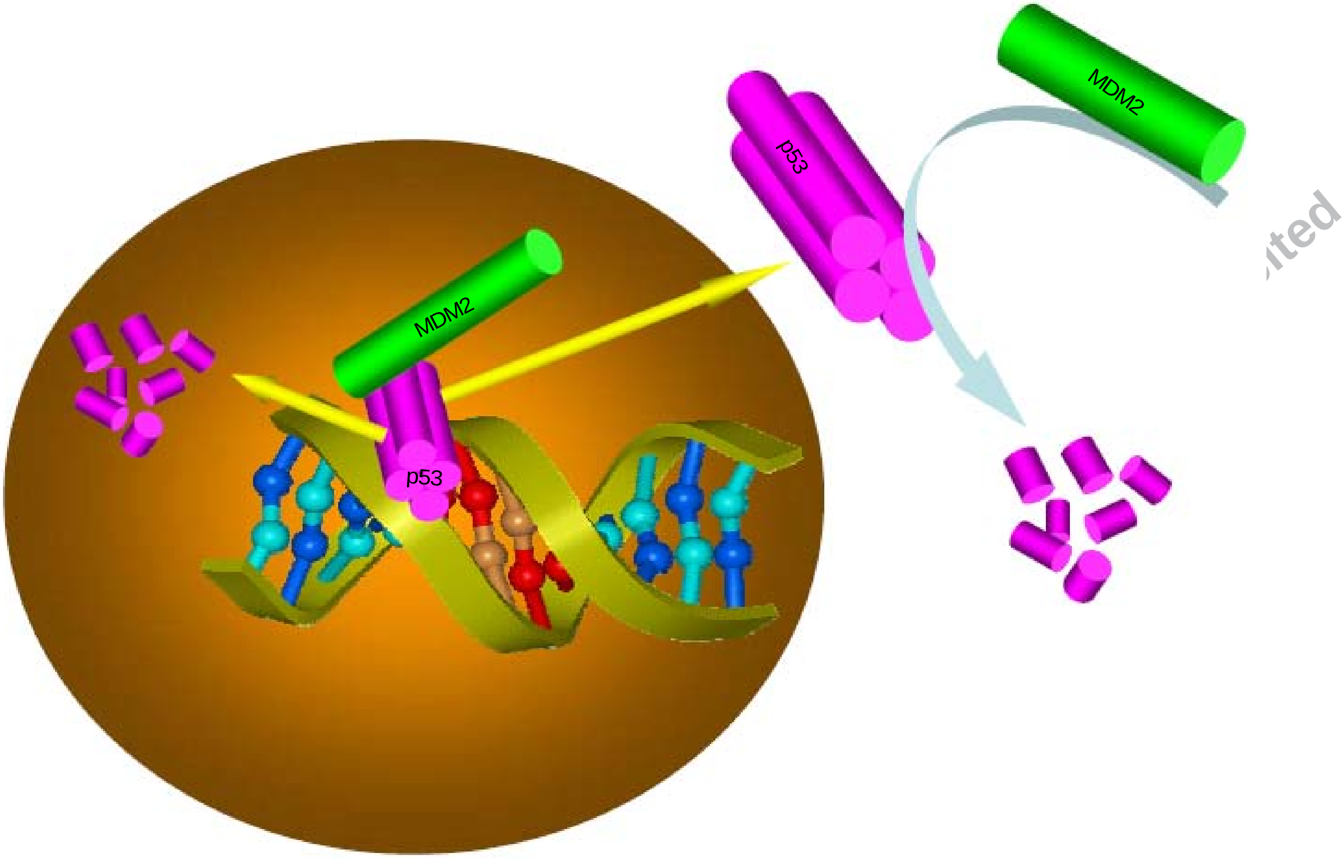

Figure 2. Simplified model of autoregulation between p53 and MDM2. p53 mediates the MDM2 expression, and in turn MDM2 regulates p53 activity through blocking its transcriptional activity, promoting its nuclear export, and stimulating its degradation in both nucleus and cytoplasm. DNA model was generated by ICM-Browser software.

Copyright of Ashley Publications Limited

loop (**Figure 2**) [36]. Therefore, as one of the approaches to stabilise p53 protein levels, MDM2 has been selected as a very attractive target for cancer therapeutics. Efforts are underway to design peptides or small molecule compounds that disrupt the p53–MDM2 interaction. Biological and functional studies have mapped residues 19 – 102 of MDM2 as the domain for p53 binding, while the MDM2 binding domain of p53 was narrowed down to a 15-amino acid residue peptide (amino acid residues 15 – 29; **Figure 1D**) [6]. The structure determination of MDM2 with the 15-mer wild-type p53 provided a precise description of the p53–MDM2 interaction. This revealed that MDM2 possesses a well-defined deep hydrophobic binding pocket. A triad of amino acid residues F19, W23 and L26 from MDM2 binding 15-mer p53 peptide occupies the deep hydrophobic pocket (**Figure 1D**) [35]. A key H-bond interaction between the indole nitrogen of W23 in p53 and the target MDM2, and several van der Walls contacts involved in the stabilisation of the complex were observed. The structure of p53-bound MDM2 provided a rational template for structure-based design of small molecule inhibitors. In the current review, the first focus will be on the patented small molecule inhibitors of the p53–MDM2 interaction. Second, recent progress towards the discovery of small molecule inhibitors that prevent MDM2-mediated p53 ubiquitylation will be covered briefly. Finally, the discovery of small molecules that have the ability to reactivate the DNA binding and apoptosis-inducing function of mutant p53 protein will be described.

2. Discovery of small molecule inhibitors of p53–MDM2 interaction

Most of the early studies employed peptides rather than small molecules to disrupt the p53–MDM2 interaction. These initial studies suggested that the peptides derived from p53 could be used as probes to investigate this specific interaction. They also confirmed the critical function of the triad motif as revealed from the p53–MDM2 complex [39-41]. Subsequently, a potent 12-mer peptide was identified by screening phage peptide libraries [42,43]. Other shorter peptides showed tighter binding as observed from the kinetic and thermodynamic studies [44].

Several small molecule inhibitors of the p53–MDM2 interaction that include chalcones and chlorofusin have previously been discovered [45-50]. However, major developments in the field were the discoveries of Nutlins (representatives of *cis*-imidazolines) and benzodiazepine compounds [50,51]. The subsequent co-crystal structures of these compounds with MDM2 greatly helped in the understanding of critical binding interactions between small molecules and the MDM2 protein. These studies established that protein–protein interactions can be successfully manipulated by small molecule inhibitors. Therefore, the p53 pathway can be effectively studied at the molecular level to develop novel anticancer drugs selectively targeting its critical interaction with MDM2.

Several reviews have summarised the early progress in the design of peptides and small molecule inhibitors targeting p53–MDM2 interaction [19,43,52-55]. However, the emergence of patented small molecules in the past 5 years has not been covered. Herein, the entire patent literature, published since 2000, for the p53–MDM2 interaction inhibitors has comprehensively reviewed. It is notable to bear in mind that many compounds claimed to be inhibitors of p53–MDM2 interaction have yet to be independently validated. These patents were not discarded. Additionally, in several patents, many compounds were disclosed but their biological activities were not presented. Even though it is very difficult to present a coherent structure–activity relationship (SAR) at this time, it was decided that it was still informative to present selected representatives from each study. The purpose is to provide a rapid access to compound structures that are claimed to be inhibitors of p53–MDM2 interaction, beneficial to interested researchers.

In general, the small molecule inhibitors fall into eight structural categories. They are *cis*-imidazolines (as represented by Nutlins [50]), benzodiazepines, fused indoles, substituted piperazines, substituted piperidines, aryl boronic acids, spiro-oxindoles and α-helix mimetic compounds. To the authors' knowledge, Nutlins, examples of *cis*-imidazolines, are the only selective and potent inhibitors that have been studied in detail in cell culture and mice xenograft. Therefore, the review begins with the discussion of *cis*-imidazolines and the recent progress in the design and discovery of potential inhibitors of p53–MDM2 interaction.

2.1 *Cis*-imidazolines

The first biological application of *cis*-imidazolines could be illustrated by TA-383 (*cis*-2-(4-chlorophenyl)-4,5-diphenyl-2-imidazoline; 1, **Figure 3**), which was recognised as a novel antirheumatic agent. Later the compound was shown to enhance macrophage migration [56,57]. In addition, 4,5-diarylimidazolines were recently evaluated as inhibitors of the $P2X_7$ receptor, which is a ligand-gated ion channel that is present on a variety of cell types, including mast cells, macrophages and lymphocytes, all thought to be involved in inflammation and autoimmune processes [58].

Nutlins are the representatives of a class of *cis*-2,4,5-triphenyl-imidazolines, and it is only in recent years that they were recognised as the first potent and selective small molecule inhibitors of the p53–MDM2 interaction [50,59,60,101-104].

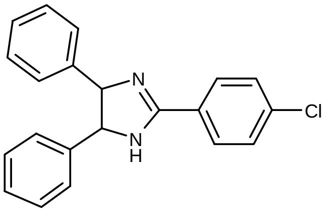

1 TA-383

Figure 3. Structure of TA-383, a *cis*-imidazoline analogue.

These compounds were identified from library screening of a large diverse synthetic chemicals database [50]. Three reported Nutlins showed potency for blocking the p53–MDM2 complex in the range of 100 to 300 nM with ~ 150- to 200-fold difference between the enantiomers [50].

Nutlins were initially examined at the cellular level for their effect on p53, MDM2, and p21 protein expression. Results confirmed that Nutlin treatment accumulated wild-type p53 levels and consistently lead to an elevation of MDM2 and p21 proteins [50]. In addition, it was shown that the increased p53 level was due to a post-translational mechanism rather than the elevated expression of the p53 gene. Cell cycle analysis of bromodeoxyuridine (BrdU)-labelled cancer cells demonstrated that G_1 and G_2/M phase fractions were increased, whereas cells progressing into S-phase were completely deleted after one-day Nutlin treatment. Results from a 3-(4,5-dimethylthiazol-2-yl)-2,5-diphenyltetrazolium bromide (MTT) assay indicated that cytotoxic activity of the compounds on the wild-type p53 cells was significantly higher than mutant p53 cells, suggesting that the p53 pathway is only turned on in wild-type p53-containing cells. The active enantiomer of Nutlin induced apoptosis in 50% of cells, whereas the inactive enantiomer had no effect. Finally, one analogue was investigated in osteosarcoma SJSA-1 tumour xenografts in nude mice. The 20-day oral administration of this compound effectively inhibited 90% tumour growth as compared to the vehicle control [50,59].

To investigate the Nutlin binding mode, the crystal structure of the human MDM2–Nutlin complex was determined at 2.3 Å [50]. **Figure 4** shows the co-crystal structure of a Nutlin analogue bound to MDM2 (PDB 1RV1). It clearly shows that the Nutlin analogue projects its functional groups into the p53 binding pocket of MDM2 by mimicking the conformation of the p53 triad motif, that is, the side chain of F19, W23 and L26.

Some representative molecules disclosed from recent patents are shown in **Figures 5 and 6** [101-104]. N-substituted imidazolines are shown in **Figure 5**, whilst un-substituted imidazolines are shown in **Figure 6**. In cell-free and cell-based assays, these molecules were observed to inhibit the p53–MDM2 interaction with a potency of ~ 100-fold greater than that of a p53-derived peptide. In addition, the cell-based assays demonstrated mechanistic activity. Incubation of

Copyright of Ashley Publications. Printing and distribution strictly prohibited

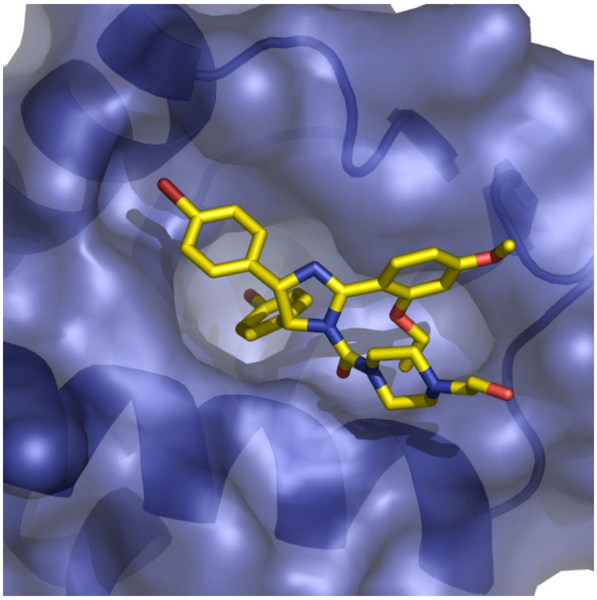

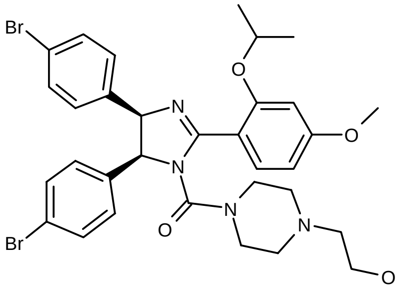

2 Nutlin analogue

Figure 4. Crystal structure of the Nutlin analogue bound MDM2 (PDB 1RV1 [50]). Blue surface represents the p53 binding pocket of MDM2 (image generated by PyMOL). The stick model shows the Nutlin analogue. Colour figure available online at www.ashley-pub.com.

Copyright of Ashley Publications. Printing and distribution prohibited

cancer cells containing wild-type p53 resulted in p53 protein accumulation, p53-regulated p21 gene induction and cell cycle arrest in G1, G2 phase, leading to potent antiproliferative activity against wild-type p53 cells *in vitro*. In contrast, similar results were not observed in p53 mutant cancer cells at comparable drug concentrations.

Another set of compounds bearing the *cis*-imdazoline group were discovered as inhibitors of the p53–MDM2 interaction and showed antiproliferative activities [105-108]. Several compounds exemplified by **I** and **II** (**Tables 1** and **2**) were claimed, and the representative molecules and their inhibitory activities are given in **Tables 1** and **2**. From a simpler formula, a group of derivatives containing 4,5-dihydro-1,4-dimethyl-2,5-diphenyl-1*H*-imidazole were also observed to induce antiproliferative activity through inhibition of the p53–MDM2 interaction. The inhibitory activity of each compound was measured as a percentage of the bound MDM2 in treated versus untreated wells. The IC_{50} values of the disclosed molecules from the invention ranged 0.5 – 150 µM. In summary, the discovery of Nutlins as potent inhibitors for the disruption of p53 with MDM2 *in vitro* and *in vivo* provided compelling evidence that such molecules have excellent therapeutic potential. Therefore, validation of p53–MDM2 disruption as a viable therapeutic target provides strong support for targeting protein–protein interactions in general. This is a clear step forward towards novel therapeutics in the future.

2.2 Benzodiazepines

The biological activities of benzodiazepine derivatives are very well documented. For example, some analogues have been recognised to bind the chemokine receptor CXCR4, a receptor for HIV, thereby inhibiting HIV infection [109]. Previously, a class of 4,5,6,7-tetrahydro-5-methylimidazo[4,5,1-*jk*]benzodiazepin-2-(1*H*)-one compounds were reported possessing significant inhibitory activity against HIV-1 with IC_{50} values ranging 0.0034 – 238 µM [61]. Separate studies showed tricyclic diazepines have antiproliferative activity on leukaemia cells [110]. Donepezil analogues have also been shown as neurocyte protective agents [111]. Recently, the imine–amine benzodiazepine dimers were also observed to efficiently bind to DNA, and exhibited *in vitro* antitumour activity in many cancer cell lines that included leukaemia, lung cancer, renal cancer and colon cancer [62-64]. Another study demonstrated that the benzothiadiazine-4-one derivatives were effective anticoagulants through inhibition of Factor Xa activity [65,66]. In addition, several benzodiazepines also showed anxiolytic and herbicidal activities [67,68].

Although the biological studies of benzodiazepine derivatives can be traced to the early 1960s, their potential as anticancer agents has only recently been discovered. Several of these compounds were found to effectively block the p53–MDM2 interaction. These compounds were identified by screening a synthetic library containing > 22,000 compounds using a high-throughput binding assay sensitive for MDM2 binding affinity [69].

A total of 217 compounds were disclosed in two recent patents each containing a critical motif; some selected compounds are shown in **Figure** 7 [112,113]. A fluorescein peptide-based assay was used to measure drug potency. Structures of 17 representative compounds are shown in **Figure** 7. Eleven compounds inhibited p53–MDM2 interaction with IC_{50} values of < 10 µM (**Table 3**).

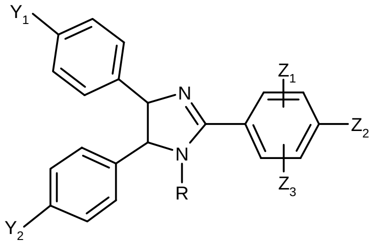

General formula

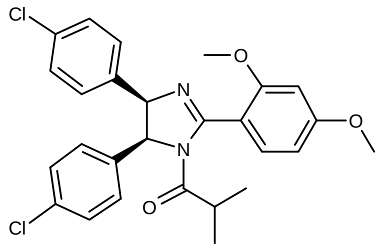

3

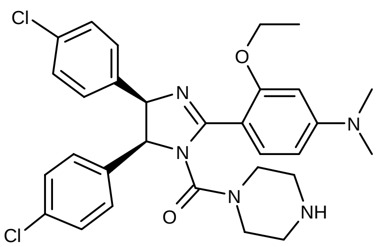

4

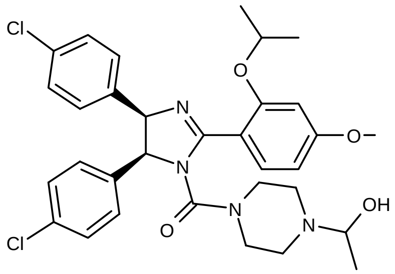

5

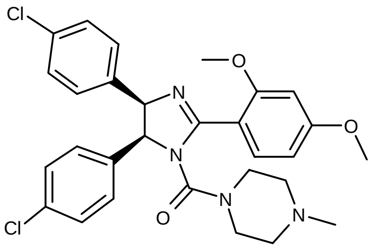

6

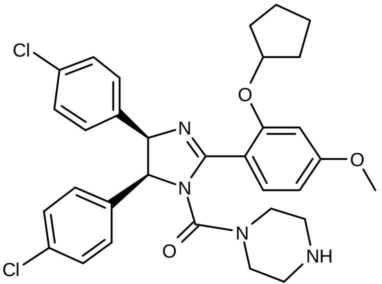

7

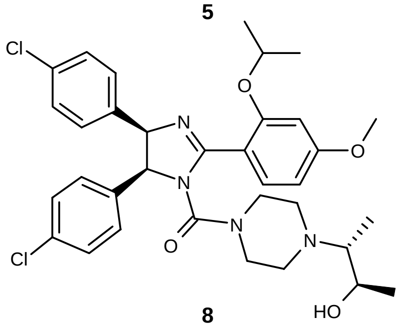

8

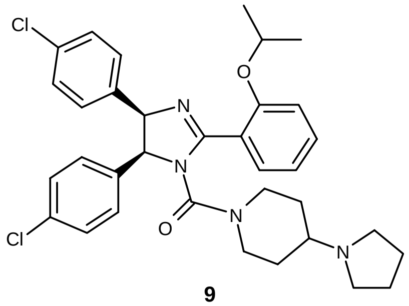

9

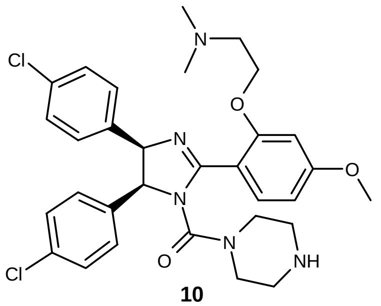

10

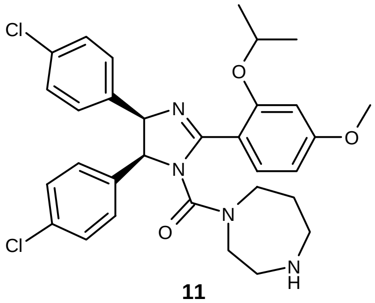

11

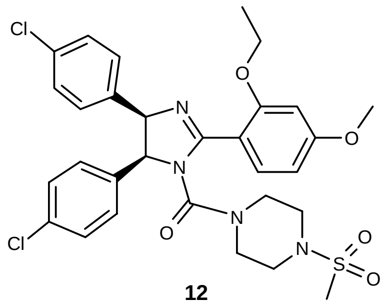

12

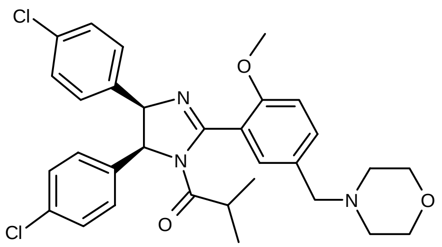

13

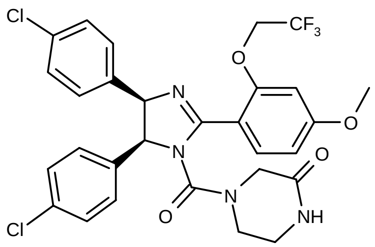

14

Figure 5. Representative examples of *cis*-imidazoline inhibitors of p53–MDM2 interaction.

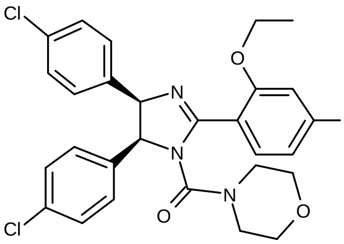

15

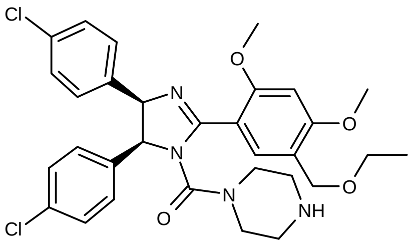

16

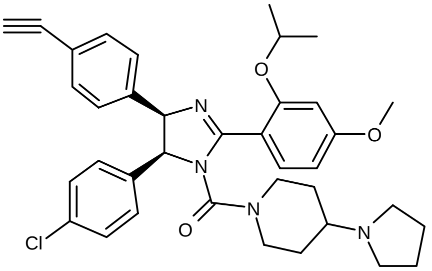

17

strictly pro ted

Figure 5. Representative examples of *cis*-imidazoline inhibitors of p53–MDM2 interaction (*Continued*).

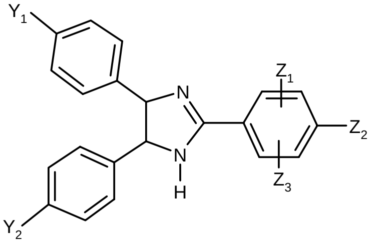

General formula

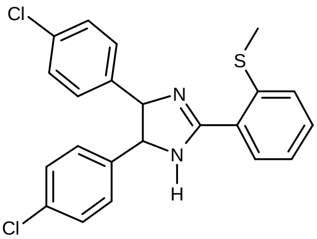

18

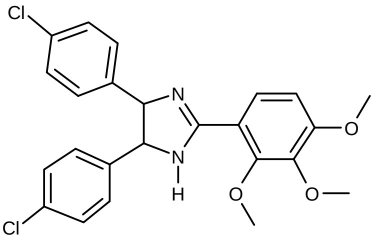

19

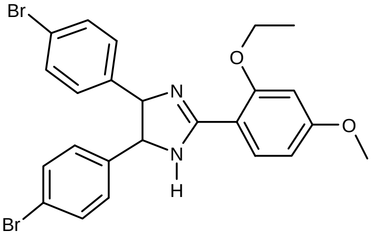

20

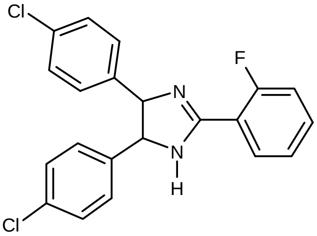

21

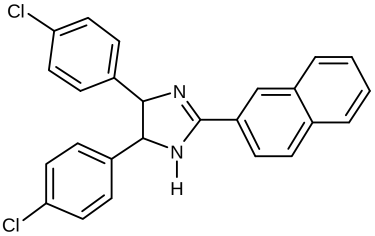

22

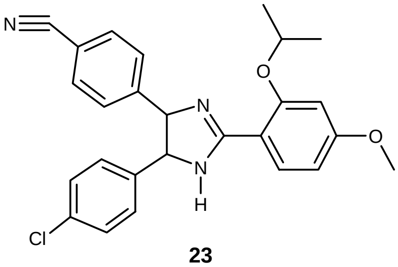

23

Copyri

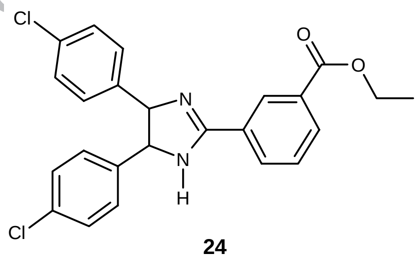

24

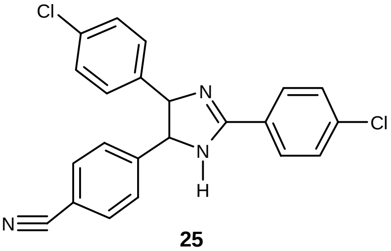

25

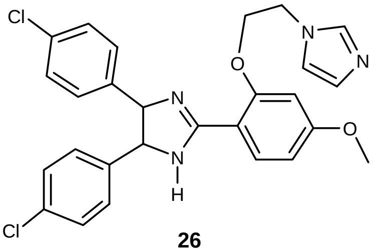

26

Figure 6. Representative *cis*-imidazoline inhibitors of p53–MDM2 interaction.

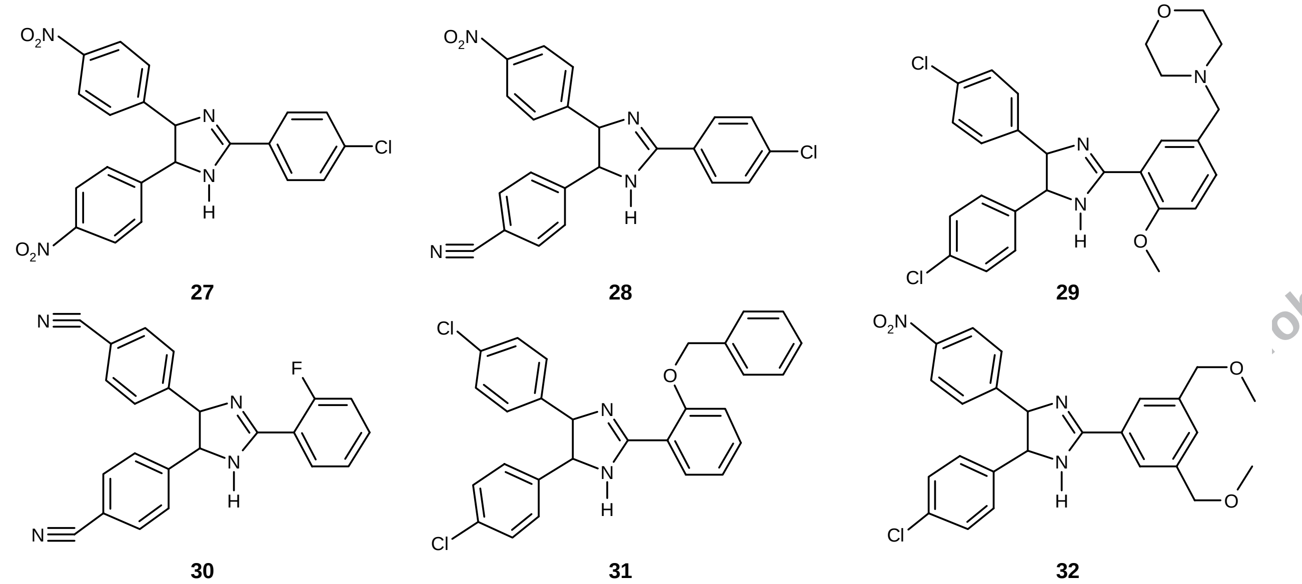

27 **28** **29**

30 **31** **32**

Figure 6. Representative *cis*-imidazoline inhibitors of p53–MDM2 interaction (*Continued*).

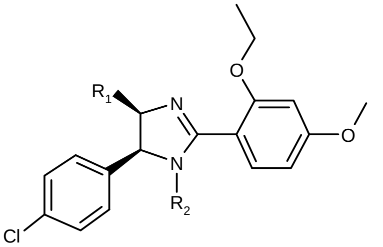

I

Table 1. Compounds exemplified by formula I and their inhibitory activities against p53–MDM2 interaction.

Compound	R_1	R_2	IC_{50} (μM)
33	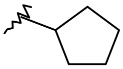	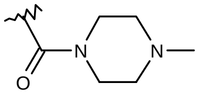	13.20
34	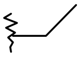	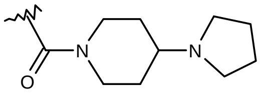	45.00
35	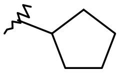	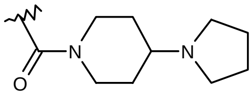	5.50
36	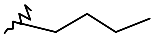	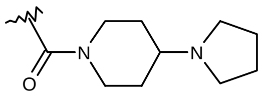	0.70

Copyright of Ashley Publica… and distri… ohibited

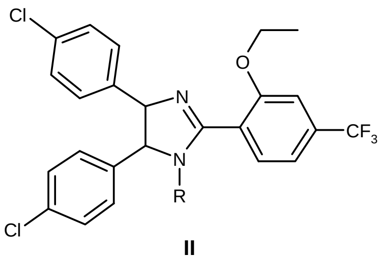

II

Table 2. Compounds exemplified by formula II and their inhibitory activities against p53–MDM2 interaction.

Compound	R	IC_{50} (μM)
37	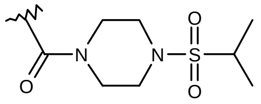	0.100
38	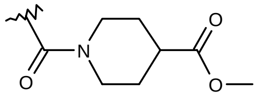	1.740
39	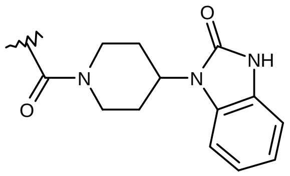	0.800
40	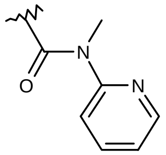	4.260
41	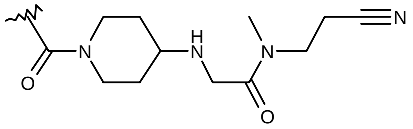	0.021

Copyright of Ashley Publications. g and distribution strictly prohibited

A modified 1,4-diazepine scaffold and some selected derivatives are shown in **Figure 8** [114,115]. A total of 114 examples was synthesised and tested [113]. The potency of these compounds ranged from 0.05 to > 100 μM. The activities of the selected representative compounds are given in **Table 4**.

To further understand the molecular detail of such types of benzodiazepinediones binding to MDM2, two representative compounds were selected for X-ray studies [116]. The chemical structures of the two compounds are shown in **Figure 9**. Coordinates of benzodiazepine analogue **64** bound to MDM2 have been determined at 2.7 Å by X-ray crystallography (PDB 1T4E), as shown in **Figure 10** [51]. From the binding conformations, it is clear that both Nutlin (see **Figure 3**) and the selected benzodiazepine analogue **64** stay in a similar orientation and interact with MDM2 in an orientation that mimics the side chain of p53. As a consequence, the p53 is released and stabilised in the cell. Cell growth suppression was measured in JAR choriocarcinoma cells that overexpress p53 and MDM2. Results with benzodiazepine analogue **64** treatment confirmed the antiproliferative activities were directly due to the selective interruption of the p53–MDM2 interaction. In addition, the discovery

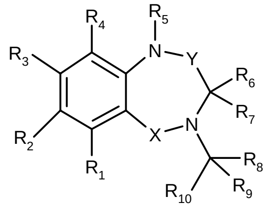
R4
R5
R3
N
Y
R6
R7
R2
X
N
R1
R8
R10
R9

General formula

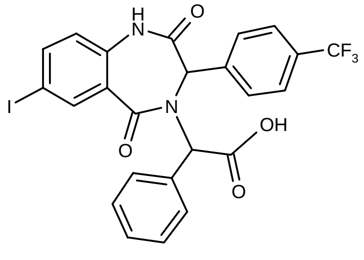

42

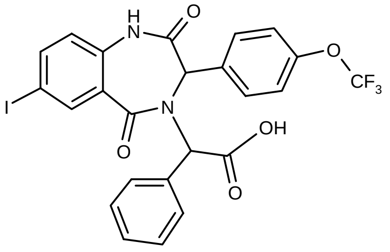

43

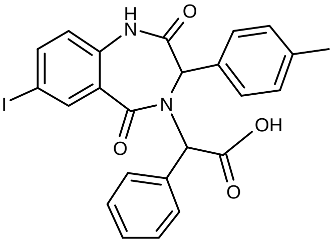

44

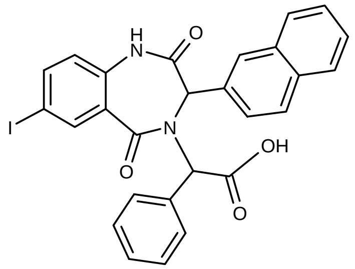

45

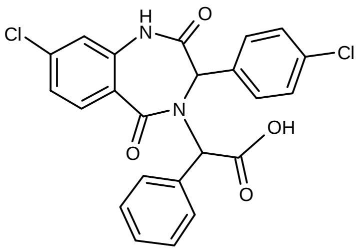

46

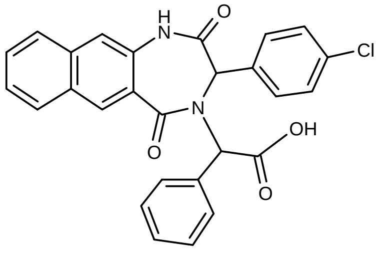

47

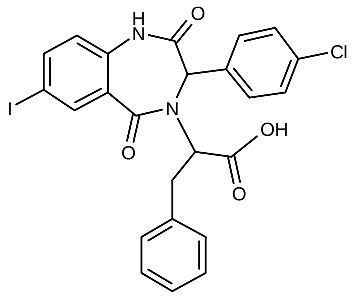

48

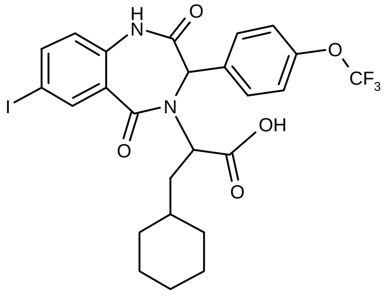

49

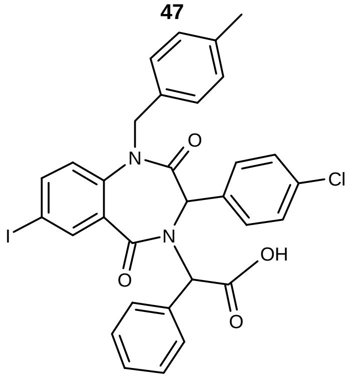

50

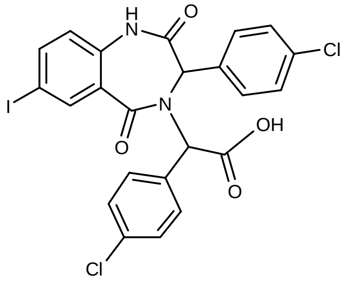

51

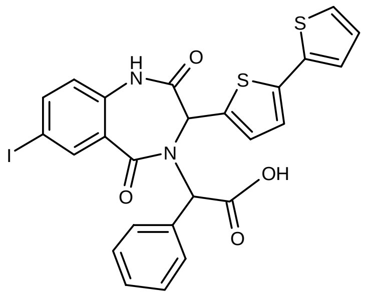

52

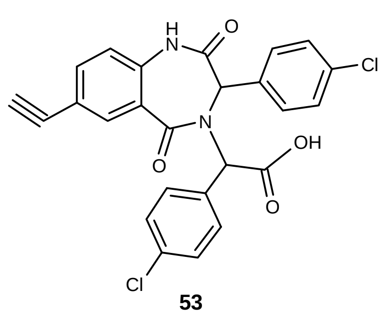

53

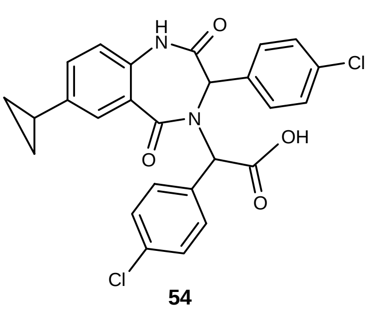

54

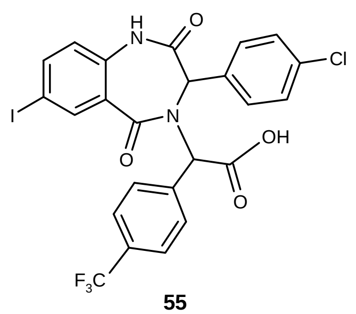

55

Figure 7. Representative examples of benzodiazepine inhibitors of p53–MDM2 interaction.

hibited

Co

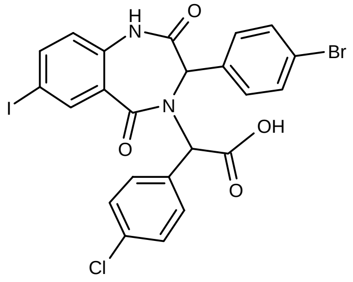

56

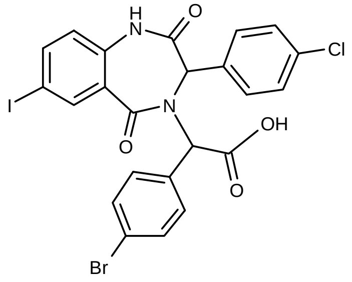

57

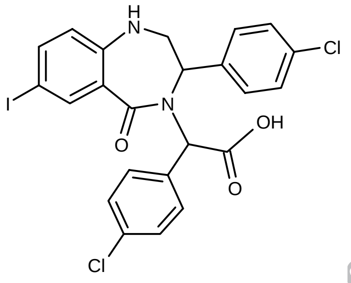

58

Figure 7. Representative examples of benzodiazepine inhibitors of p53–MDM2 interaction (*Continued*).

Table 3. Inhibition of MDM2 binding to p53 by representative benzodiazepines.

Compound	Inhibition of MDM2 binding to p53 (IC$_{50}$ μM)
42	1.7
43	1.8
44	13
45	56
46	7.8
47	10.1
48	11.7
49	10.5
50	1.9
51	0.22
52	10
53	0.87
54	1.70
55	0.62
56	0.47
57	0.62
58	0.58

of benzodiazepines as inhibitors of p53–MDM2 interaction was the first report of such types of compound acting as α-helix mimetics [51]. Therefore, this finding further suggests that the exploration of the benzodiazepinedione scaffold towards the design of inhibitors for the disruption of protein–protein interaction is a valid approach [51].

2.3 Substituted piperazines

Numerous studies on the biological activities of 4-phenylpiperazine-1-carboxamide substituents have been reported. Some have been shown to be orally-active nonsteroidal androgen receptor inhibitors, whilst some have shown antibacterial activity [70-72]. A new synthetic piperazine derivative, which inhibits microtubule activity, is reported to exhibit antiangiogenic and anticancer activities [73]. Another study indicated that several piperazine-based synthetic molecules were potent inhibitors of plasminogen activator inhibitor-1, a member of the serine protease inhibitor (serpin) family acting as the major negative regulator of tPA and uPA [74]. Some piperazine derivatives were recently reported as histone deacetylase and NK1 inhibitors [117-119].

Recently, the piperazine derivatives were proposed as useful probes of the p53–MDM2 interaction and as novel agents for the treatment of cancer [120]. The activities were measured by a modified ELISA using a histidine-tagged MDM2, a GST–p53 fusion protein and a nickel chelate-alkaline phosphatase (NTA-AP).

4-Phenylpiperazine derivatives are another example of p53–MDM2 interaction inhibitors that have been reviewed recently [75,76,121]. The IC$_{50}$ value of these compounds ranged 0.03 – 200 μM. Compound **70** has an IC$_{50}$ value of ~ 4 μM. Representative compounds are shown in **Figure 11**. These compounds are claimed to be useful in combination with other anticancer drugs to treat tumours where MDM2 is overexpressed [75].

2.4 Substituted piperidines

A separate discovery provided a novel series of piperidines with *cis*-3,4-dialkoxy substitutions. These compounds were claimed as small molecule inhibitors of the p53–MDM2 interaction. The 3,4-bis(benzyloxy) piperidines displayed a variety of biological activities. For example, several derivatives were useful to treat Gaucher disease, a genetic disorder, and cancer, whereas some other examples were claimed to be effective in the prevention and treatment of Alzheimer's disease [122-124]. Moreover, the piperidine motif has also been recognised as a core structure in several HIV and feline immunodeficiency virus (FIV) protease inhibitors [125]. Some examples were reported to target human coronavirus severe acute respiratory syndrome.

Amongst the 15 patents covering piperidines, two describe their potential as inhibitors of the p53–MDM2 interaction [126-127]. Representative examples are shown in **Figure 12**. The

Copyright of Ashley Publications. Printing and distribution strictly prohibited

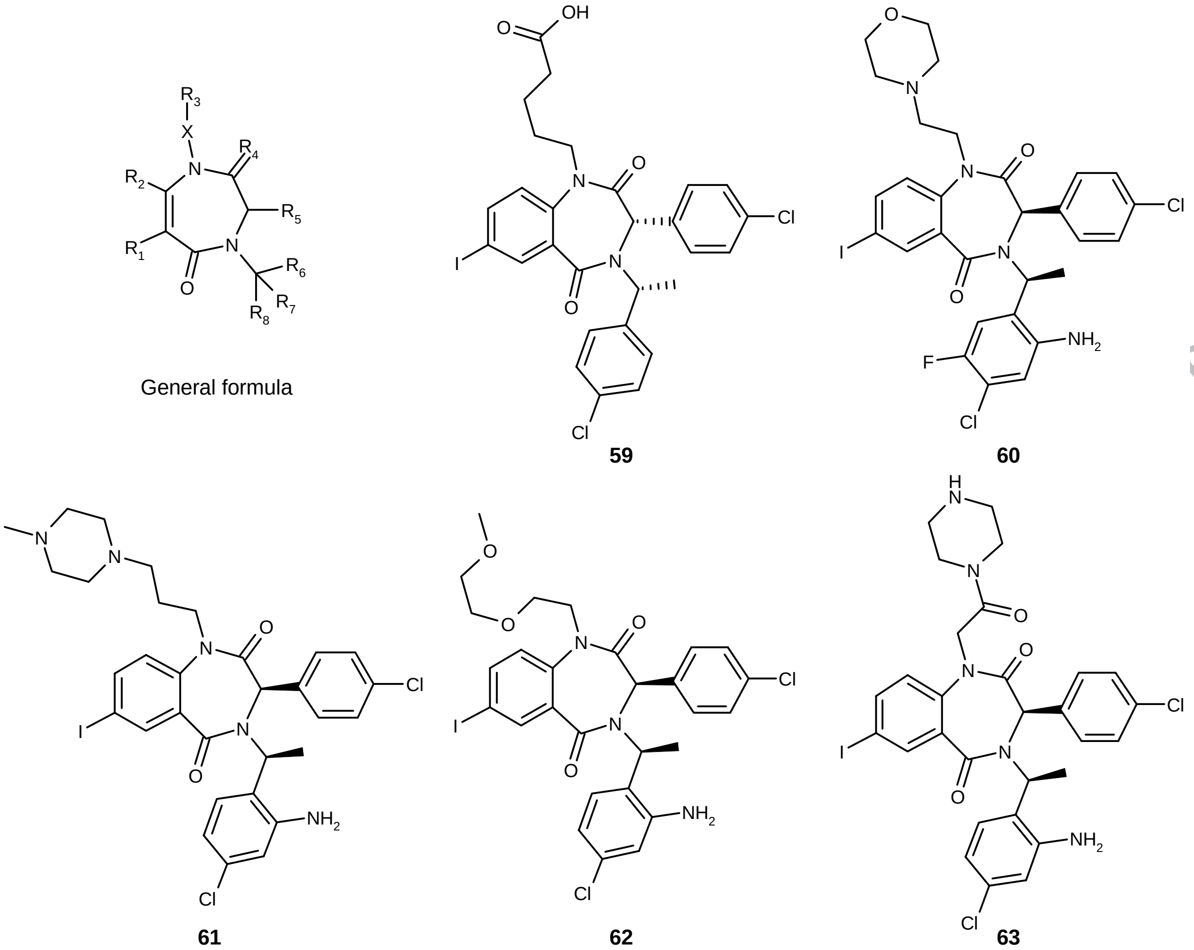

Figure 8. Representative diazepine inhibitors of p53–MDM2 interaction.

Copyright of Ashley Publications.

prohibited

Table 4. Inhibition of MDM2 binding to p53 by representative compounds.

Compound	Inhibition of MDM2 binding to p53 (IC_{50} µM)
59	0.1 – 1.0
60	1.0 – 3.0
61	0.1 – 1.0
62	0.1 – 1.0
63	1.0 – 2.0

binding orientation of the selected compounds to the p53-binding pocket of MDM2 was validated by NMR studies.

2.5 Aryl boronic acids

Several aryl and heteroaryl boronic acids were recently tested *in vitro* for their hormone-sensitive lipase inhibitory properties. The most potent compound had an IC_{50} value of 17 nM [77]. Another study showed that some boronic acids were potent inhibitors of EGFR and VEGFR-1 tyrosine kinases [78]. Other activities, such as the inhibition of β-lactamases and serine protease, were also documented [128-130].

A recent study described their anticancer activities [131]. The compounds were claimed to inhibit MDM2 expression and disrupt the p53–MDM2 protein complex. Structures of four selected aryl boronic acids are shown in **Figure 13**. The anticancer activities of a representative compound **88** are given in **Table 5**.

2.6 Fused indoles

A series of fused indoles shown in **Figure 14** were reported to interrupt the wild-type p53–MDM2 interaction [132]. These were demonstrated to induce cell death in different types of human tumour cells, for example, lung, colon and breast cancer. Moreover, the compounds were shown to stabilise the p53 expression and prevent its degradation in living cells. Restoration of p53 transcriptional activity was also validated by the standard biological assay. Selective growth suppression activities of a set of representative compounds in wild-type p53-expressing colon cancer cells are given in **Table 6**.

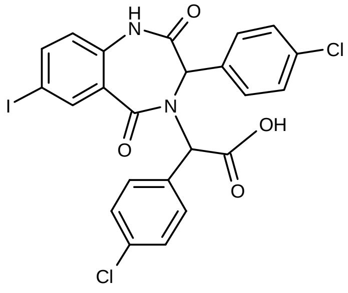

64

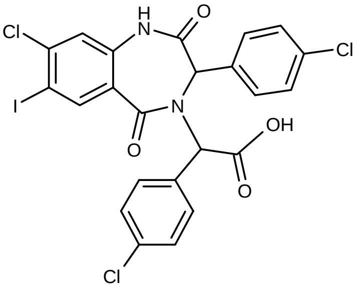

64a

Figure 9. Compounds 64 and 64a were co-crystallised with MDM2.

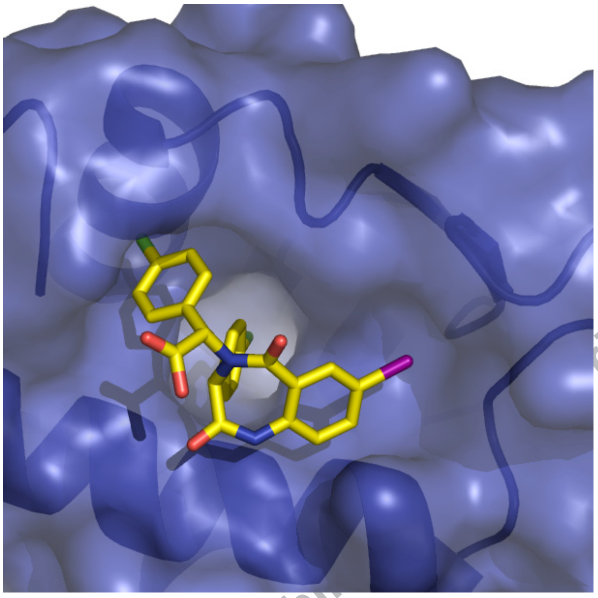

Figure 10. Crystal structure of the MDM2 complexed with benzodiazepine analogue 64 (PDB 1T4E [51]). Blue surface represents the p53 binding pocket of MDM2. The stick model shows the benzodiazepine analogue (image generated by PyMOL). Colour figure available online at www.ashley-pub.com.

2.7 Spiro-oxindoles

From the biological mapping studies and X-ray structural validation, it was envisaged that W23 of p53 appears to be most critical for MDM2 by forming hydrophobic and H-bond interactions. A recent study clearly showed that oxindoles can mimic the side chain of W23 for interaction with MDM2 [79]. These compounds were designed on the basis of a spiro-oxindole core structure, which was identified as a scaffold from a substructure search of natural products. **Figure 15** shows the structures and the competitive binding activities of representative compounds optimised on the basis of the spiro-oxindole template. The spiro-oxindoles are, therefore, exciting new additions of small molecules to the field. Their co-crystal structures with MDM2 and *in vivo* efficacy studies are eagerly awaited.

2.8 α-Helix mimetic compounds

A peptidomimetic approach in general can result in different classes of small molecules. Protein binding interfaces are largely comprised of β-sheets, α-helices, turns and secondary loop structures. It is possible to design inhibitors of protein–protein interaction mimicking each of these structural patterns [80]. Previously, several compounds were successfully designed to emulate β-turn conformations, which is defined by the ϕ and ψ torsion angles of the i+1 and i+2 residues occupying the turn region [80-85]. Recently, an α-helix mimetic was reported based on terphenyl derivatives as inhibitors of the interaction between calmodulin (CaM) and small muscle myosin light chain kinase [86]. Such terphenyl scaffolds were recently reported to interfere with the p53–MDM2 interaction [45].

Several novel inhibitors of the p53–MDM2 interaction were designed as α-helix mimics using structure-based computer-aided drug design methods. The CAVEAT software program was applied to search the Available Chemical Directory and other databases to identify lead compounds having nearly similar geometrical relationship as the Cα-Cβ of the triad motif residues (F19, W23, and L26) of MDM2-binding p53 peptide. The identified hits were further evaluated by surface docking procedure, and the synthetically accessible scaffolds were chosen for library synthesis (**Figure 16**). Furthermore, the procedure in general could be used to design small molecule inhibitors to interfere with the protein–protein interactions that are largely comprised of helices of each protein [133]. The compounds obtained from this approach have a variety of structural templates for lead optimisation.

3. Discovery of small molecule ubiquitin ligase inhibitors

Another approach to stabilise the p53 cellular level is by ubiquitin ligase inhibitors that protect p53 from MDM2-mediated ubiquitylation. The ubiquitylation of target

Copyright of Ashley Publications Ltd. Printing and distribution strictly prohibited

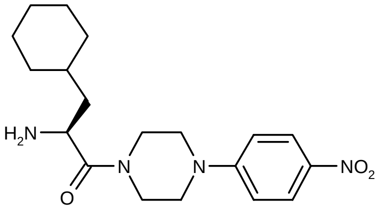

65

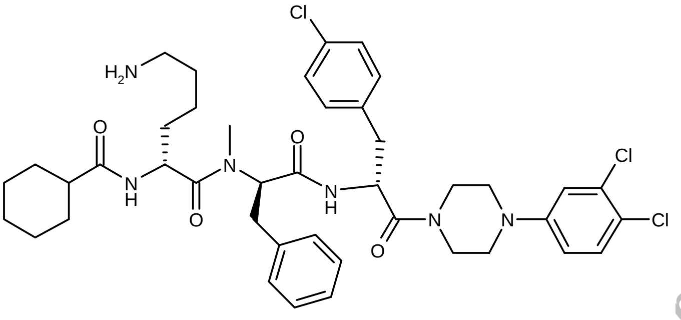
Cl
H2N
O
N
H
O
N
O
O
N
H
O
N
N
Cl
Cl

66

nibited

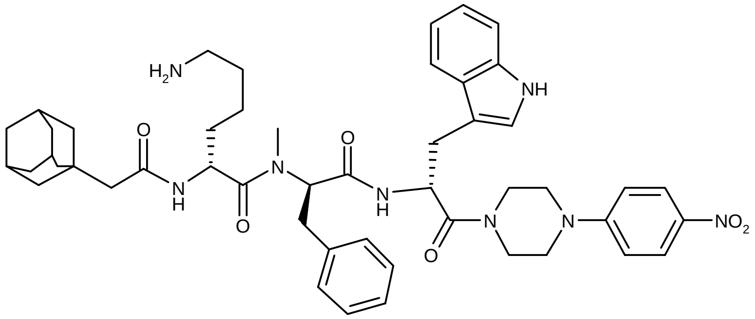
H2N
NH
O
N
H
O
N
O
N
H
O
N
N
NO2

67

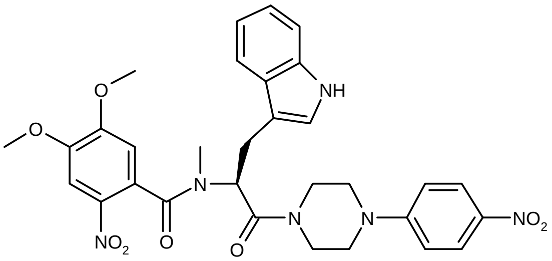
O
O
NH
N
NO2
O
O
N
N
NO2

68

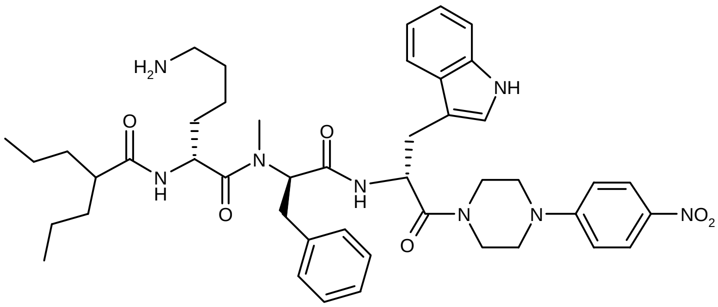
H2N
NH
O
N
H
O
N
O
N
H
O
N
N
NO2

69

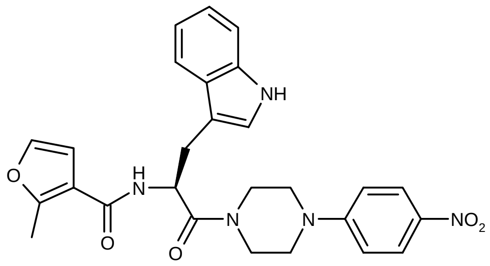
NH
O
H
N
O
O
N
N
NO2

70

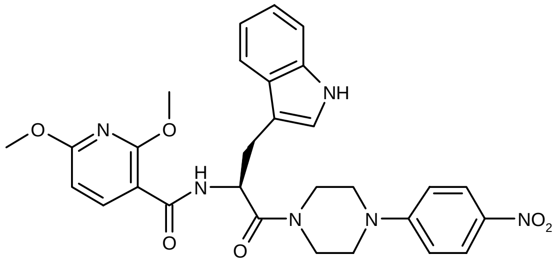
NH
O
N
O
H
N
O
O
N
N
NO2

71

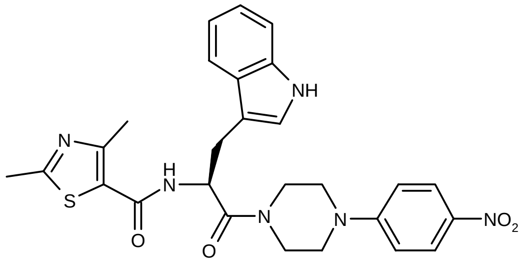
NH
N
S
H
N
O
O
N
N
NO2

72

Co

Figure 11. Representative substituted piperizine inhibitors of p53–MDM2.

proteins is regulated by the enzymatic activity of three proteins. They are the E1 ubiquitin-activating enzymes, the E2 ubiquitin-conjugating enzymes and E3 ubiquitin-protein ligases. It has been proposed that E3 functions as 'docking proteins' for specific substrate protein and E2 binding, and that ubiquitin is then transferred directly from E2s to substrates [87,88]. MDM2 belongs to the second subclass of single subunit E3 ligase that have the RING finger domain and substrate recognition domain on a single subunit, whereas the other subclass contains the RING finger domain and the

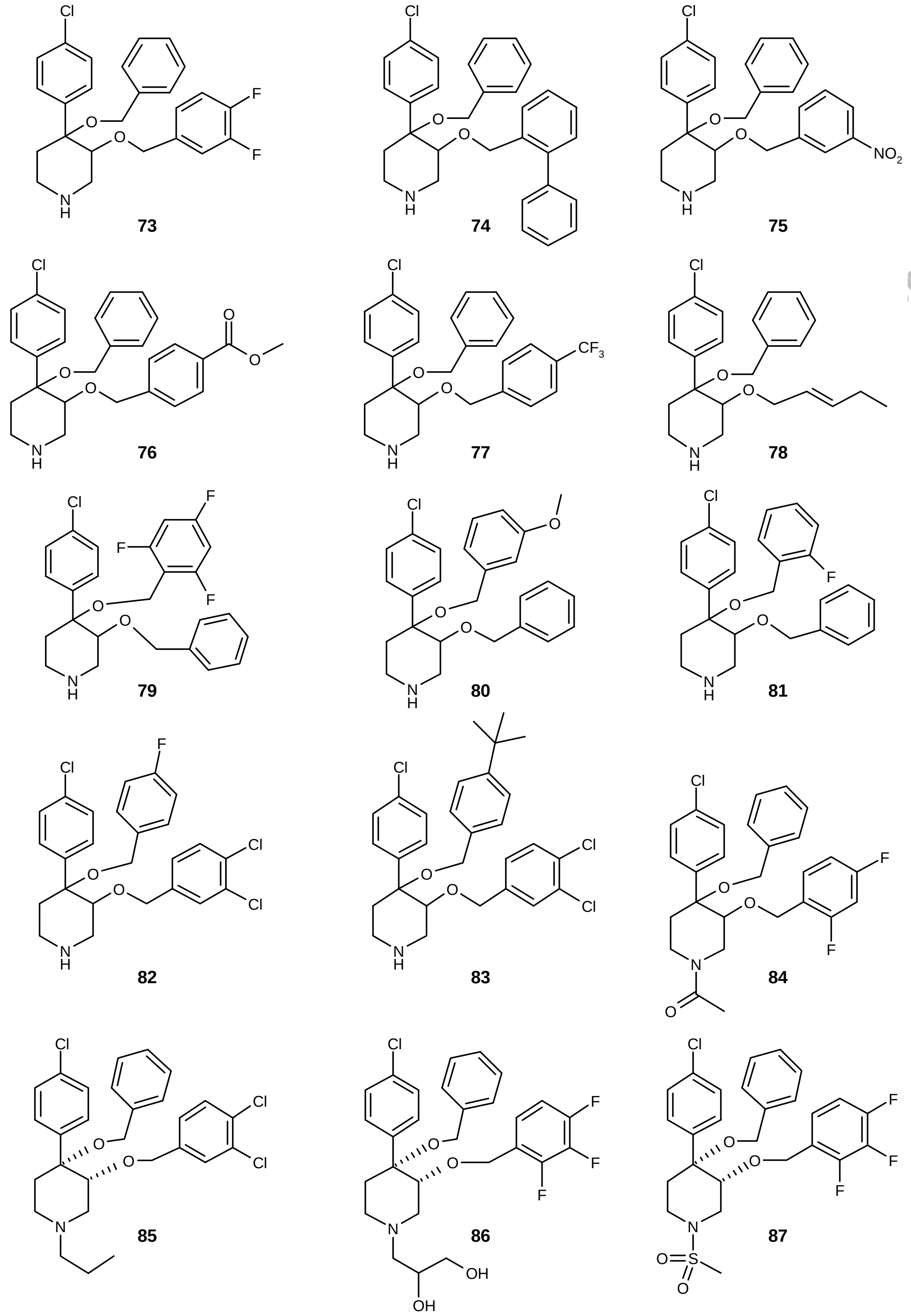
73
74
75
76
77
78
79
80
81
82
83
84
85
86
87

Figure 12. Representative substituted piperidine inhibitors of p53–MDM2 interaction.

rohibited

Copyright of

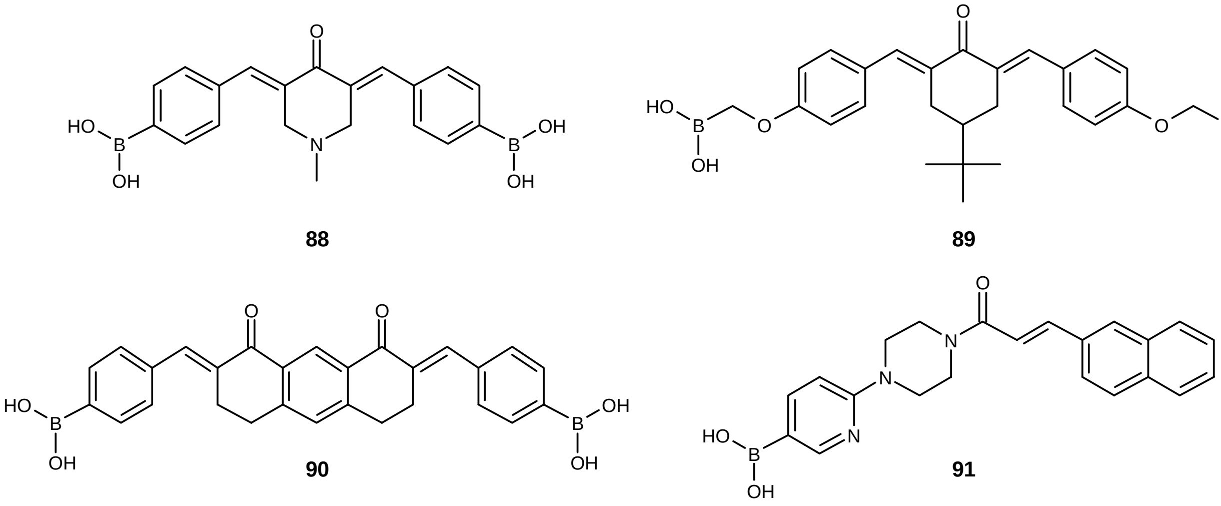

Figure 13. Representative aryl boronic acid inhibitors of p53–MDM2 interaction.

Table 5. Growth inhibition of a panel of human breast cancer cells by compound 88.

Cell line	IC_{50} (µM)
MCF7	1.9
MDA-MB-231	1.3
MCF-10A	2.5
MCF-12A	4.4

Table 6. Selective growth suppression of wild-type p53-expressing cells by fused indole (92 – 97) inhibitors of p53–MDM2 interaction.

Compound	IC_{50} (µM)	
	HCT116p53$^{+/+}$	HCT116p53$^{-/-}$
92	7.3	17
93	3.1	17
94	1.8	5.6
95	< 1	43
96	1.1	12
97	10	48

substrate recognition domain on different subunits [89]. A recent study showed that small molecules, such as benzenesulfonamides, ureas and imidazolone derivatives, inhibit MDM2-mediated p53 ubiquitylation (**Figure 17**) [90]. Another set of compounds, including 5-deazaflavin, were shown to inhibit MDM2 autoubiquitylation and clearly lead to the activation of p53 function despite allowing the stabilisation of both MDM2 and p53 [91].

5-Deazaflavin compounds were shown to effectively regulate p53 activity and anticancer activities by inhibiting MDM2-regulated ubiquitylation [134]. This finding demonstrated that p53 levels can be stabilised in mammalian cells after the treatment of 7-nitro-5-deazaflavin. Three representative compounds are shown in **Figure 18**. Biological assays demonstrated that the compounds only increased the amount of MDM2 and p53 but not p21, indicating they are specific for E3 activity of MDM2.

A recent invention provided a group of compounds as inhibitors of ubiquitin ligases [135]. The molecules can also be used in treating different diseases where ubiquitylation is involved. Because MDM2 mediates multiple monoubiquitylation of p53 by a mechanism requiring enzyme isomerisation, such compounds can stabilise p53 cell levels. Several representative compounds are shown in **Figure 19**.

4. Small molecule activators of mutant p53

The previously mentioned compounds are aimed at restoring or stabilising the wild-type p53 level to control cell growth and death. However, considering the fact that over half of all cancers carry p53 mutations, the reactivation of p53-specific DNA binding is very important to trigger p53-mediated apoptosis in cancer cells under pathological conditions. Accordingly, such strategies for the treatment of mutant p53-carrying cancers should greatly improve clinical outcome [92]. Several studies were earlier reviewed to provide methods to restore normal function of mutant p53 [93]. Some small molecules were identified by a chemical library screening showing anticancer activity through their ability to restore the DNA-binding activity of a mutant p53 (**Figure 20**) [94]. Separate chemical library screening from the National Cancer Institute discovered a novel compound, PRIMA-1, to induce mutant

Copyright of Ashley Publications. Printing and distribution prohibited

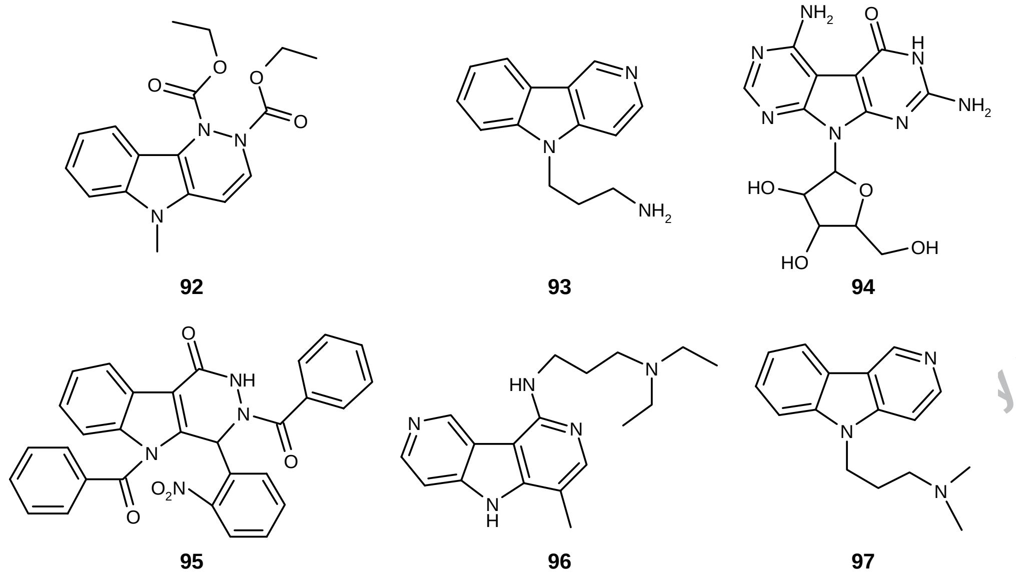

Figure 14. Representative fused indole inhibitors of p53–MDM2.

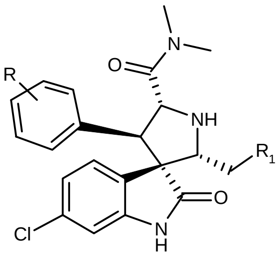

98a R = H, R_1 = *i*-Pr; K_i = 8.46 ± 1.44 µM
98b R = 3-Cl, R_1 = *i*-Pr; K_i = 0.30 ± 0.09 µM
98c R = 4-Cl, R_1 = *i*-Pr; K_i = 7.68 ± 1.68 µM
98d R = 3-Cl, R_1 = *t*-Bu; K_i = 0.086 ± 0.02 µM
98e R = 3-Cl, R_1 = C_2H_5; K_i = 0.65 ± 0.14 µM
98f R = 3-Cl, R_1 = *i*-Bu; K_i = 0.39 ± 0.08 µM

Figure 15. Representative spiro-oxindoles.

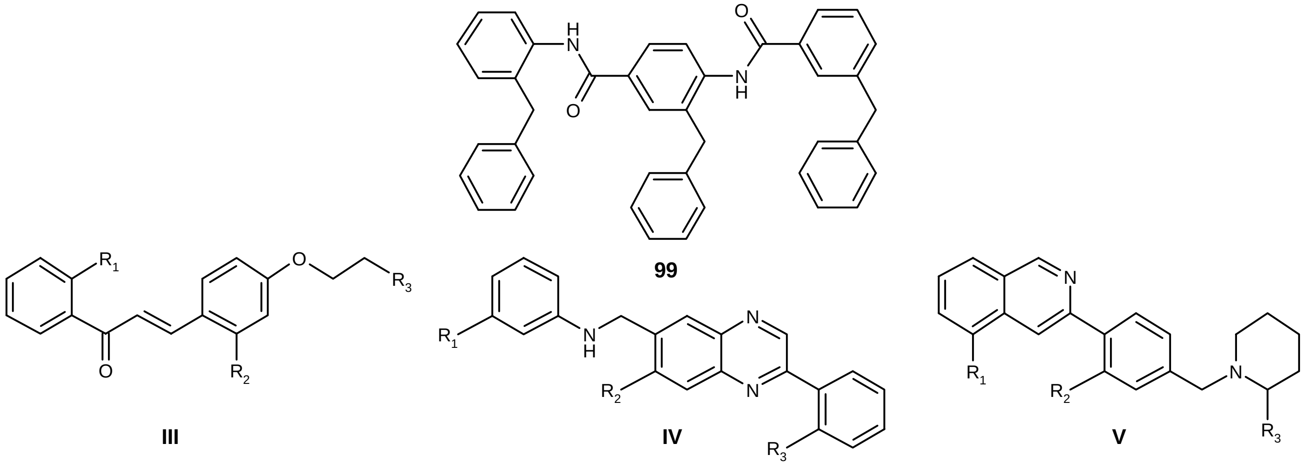

Figure 16. Representative α-helix mimetic inhibitors of p53–MDM2 interaction.

Copyri … Publicati … nd distrib … y prohibited

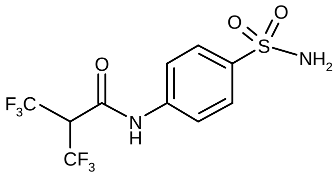

100

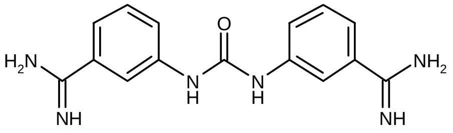

101

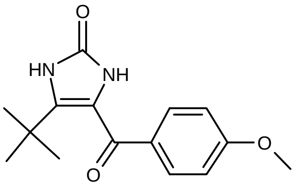

102

Figure 17. Small molecule inhibitors of MDM2-mediated p53 ubiquitiylation.

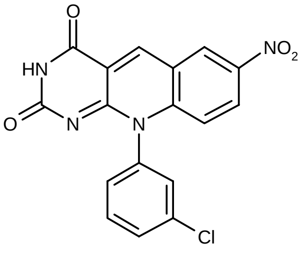

103

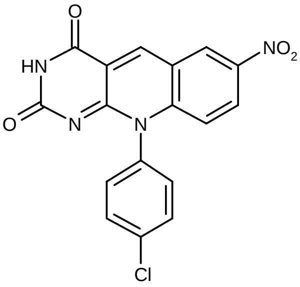

104

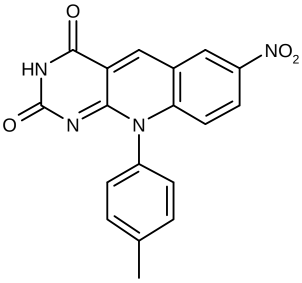

105

Figure 18. Deazaflavin ubiquitin ligase inhibitors.

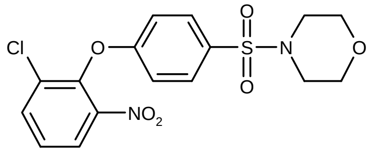

106

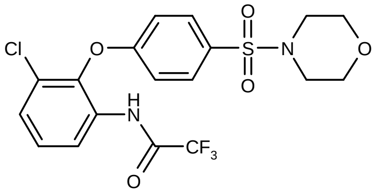

107

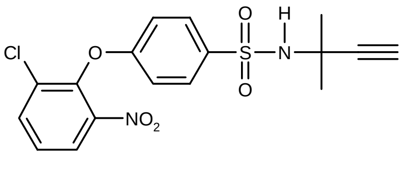

108

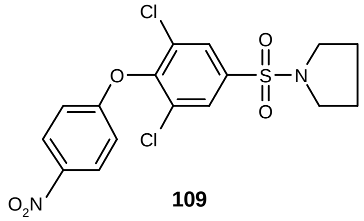

109

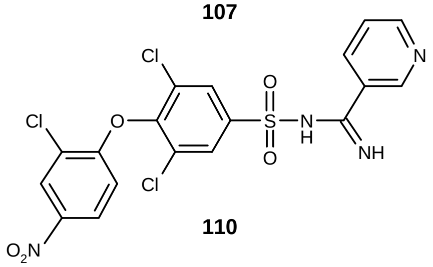

110

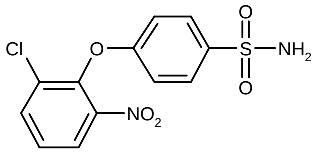

111

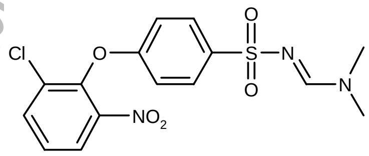

112

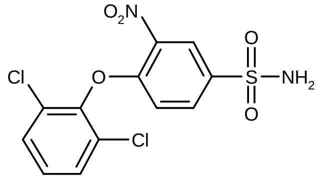

113

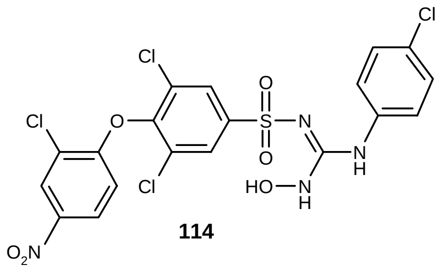

114

Figure 19. Arylsulfonamide and amide ubiquitin ligase inhibitors.

Cop Printing a ctly prohibited

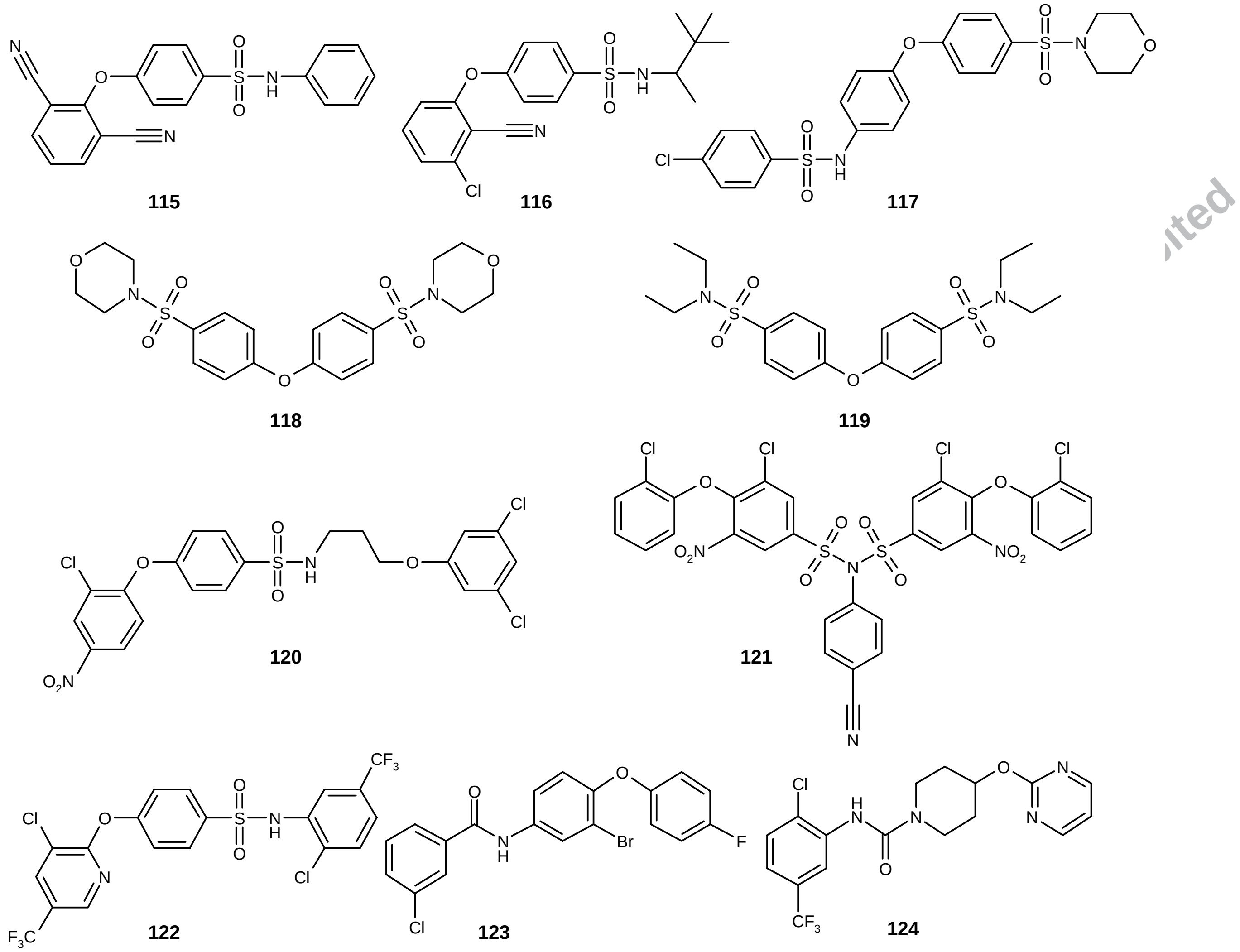

115
116
117
118
119
120
121
122
123
124

Copyright of Ashley Public ... ited

Figure 19. Arylsulfonamide and amide ubiquitin ligase inhibitors (*Continued*).

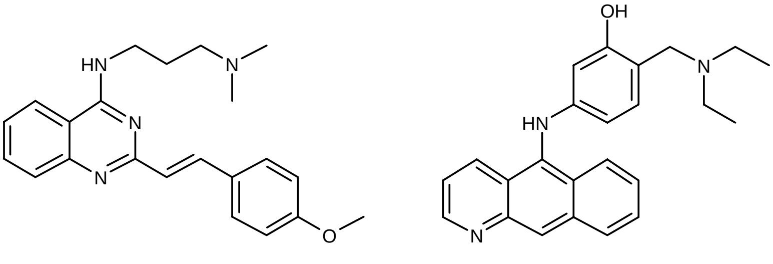

125 CP-31398

126 CP-257042

Figure 20. Examples of compounds reactivating the DNA binding activity of mutant p53.

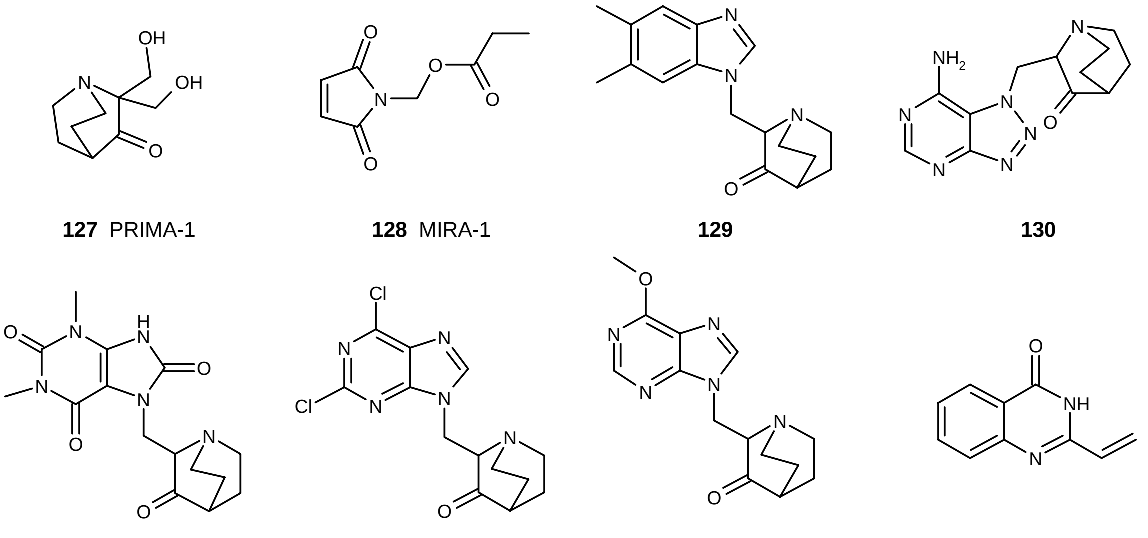

Figure 21. Representative compounds restoring apoptosis inducing function of mutant p53.

Copyright of Ashley Publications. Printing and distrib prohibited

Table 7. Calculated physicochemical properties of some of the patented inhibitors of p53–MDM2 interaction.

Compound	Calculated physicochemical properties				
	MW	S^+logP	HBA	HBD	RB
3	497.41	5.49	5	0	7
8	639.61	5.40	8	1	11
9	605.59	6.32	6	0	8
12	631.56	4.05	9	0	9
18	413.36	6.04	2	1	4
31	473.39	6.77	3	1	6
42	580.29	4.78	6	2	5
52	600.44	4.57	6	2	6
54	495.35	4.94	6	2	6
59	651.31	5.89	6	1	9
61	706.44	5.6	7	1	7
65	360.45	2.92	6	1	5
66	812.26	6.49	10	3	20
67	859.06	6.32	12	4	21
72	532.61	3.35	8	2	8
73	443.91	5.91	3	1	7
78	385.92	5.10	3	1	8
86	535.98	5.13	5	2	12
92	315.32	2.64	6	1	6
94	349.30	-1.88	10	6	5
95	516.50	3.69	7	1	5
99	586.72	8.40	4	2	12

HBA: Number of hydrogen-bond acceptors; HBD: Number of hydrogen-bond donors; MW: Molecular weight; RB: Number of rotatable bonds; S^+logP: Logarithm of the octanol-water partition coefficient (calculated using ADMET Predictor [Simulations Plus, Inc.]).

p53-dependent apoptosis and inhibit *in vivo* tumour growth [95]. Furthermore, PRIMA-1 was synergistic with cisplatin in inducing apoptosis [96]. Recently, maleimide analogues were reported to induce apoptosis in human tumours by restoring the normal function of mutant p53 [92,136]. The structures of representative compounds are shown in **Figure 21**.

5. Expert opinion

p53 is a transcription factor forming an autoregulartory loop with MDM2. Over 50% of all cancers have mutant p53, indicating its critical role in the cell. Therefore, restoring or stabilising the p53 cellular level and its normal function has become one of the major targets for cancer therapy. The disruption of the p53–MDM2 interaction has been validated as a novel drug target for the development of cancer therapeutics. In particular, the discovery of the Nutlin series of compounds provided compelling evidence that the p53–MDM2 interaction can be successfully manipulated with small molecule inhibitors. The success of these compounds also provides strong support for the therapeutic application of selective disruption of protein–protein interactions. Protein–protein interactions consist of large surfaces and multiple interactions of diverse nature. Many of the inhibitors of the p53–MDM2 interaction discussed in this review contain several hydrophobic groups and have a high molecular weight. To put these compounds into perspective the authors have calculated drug-like properties (Lipinski's rule-of-five) of some of the selected compounds from each class of patented inhibitors (**Table 7**). Interestingly, several of these inhibitors do not satisfy Lipinski's rule-of-five. Many of these inhibitors violate molecular weight (> 500) and logP (> 5), which is a result of their large size and hydrophobic functional groups. These inhibitors represent a novel class of therapeutics targeted at protein–protein interactions; upon their *in vivo* success some modifications to Lipinski's rule-of-five, which was formulated on the basis of properties of drugs aimed at conventional drug targets, are warrented.

In conclusion, the inhibitors of p53–MDM2 interaction represent a major step in the design of disrupting protein–protein interaction and a giant leap towards the targeted therapeutics.

Acknowledgements

This work was financially supported by funds from DOD Concept Award and Gustavus and Louise Pfeiffer Research Foundation grant to N Neamati. The authors thank Laith Al-Mawsawi for critical reading of the manuscript.

Copyright of Ashley Publications. Printing and distribution strictly prohibited

Bibliography

Papers of special note have been highlighted as either of interest (•) or of considerable interest (••) to readers.

1. CAHILLY-SNYDER L, YANG-FENG T, FRANCKE U, GEORGE DL: Molecular analysis and chromosomal mapping of amplified genes isolated from a transformed mouse 3T3 cell line. *Somat. Cell Mol. Genet.* (1987) **13**:235.
2. MOMAND J, ZAMBETTI GP, OLSON DC, GEORGE D, LEVINE AJ: The MDM-2 oncogene product forms a complex with the p53 protein and inhibits p53-mediated transactivation. *Cell* (1992) **69**(7):1237-1245.
3. OLINER JD, KINZLER KW, MELTZER PS, GEORGE DL, VOGELSTEIN B: Amplification of a gene encoding a p53-associated protein in human sarcomas. *Nature* (1992) **358**(6381):80-83.
- **The first report of MDM2 overexpression in sarcomas.**
4. STEFANOU DG, NONNI AV, AGNANTIS NJ *et al.*: p53/MDM-2 immunohistochemical expression correlated with proliferative activity in different subtypes of human sarcomas: a ten-year follow-up study. *Anticancer Res.* (1998) **18**(6B):4673-4681.
5. ZIETZ C, ROSSLE M, HAAS C *et al.*: MDM-2 oncoprotein overexpression, p53 gene mutation, and VEGF up-regulation in angiosarcomas. *Am. J. Pathol.* (1998) **153**(5):1425-1433.
6. ZHELEVA DI, LANE DP, FISCHER PM: The p53-MDM2 pathway: targets for the development of new anticancer therapeutics. *Mini Rev. Med. Chem.* (2003) **3**(3):257-270.
7. RAYBURN E, ZHANG R, HE J, WANG H: MDM2 and human malignancies: expression, clinical pathology, prognostic markers, and implications for chemotherapy. *Curr. Cancer Drug Targets* (2005) **5**(1):27-41.
8. YAM CH, SIU WY, AROOZ T *et al.*: MDM2 and MDMX inhibit the transcriptional activity of ectopically expressed SMAD proteins. *Cancer Res.* (1999) **59**(20):5075-5078.
9. BOND GL, HU W, LEVINE AJ: MDM2 is a central node in the p53 pathway: 12 years and counting. *Curr. Cancer Drug Targets* (2005) **5**(1):3-8.
10. HORIE S, ENDO K, KAWASAKI H, TERADA T: Overexpression of MDM2 protein in intrahepatic cholangiocarcinoma: relationship with p53 overexpression, Ki-67 labeling, and clinicopathological features. *Virchows Arch.* (2000) **437**(1):25-30.
11. COCKER HA, HOBBS SM, TIFFIN N *et al.*: High levels of the MDM2 oncogene in paediatric rhabdomyosarcoma cell lines may confer multidrug resistance. *Br. J. Cancer* (2001) **85**(11):1746-1752.
12. SUZUKI A, TOI M, YAMAMOTO Y *et al.*: Role of MDM2 overexpression in doxorubicin resistance of breast carcinoma. *Jpn. J. Cancer Res.* (1998) **89**(2):221-227.
13. RODRIGUEZ-LOPEZ AM, XENAKI D, EDEN TO, HICKMAN JA, CHRESTA CM: MDM2 mediated nuclear exclusion of p53 attenuates etoposide-induced apoptosis in neuroblastoma cells. *Mol. Pharmacol.* (2001) **59**(1):135-143.
14. MATHEW R, ARORA S, KHANNA R *et al.*: Alterations in p53 and pRb pathways and their prognostic significance in oesophageal cancer. *Eur. J. Cancer* (2002) **38**(6):832-841.
15. ZHANG L, HILL RP: Hypoxia enhances metastatic efficiency by up-regulating MDM2 in KHT cells and increasing resistance to apoptosis. *Cancer Res.* (2004) **64**(12):4180-4189.
16. IWAKUMA T, LOZANO G: MDM2, an introduction. *Mol. Cancer Res.* (2003) **1**(14):993-1000.

17. ZHANG Z, ZHANG R: p53-Independent activities of MDM2 and their relevance to cancer therapy. *Curr. Cancer Drug Targets* (2005) **5**(1):9-20.
18. FINLAY CA, HINDS PW, LEVINE AJ: The p53 proto-oncogene can act as a suppressor of transformation. *Cell* (1989) **57**(7):1083-1093.
19. BUOLAMWINI JK, ADDO J, KAMATH S *et al.*: Small molecule antagonists of the MDM2 oncoprotein as anticancer agents. *Curr. Cancer Drug Targets* (2005) **5**(1):57-68.
20. WOODS DB, VOUSDEN KH: Regulation of p53 function. *Exp. Cell Res.* (2001) **264**(1):56-66.
21. MALKIN D: The role of p53 in human cancer. *J. Neurooncol.* (2001) **51**(3):231-243.
22. HOLLSTEIN M, SIDRANSKY D, VOGELSTEIN B, HARRIS CC: p53 mutations in human cancers. *Science* (1991) **253**(5015):49-53.
23. HOLLSTEIN M, RICE K, GREENBLATT MS *et al.*: Database of p53 gene somatic mutations in human tumors and cell lines. *Nucleic Acids Res.* (1994) **22**(17):3551-3555.
24. HARRIS CC: Structure and function of the p53 tumor suppressor gene: clues for rational cancer therapeutic strategies. *J. Natl. Cancer Inst.* (1996) **88**(20):1442-1455.
25. MOMAND J, WU HH, DASGUPTA G: MDM2-master regulator of the p53 tumor suppressor protein. *Gene* (2000) **242**(1-2):15-29.
26. CHO Y, GORINA S, JEFFREY PD, PAVLETICH NP: Crystal structure of a p53 tumor suppressor-DNA complex: understanding tumorigenic mutations. *Science* (1994) **265**(5170):346-355.
27. MCCOY M, STAVRIDI ES, WATERMAN JL *et al.*: Hydrophobic side-chain size is a determinant of the three-dimensional structure of the p53 oligomerization domain. *EMBO J.* (1997) **16**(20):6230-6236.
28. CLORE GM, ERNST J, CLUBB R *et al.*: Refined solution structure of the oligomerization domain of the tumour suppressor p53. *Nat. Struct. Biol.* (1995) **2**(4):321-333.
29. LEE W, HARVEY TS, YIN Y *et al.*: Solution structure of the tetrameric minimum transforming domain of p53. *Nat. Struct. Biol.* (1994) **1**(12):877-890.
30. WU H, MACIEJEWSKI MW, MARINTCHEV A *et al.*: Solution structure of a dynein motor domain associated light chain. *Nat. Struct. Biol.* (2000) **7**(7):575-579.
31. JEFFREY PD, GORINA S, PAVLETICH NP: Crystal structure of the tetramerization domain of the p53 tumor suppressor at 1.7 angstroms. *Science* (1995) **267**(5203):1498-1502.
32. MITTL PR, CHENE P, GRUTTER MG: Crystallization and structure solution of p53 (residues 326-356) by molecular replacement using an NMR model as template. *Acta Crystallogr. D Biol. Crystallogr.* (1998) **54**(Pt.1):86-89.
33. JOERGER AC, ALLEN MD, FERSHT AR: Crystal structure of a superstable mutant of human p53 core domain. Insights into the mechanism of rescuing oncogenic mutations. *J. Biol. Chem.* (2004) **279**(2):1291-1296.
34. JOERGER AC, ANG HC, VEPRINTSEV DB, BLAIR CM, FERSHT AR: Structures of p53 cancer mutants and mechanism of rescue by second-site suppressor mutations. *J. Biol. Chem.* (2005) **280**(16):16030-16037.
35. KUSSIE PH, GORINA S, MARECHAL V *et al.*: Structure of the MDM2 oncoprotein bound to the p53 tumor suppressor transactivation domain. *Science* (1996) **274**(5289):948-953.

•• **The first co-crystal structure of MDM2 with p53 peptide.**

36. FREEDMAN DA, WU L, LEVINE AJ: Functions of the MDM2 oncoprotein. *Cell. Mol. Life Sci.* (1999) **55**(1):96-107.
37. GOTTIFREDI V, PRIVES C: Molecular biology. Getting p53 out of the nucleus. *Science* (2001) **292**(5523):1851-1852.
38. CHENE P, FUCHS J, CARENA I, FURET P, GARCIA-ECHEVERRIA C: Study of the cytotoxic effect of a peptidic inhibitor of the p53-HDM2 interaction in tumor cells. *FEBS Lett.* (2002) **529**(2-3):293-297.
39. LIN J, CHEN J, ELENBAAS B, LEVINE AJ: Several hydrophobic amino acids in the p53 amino-terminal domain are required for transcriptional activation, binding to MDM2 and the adenovirus 5 E1B 55 kD protein. *Genes Dev.* (1994) **8**(10):1235-1246.

• **The first study on the MDM2 binding motif.**

40. PICKSLEY SM, VOJTESEK B, SPARKS A, LANE DP: Immunochemical analysis of the interaction of p53 with MDM2; fine mapping of the MDM2 binding site on p53 using synthetic peptides. *Oncogene* (1994) **9**(9):2523-2529.
41. BOTTGER A, BOTTGER V, GARCIA-ECHEVERRIA C *et al.*: Molecular characterization of the hdm2-p53 interaction. *J. Mol. Biol.* (1997) **269**(5):744-756.
42. BOTTGER V, BOTTGER A, HOWARD SF *et al.*: Identification of novel mdm2 binding peptides by phage display. *Oncogene* (1996) **13**(10):2141-2147.
43. CHENE P: Inhibition of the p53–MDM2 interaction: targeting a protein–protein interface. *Mol. Cancer Res.* (2004) **2**(1):20-28.
44. SCHON O, FRIEDLER A, FREUND S, FERSHT AR: Binding of p53-derived ligands to MDM2 induces a variety of long range conformational changes. *J. Mol. Biol.* (2004) **336**(1):197-202.
45. CHEN L, YIN H, FAROOQI B *et al.*: p53 α-Helix mimetics antagonize p53/MDM2 interaction and activate p53. *Mol. Cancer Ther.* (2005) 4(6):1019-1025.
46. STOLL R, RENNER C, HANSEN S *et al.*: Chalcone derivatives antagonize interactions between the human oncoprotein MDM2 and p53. *Biochemistry* (2001) **40**(2):336-344.
47. DUNCAN SJ, GRUSCHOW S, WILLIAMS DH *et al.*: Isolation and structure elucidation of Chlorofusin, a novel p53-MDM2 antagonist from a *Fusarium* sp. *J. Am. Chem. Soc.* (2001) **123**(4):554-560.
48. ZHAO J, WANG M, CHEN J *et al.*: The initial evaluation of non-peptidic small-molecule HDM2 inhibitors based on p53-HDM2 complex structure. *Cancer Lett.* (2002) **183**(1):69-77.
49. KUMAR SK, HAGER E, PETTIT C *et al.*: Design, synthesis, and evaluation of novel boronic-chalcone derivatives as antitumor agents. *J. Med. Chem.* (2003) **46**(14):2813-2815.
50. VASSILEV LT, VU BT, GRAVES B *et al.*: *In vivo* activation of the p53 pathway by small-molecule antagonists of MDM2. *Science* (2004) **303**(5659):844-848.

•• **The first co-crystal structure of a potent small molecule bound to MDM2.**

Copyright of Ashley Publications. Printing and distribution strictly prohibited

51. GRASBERGER BL, LU T, SCHUBERT C *et al.*: Discovery and cocrystal structure of benzodiazepinedione HDM2 antagonists that activate p53 in cells. *J. Med. Chem.* (2005) **48**(4):909-912.

- **The second co-crystal structure of a small molecule bound to MDM2.**

52. MOLL UM, PETRENKO O: The MDM2–p53 interaction. *Mol. Cancer Res.* (2003) **1**(14):1001-1008.

53. CHENE P: Inhibiting the p53–MDM2 interaction: an important target for cancer therapy. *Nat Rev Cancer* (2003) **3**(2):102-109.

54. ALARCON-VARGAS D, RONAI Z: p53-MDM2 – the affair that never ends. *Carcinogenesis* (2002) **23**(4):541-547.

55. CHENE P, FUCHS J, BOHN J *et al.*: A small synthetic peptide, which inhibits the p53–HDM2 interaction, stimulates the p53 pathway in tumour cell lines. *J. Mol. Biol.* (2000) **299**(1):245-253.

56. UENO M, IMAIZUMI K, SUGITA T, TAKATA I, TAKESHITA M: Effect of a novel anti-rheumatic drug, TA-383, on type II collagen-induced arthritis. *Int. J. Immunopharmacol.* (1995) **17**(7):597-603.

57. UENO M, SUGITA T, MURAKAMI T, TAKATA I: The novel anti-rheumatic drug TA-383 has a macrophage migration enhancing activity. *Jpn. J. Pharmacol.* (1997) **74**(2):221-224.

58. MERRIMAN GH, MA L, SHUM P *et al.*: Synthesis and SAR of novel 4,5-diarylimidazolines as potent P2X7 receptor antagonists. *Bioorg. Med. Chem. Lett* (2005) **15**(2):435-438.

59. VASSILEV LT: p53 activation by small molecules: application in oncology. *J. Med. Chem.* (2005) **48**(14):4491-4499.

60. KLEIN C, VASSILEV LT: Targeting the p53–MDM2 interaction to treat cancer. *Br. J. Cancer* (2004) **91**(8):1415-1419.

61. BRESLIN HJ, KUKLA MJ, KROMIS T *et al.*: Synthesis and anti-HIV activity of 1,3,4,5-tetrahydro-2*H*-1,4-benzodiazepin-2-one (TBO) derivatives. Truncated 4,5,6,7-tetrahydro-5-methylimidazo[4,5,1-jk][1,4]benzodiazepin-2(1H)-ones (TIBO) analogues. *Bioorg. Med. Chem.* (1999) **7**(11):2427-2436.

62. KAMAL A, RAMESH G, SRINIVAS O *et al.*: Design, synthesis, and evaluation of mixed imine–amine pyrrolobenzodiazepine dimers with efficient DNA binding affinity and potent cytotoxicity. *Bioorg. Med. Chem.* (2004) **12**(20):5427-5436.

63. KAMAL A, SRINIVAS O, RAMULU P *et al.*: Synthesis and DNA binding affinity of novel A-C8/C-C2-exo unsaturated alkoxyamido-linked pyrrolo[2,1-c][1,4]benzodiazepine dimers. *Bioorg. Med. Chem.* (2004) **12**(16):4337-4350.

64. GREGSON SJ, HOWARD PW, HARTLEY JA *et al.*: Design, synthesis, and evaluation of a novel pyrrolobenzodiazepine DNA-interactive agent with highly efficient cross-linking ability and potent cytotoxicity. *J. Med. Chem.* (2001) **44**(5):737-748.

65. HIRAYAMA F, KOSHIO H, KATAYAMA N *et al.*: Design, synthesis and biological activity of YM-60828 derivatives. Part 2: potent and orally-bioavailable Factor Xa inhibitors based on benzothiadiazine-4-one template. *Bioorg. Med. Chem.* (2003) **11**(3):367-381.

66. KAMAL A, RAMESH G, LAXMAN N *et al.*: Design, synthesis, and evaluation of new noncross-linking pyrrolobenzodiazepine dimers with efficient DNA binding ability and potent antitumor activity. *J. Med. Chem.* (2002) **45**(21):4679-4688.

67. KOSSAKOWSKI J, ZAWADOWSKI T, TURLO J: Synthesis of new N-substituted benzodiazepine derivatives with potential anxiolytic activity. *Acta Pol. Pharm.* (1997) **54**(6):483-485.

68. KARP G, MANFREDI MC, GUACIARO MA *et al.*: Synthesis and herbicidal activity of 1*H*-1,4-benzodiazepine-2,5-diones. *J. Agric. Food Chem.* (1997) **45**(2):493-500.

69. RABOISSON P, MARUGAN JJ, SCHUBERT C *et al.*: Structure-based design, synthesis, and biological evaluation of novel 1,4-diazepines as HDM2 antagonists. *Bioorg. Med. Chem. Lett.* (2005) **15**(7):1857-1861.

70. KINOYAMA I, TANIGUCHI N, KAWAMINAMI E *et al.*: N-Arylpiperazine-1-carboxamide derivatives: a novel series of orally active nonsteroidal androgen receptor antagonists. *Chem. Pharm. Bull.* (2005) **53**(4):402-409.

71. KINOYAMA I, TANIGUCHI N, YODEN T *et al.*: Synthesis and pharmacological evaluation of novel arylpiperazine derivatives as nonsteroidal androgen receptor antagonists. *Chem. Pharm. Bull.* (2004) **52**(11):1330-1333.

72. KHALAJ A, ADIBPOUR N, SHAHVERDI AR, DANESHTALAB M: Synthesis and antibacterial activity of 2-(4-substituted phenyl)-3(2*H*)-isothiazolones. *Eur J. Med. Chem.* (2004) **39**(8):699-705.

73. YI EY, JEONG EJ, SONG HS *et al.*: Antiangiogenic and anti-tumor apoptotic activities of SJ-8002, a new piperazine derivative. *Int. J. Oncol.* (2004) **25**(2):365-372.

74. YE B, CHOU YL, KARANJAWALA R *et al.*: Synthesis and biological evaluation of piperazine-based derivatives as inhibitors of plasminogen activator inhibitor-1 (PAI-1). *Bioorg. Med. Chem. Lett.* (2004) **14**(3):761-765.

75. PICKSLEY SM, DART DA, MANSOOR MS, LOADMAN PM: Current advances in the inhibition of the auto-regulatory interaction between the p53 tumour suppressor protein and MDM2 protein. *Expert Opin. Ther. Patents* (2001) **11**(12):1825-1835.

76. CHENE P: p53 as drug target in cancer therapy. *Expert Opin. Ther. Patents* (2001) **11**(6):923-935.

77. EBDRUP S, JACOBSEN P, FARRINGTON AD, VEDSO P: Structure–activity relationship for aryl and heteroaryl boronic acid inhibitors of hormone-sensitive lipase. *Bioorg. Med. Chem.* (2005) **13**(6):2305-2312.

78. ASANO T, NAKAMURA H, UEHARA Y, YAMAMOTO Y: Design, synthesis, and biological evaluation of aminoboronic acids as growth-factor receptor inhibitors of EGFR and VEGFR-1 tyrosine kinases. *Chembiochem* (2004) 5(4):483-490.

79. DING K, LU Y, NIKOLOVSKA-COLESKA Z *et al.*: Structure-based design of potent non-peptide MDM2 inhibitors. *J. Am. Chem. Soc.* (2005) **127**(29):10130-10131.

- **An excellent example of structure-based drug design and identification of an entirely new class of MDM2 antagonist.**

80. TOOGOOD PL: Inhibition of protein–protein association by small molecules: approaches and progress. *J. Med. Chem.* (2002) **45**(8):1543-1558.

81. STIGERS KD, SOTH MJ, NOWICK JS: Designed molecules that fold to mimic protein secondary structures. *Curr. Opin. Chem. Biol.* (1999) **3**(6):714-723.

82. SOMU RV, JOHNSON RL: Synthesis of pipecolic acid-based spiro bicyclic lactam scaffolds as beta-turn mimics. *J. Org. Chem.* (2005) **70**(15):5954-5963.

Copyright of Ashley Publications Printing and distribution strictly prohibited

83. CREIGHTON CJ, LEO GC, DU Y, REITZ AB: Design, synthesis, and conformational analysis of eight-membered cyclic peptidomimetics prepared using ring closing metathesis. *Bioorg. Med. Chem.* (2004) **12**(16):4375-4385.

84. KAUL R, SURPRENANT S, LUBELL WD: Systematic study of the synthesis of macrocyclic dipeptide β-turn mimics possessing 8-, 9- and 10-membered rings by ring-closing metathesis. *J. Org. Chem.* (2005) **70**(10):3838-3844.

85. HALAB L, LUBELL WD: Effect of sequence on peptide geometry in 5-*tert*-butylprolyl type VI β-turn mimics. *J. Am. Chem. Soc.* (2002) **124**(11):2474-2484.

86. ORNER BP, ERNST JT, HAMILTON AD: Toward proteomimetics: terphenyl derivatives as structural and functional mimics of extended regions of an α-helix. *J. Am. Chem. Soc.* (2001) **123**(22):5382-5383.

87. SCHEFFNER M, NUBER U, HUIBREGTSE JM: Protein ubiquitination involving an E1-E2-E3 enzyme ubiquitin thioester cascade. *Nature* (1995) **373**(6509):81-83.

88. WEISSMAN AM: Themes and variations on ubiquitylation. *Nat. Rev. Mol. Cell. Biol.* (2001) **2**(3):169-178.

89. TYERS M, WILLEMS AR: One ring to rule a superfamily of E3 ubiquitin ligases. *Science* (1999) **284**(5414):601, 603-604.

90. LAI Z, YANG T, KIM YB *et al.*: Differentiation of HDM2-mediated p53 ubiquitination and HDM2 autoubiquitination activity by small molecular weight inhibitors. *Proc. Natl. Acad. Sci. USA* (2002) **99**(23):14734-14739.

91. YANG Y, LUDWIG RL, JENSEN JP *et al.*: Small molecule inhibitors of HDM2 ubiquitin ligase activity stabilize and activate p53 in cells. *Cancer Cell* (2005) **7**(6):547-559.

92. BYKOV VJ, ISSAEVA N, ZACHE N *et al.*: Reactivation of mutant p53 and induction of apoptosis in human tumor cells by maleimide analogs. *J. Biol. Chem.* (2005) **280**(34):30384-30391.

93. BYKOV VJ, SELIVANOVA G, WIMAN KG: Small molecules that reactivate mutant p53. *Eur. J. Cancer* (2003) **39**(13):1828-1834.

94. FOSTER BA, COFFEY HA, MORIN MJ, RASTINEJAD F: Pharmacological rescue of mutant p53 conformation and function. *Science* (1999) **286**(5449):2507-2510.

95. BYKOV VJ, ISSAEVA N, SHILOV A *et al.*: Restoration of the tumor suppressor function to mutant p53 by a low-molecular-weight compound. *Nat. Med.* (2002) **8**(3):282-288.

96. BYKOV VJ, ZACHE N, STRIDH H *et al.*: PRIMA-1(MET) synergizes with cisplatin to induce tumor cell apoptosis. *Oncogene* (2005) **24**(21):3484-3491.

Patents

101. HOFFMANN-LA ROCHE AG: WO03051359 (2003).

102. HOFFMANN-LA ROCHE, INC.: US20040204410 (2004).

103. HOFFMANN-LA ROCHE, INC.: US006617346 (2003).

104. HOFFMANN-LA ROCHE, INC.: US20030153580 (2003).

105. HOFFMANN-LA ROCHE, INC.: US20040259884 (2004).

106. HOFFMANN-LA ROCHE AG: WO2005003097 (2005).

107. HOFFMANN-LA ROCHE, INC.: US20040259867 (2004).

108. HOFFMANN-LA ROCHE AG: WO2005002575 (2005).

109. MARSHALL, GARLAND: US192272 (2005).

110. KYOWA HAKKO KOGYO CO. LTD: WO2005040172 (2005).

111. JAPAN TOBACCO, INC.: WO2004113345 (2004).

112. 3-DIMENSIONAL PHARM., INC.: WO03095625 (2003).

113. LU TIAN BIAO *ET AL.*: US20030109518 (2003).

114. JOHNSON & JOHNSON: US20040220179 (2004).

115. 3-DIMENSIONAL PHARM., INC.: WO2004096134 (2004).

116. JOHNSON & JOHNSON: US20040197893 (2004).

117. METHYLGENE, INC.: WO2005030705 (2005).

118. METHYLGENE, INC.: WO2005030704 (2005).

119. PFIZER PRODUCTS, INC.: WO2004110996 (2004).

120. ZENECA LTD: US006770627 (2004).

121. ZENECA LTD: WO0015657 (2000).

122. AMICUS THERAPEUTICS, INC.: WO2005046612 (2005).

123. RANBAXY LAB. LTD: WO2004074251 (2004).

124. ELAN PHARM., INC.: WO02076440 (2002).

125. SCRIPPS RES. INST.: WO9721100 (1997).

126. HOFFMANN-LA ROCHE, INC.: US20040180929 (2004).

127. HOFFMANN-LA ROCHE, INC.: WO2004080460 (2004).

128. NORTHWESTERN UNIV.: US6184363 (1998).

129. ASTRA PHARMA PRODUCTS: WO9842670 (1998).

130. TRIGEN LTD: WO02057273 (2002).

131. UNIV. JOHNS HOPKINS: WO2005063774 (2005).

132. APREA AB: WO2004035580 (2004).

133. UNIV. ILLINOIS: US20030144331 (2003).

134. US HEALTH: WO2004073615 (2004).

135. RIGEL PHARM., INC.: US20050009871 (2005).

136. KAROLINSKA INNOVATIONS AB: WO03070250 (2003).

Affiliation

Jinxia Deng[1], Raveendra Dayam[2] &
Nouri Neamati[†3]
[†]Author for correspondence
[1]Postdoctoral Fellow
[2]Research Fellow
[3]Assistant Professor, Department of Pharmaceutical Sciences, School of Pharmacy, University of Southern California, 1985 Zonal Avenue, PSC304A, Los Angeles, California 90089, USA
Tel: +1 323 442 2341; Fax: +1 323 442 1390;
E-mail: neamati@usc.edu

Copyright of Ashley Publications. Printing and distribution strictly prohibited

Expert Opinion

1. Introduction
2. Anticancer therapeutics targeting HER2
3. Expert opinion

informa
healthcare

Recent advances in the design and discovery of small-molecule therapeutics targeting HER2/neu

Raveendra Dayam, Fedora Grande, Laith Q Al-Mawsawi & Nouri Neamati[†]
[†]*Department of Pharmacology & Pharmaceutical Sciences, School of Pharmacy, University of Southern California, 1985 Zonal Avenue, PSC304A, Los Angeles, CA90089, USA*

The human epidermal growth factor receptor (HER) family is a highly explored and promising anticancer drug target. At present, several investigational agents targeted to the HER family of receptors are in various stages of development. Five drugs are already in the clinic for the treatment of cancers that overexpress HER family receptors. Two FDA-approved small-molecule drugs, gefitinib and erlotinib, inhibit HER1 tyrosine kinase activity. Two mAbs, cetuximab and panitumumab, target the extracellular domain of HER1, and another, trastuzumab, targets the extracellular domain of HER2. HER2 is a prominent member of the HER family of receptor tyrosine kinases and serves as a preferred dimerization partner for other HER family members. This paper reviews recently patented small-molecule inhibitors of HER2 receptor kinase activity, and inhibitors of HER2 expression and shedding. Apart from the well-explored quinazoline class of compounds (e.g., lapatinib), arylazole, benzodithiazole, pyrrolopyridazine, pyrrolotriazine and pyrrolopyrimidine classes of compounds were also claimed as HER2 tyrosine kinase inhibitors. Most of these compounds show considerable activity against all the HER family as well as members from different families of tyrosine kinases. It remains to be established how the combination of selective HER inhibitors compare with the single-agent pan-kinase inhibitors in disrupting HER family mediated signalling pathways. Such information is of paramount importance in the clinical development of HER-targeted inhibitors.

Keywords: anticancer drug, HER2, monoclonal antibody, small-molecule, tyrosine kinase inhibitor

Expert Opin. Ther. Patents (2007) 17(1):83-102

1. Introduction

Molecularly targeted anticancer drugs represent a rational advancement in the modern drug discovery paradigm. In addition to cytotoxic and DNA-targeted anticancer agents, a large number of mechanism-based molecular targets are under intensive investigation. Clinical success of several molecularly targeted therapeutics has accelerated tremendous interest in this field. The human epidermal growth factor receptor (HER, ErbB) family is an excellent example for mechanism-based anticancer molecular targets. The HER family consists of four closely related transmembrane proteins, epidermal growth factor receptor (EGFR/ErbB1/HER1), human epidermal growth factor receptor-2 (HER2/Neu/ErbB2), HER3/ErbB3 and HER4/ErbB4. The HER family receptors are among the most studied cell signalling families in cancer biology [1]. Each protein has an extracellular ligand-binding domain, a transmembrane region and an intracellular cytoplasmic domain [2]. The extracellular domain is involved in recognizing and binding ligands that are able to activate receptor. The cytoplasmic domain contains a tyrosine kinase region and a

Copyright Informa UK Ltd. Printing and distribution strictly prohibited

10.1517/13543776.17.1.83 © 2007 Informa UK Ltd ISSN 1354-3776

carboxy terminal tail that harbors tyrosine autophosphorylation sites. The HER family receptors have similar structures and a high degree of homology in the tyrosine kinase region, although they possess diverse characteristics that determine their signalling specificity. The tyrosine kinase domains of HER2 and -4 show ~ 80% homology to that of HER1, whereas HER3 lacks intrinsic tyrosine kinase activity [3]. Interestingly, the extracellular domains are less conserved among the four receptors, which is indicative of different specificity in ligand binding.

The HER receptors exist as inactive monomers. A variety of epidermal growth factor ligands can bind to extracellular domains of HER1, -3 and -4 and activate these receptors. These ligands have different specificities for each receptor, resulting in different cellular signalling effects [4,5]. There is no known ligand for HER2, rendering it an orphan receptor. On binding to ligands, the extracellular domains of HER1, -3 and -4 receptors undergo conformational changes that allow activation of the receptors by either a homodimerization or a heterdimerization process, which is essential to stimulate the tyrosine kinase activity of the receptors for subsequent generation of an intracellular signal. The pairing of two receptors of the same type results in homodimers, whereas pairing of two different type of receptors produces heterodimers. Interestingly, constitutive conformation of the extracellular domain of HER2, an orphan receptor, resembles the conformation of ligand activated extracellular domains of the other HER receptors [6,7]. This autoactivated conformation enables HER2 to perform as a preferred dimerization partner for all the other HER receptors. It has been observed that the relative expression levels of HER receptors and the ligands dictate a receptors' ability to form either a 'homo' or a 'hetero' dimer. It also has been demonstrated that HER receptors can acquire different signalling properties following dimerization with different partners. For example, a heterodimeric complex containing HER2, and an inactive tyrosine kinase receptor, HER3, can form the most potent HER signalling complex in terms of cell proliferation and transformation [8].

HER receptor dimerization induces tyrosine kinase catalytic activity, which leads to autophosphorylation of several key tyrosine residues in the activation loop of the tyrosine kinase domain within the receptor's carboxyl-terminal tail via transfer of γ-phosphates from bound ATP. The resulting phosphotyrosine residues act as docking sites for a number of signal-transducing enzymes and adaptor proteins [1]. At least two major pathways are involved in HER signalling, the MAPK and phosphatidylinositol 3-kinase (PI3K)/Akt pathways (**Figure 1**) [9,10]. The four HER receptors share most of the same intracellular second messengers generated when they are activated [11]. These include adaptor proteins such as Shc and Grb2, which couple the HER receptors to the MAPK pathway, kinases such as *c-src* and PI3K, and protein tyrosine phosphatases such as SHP1 and -2 [11]. The various postreceptor downstream signalling cascades activated upon ligand binding and receptor dimerization result in different cellular effects. For example, the MAPK pathway is important for cell proliferation, whereas the PI3K pathway has a predominant role in cell survival [12,13]. The HER receptors and their ligands are frequently amplified in various human cancers and play an important role in the pathogenesis of these diseases.

1.1 The HER family: a rational anticancer drug target

In a variety of human cancer cells, aberrant signalling involving HER receptors stimulates pathways that activate many of the properties associated with cancer, including proliferation, migration, metastases, angiogenesis and resistance to apoptosis. Due to the high frequency of abnormalities in receptor signalling in human cancers, the HER family is an attractive target for therapeutic development. The frequently observed causes of signalling abnormalities in cancers involving HER receptors are overexpression of receptors, overproduction of growth factor ligands and ligand-independent receptor activation. The third condition is related to a mutant receptor, EGFRvIII, which is commonly detected in many types of cancers. EGFRvIII lacks a major segment in the extracellular ligand binding domain. This mutation results in ligand-independent, constitutive activation of the receptor [14]. The HER receptors are overexpressed or dysregulated in a wide variety of cancers including breast, colorectal, ovarian, prostate and non-small-cell lung cancers. Importantly, overexpression of HER receptors is associated with poor disease prognosis and reduced survival. Mounting preclinical and clinical evidence supports the rationale behind the HER family targeted anticancer therapeutic approaches. Although the complexities of the signalling pathways involving the HER family of receptors are not fully understood, several possible points within the pathways have been identified to be therapeutically advantageous if interrupted [15]. The most promising and advanced therapeutic strategies targeting HER receptors are mAbs and small-molecule tyrosine kinase inhibitors. Intensive research over the last 20 years in these areas has yielded a number of promising anticancer therapeutics. As of today, five anticancer therapeutics targeting the HER receptor family have been approved by the US FDA. Two of them are small-molecule tyrosine kinase inhibitors, gefitinib (**Figure 2**) and erlotinib (**Figure 2**), targeted to the HER1 tyrosine kinase domain. The remaining three are mAbs. Trastuzumab, a humanized mAb, is targeted to the extracellular domain of HER2. Cetuximab is also a humanized mAb targeted to the extracellular domain of HER1. Recently, the US FDA approved panitumumab, the first fully human mAb for the treatment of patients with HER1-expressing metastatic colorectal cancer. Like cetuximab, panitumumab is also targeted to the extracellular domain of HER1. At present, several small-molecule HER tyrosine kinase inhibitors and HER extracellular domain-targeted antibodies are being investigated in various stages of clinical trials. Considering the enormous research activity in the discovery of anticancer therapeutics targeting the HER receptor family, the emphasis of this review is restricted to HER2-targeted small-molecule therapeutics. Recently patented small-molecule inhibitors of tyrosine kinase activity and expression and shedding of HER2 are reviewed.

Copyright of Informa UK Ltd. Printing and distribution strictly prohibited

prohibited

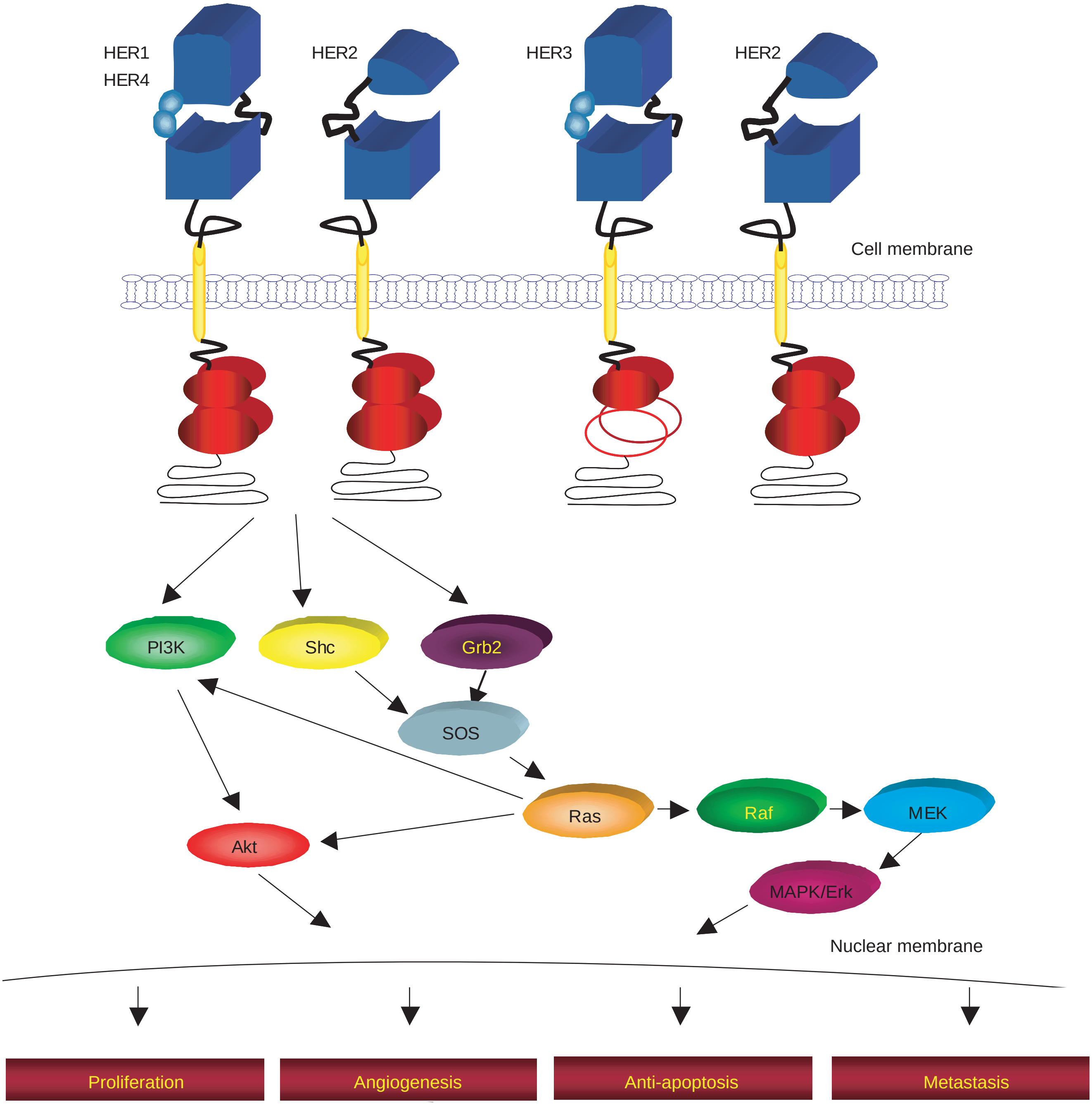
HER1
HER4
HER2
HER3
HER2
Cell membrane
PI3K
Shc
Grb2
SOS
Ras
Raf
MEK
Akt
MAPK/Erk
Nuclear membrane
Proliferation
Angiogenesis
Anti-apoptosis
Metastasis

Copyright of

Figure 1. Schematic representation of the HER family mediated signaling pathways. HER3 lacks intracellular tyrosine kinase activity; however, it acts as a dimerization partner for other members of the HER family of receptors.

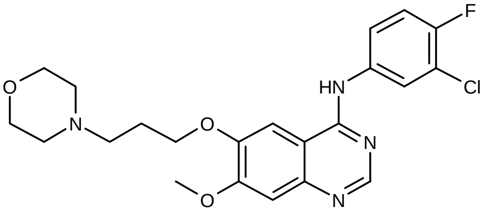

1 Gefitinib/Iressa

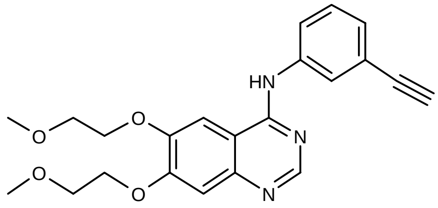

2 Erlotinib/Traceva

Figure 2. The US FDA approved small-molecule HER tyrosine kinase inhibitors.

2. Anticancer therapeutics targeting HER2

HER2 is a unique member of the HER receptor family. As discussed above, HER2 is an orphan receptor and operates as a preferred heterodimeric partner to the other HER receptors. The HER2 extracellular domain exists in a heterodimerization-favorable conformation on the cell surface, which underlies its enhanced capacity for heterodimerization with other HER family members. Although both homo- and hetrodimerization stimulate HER signalling cascades, heterodimers are more potent and mitogenic. HER2 is overexpressed in 25 – 30% of breast cancers and high expression levels correlate with poor prognosis in cancers of breast, ovary, colon and bladder [16-18]. HER2 has become an important anticancer therapeutic target, particularly for HER2-expressing primary and metastatic breast cancers. The first clinically used HER2 specific anticancer therapeutic is trastuzumab, a recombinant humanized mAb targeted at the extracellular domain of HER2. Several antibodies and small-molecule tyrosine kinase inhibitors targeting HER2 are in various stages of development at present.

2.1 Monoclonal antibodies targeting the HER2 extracellular domain

mAbs are highly specific therapeutics. Several antibodies targeted at HER family members are in development for treatment of various cancers. At present, trastuzumab is the only therapy approved for the treatment of HER2-positive cancers. A recent X-ray crystal structure reveals several critical interactions between the HER2 extracellular domain and trastuzumab. Trastuzumab shows both cytostatic and cytotoxic activities [19]. It inhibits tumor growth by accelerating the internalization and degradation of the HER2 receptor [20,21]. It has been also shown that trastuzumab has antiangiogenic activity and downregulates proteins involved in angiogenesis [22]. It also has been demonstrated that trastuzumab shows synergism in combination with a variety of chemotherapeutic agents in HER2 positive cancers. However, the majority of cancers that initially respond to trastuzumab treatment start to progress over the course of a year. Some of the reasons for resistance to trastuzumab include altered HER2–trastuzumab interactions and increased compensatory cell signalling by other HER family members. A recently completed Herceptin Adjuvant (HERA) trial study concludes that treatment with trastuzumab after adjuvant chemotherapy significantly improves disease-free survival among women with HER2-positive breast cancer [23]. To maximize trastuzumab-based treatment in patients with HER-positive cancers, novel combinations that include tyrosine kinase inhibitors and antibodies targeting other HER receptors should be explored.

Pertuzumab is a second antibody targeted to the HER2 extracellular domain. It disrupts HER2-mediated signalling by sterically blocking a binding pocket in the extracellular domain, which is required for HER2 heterodimerization with other members of the HER family [24,25]. Several preclinical studies show that pertuzumab is as active as trastuzumab on breast cancer cells expressing high levels of HER2. However, unlike trastuzumab, it is also effective in inhibiting the growth of cancer cells that do not overexpress the HER2 receptor. Its efficacy in cancers with low HER2 expression levels could be attributed to its ability to disrupt HER2 heterodimerization with other HER receptors. Pertuzumab is presently in Phase II clinical evaluation for its effect on patients with HER2-overexpressing advanced or metastatic breast cancers [26].

2.2 Small molecules targeting the HER2 tyrosine kinase domain

Small-molecule tyrosine kinase inhibitors targeted to the HER receptor family act at an intracellular level. These compounds compete with ATP for binding to the ATP site on the receptor's intracellular tyrosine kinase domain. By binding to the ATP site and inhibiting catalytic activity, they block autophosphorylation of key tyrosine residues on the receptor kinase domain. This disrupts activation of the receptor mediated downstream signalling cascades. Several small-molecule HER tyrosine kinase inhibitors are in clinical development. At present, there are no FDA-approved tyrosine kinase inhibitors selectively targeting HER2 available for cancer treatment. However, the two clinically approved HER1-specific tyrosine kinase inhibitors gefitinib and erlotinib also inhibit HER2 phosphorylation and downstream signalling cascades in HER2/HER3-overexpressing cancer cells [27-29]. It has been observed that most of the HER tyrosine kinase inhibitors in

Copyright of Informa UK Ltd. Printing and distributors ibited

Table 1. Growth inhibitory activities of representative arylalkoxy oxazole and thiazole-based HER tyrosine kinase inhibitors in A549 cells.

Compound	Structure	IC_{50} (nM)
12	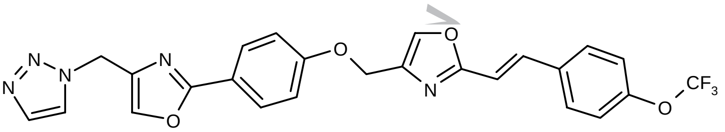	46
13	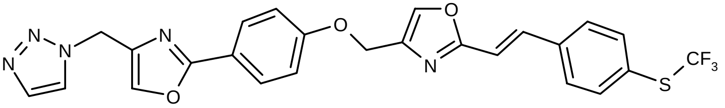	46
14	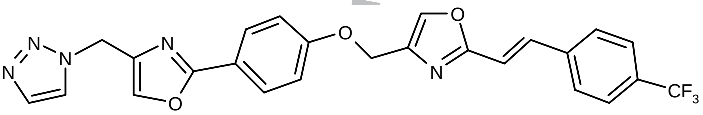	45
15	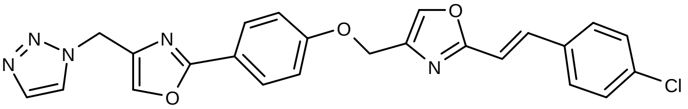	69
16	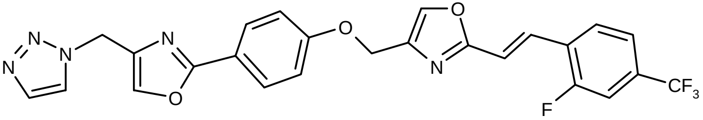	7
17	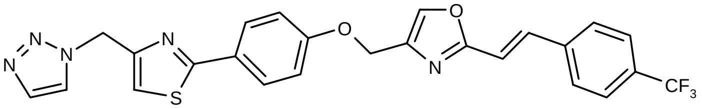	37
18	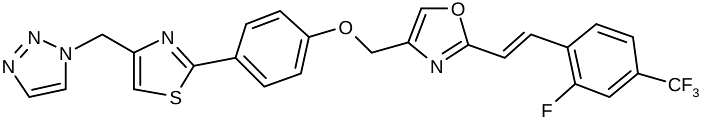	70
19	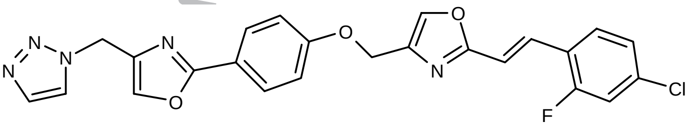	11
20	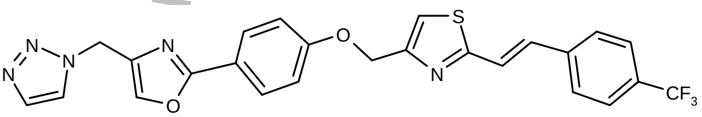	60

Table 2. Inhibition of HER2 phosphorylation by representative pentaflurosulfanyl derivatives of arylalkoxyoxazole-based HER2 tyrosine kinase inhibitors.

Compound	Structure	Percent inhibition of HER2 phosphorylation at 1 μM
21	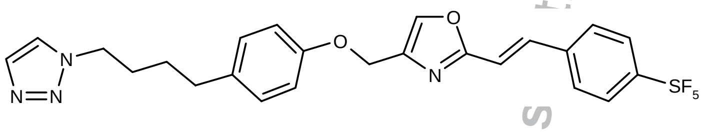	87.5
22	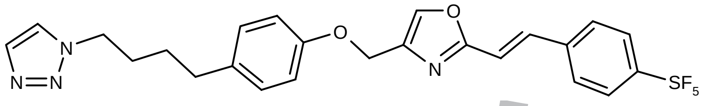	86.1
23	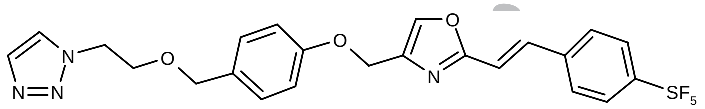	52.9
24	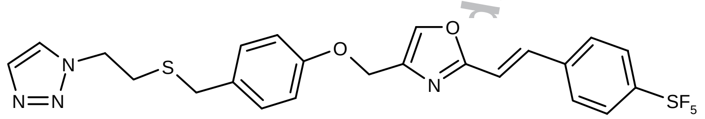	59.7
25	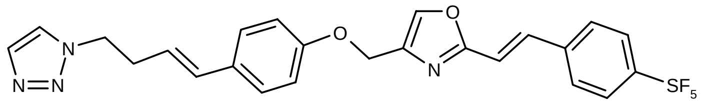	68.8
26	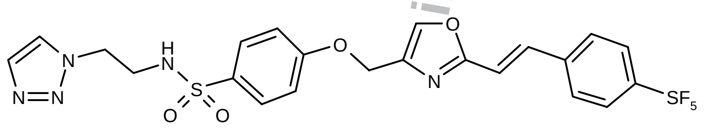	71.7
27	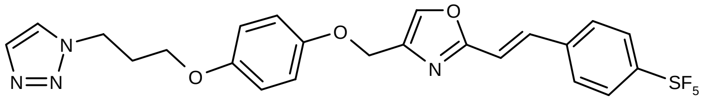	97.5
28	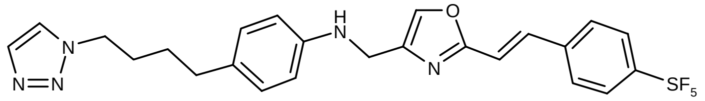	91.9

clinical development also show cross receptor activity. This phenomenon could be attributed to the high homology present in kinase domains of HER receptors. At this point of time, it is not clear that HER tyrosine kinase inhibitors that show either a broad activity spectrum (those that inhibit more than one receptor simultaneously) or receptor specificity yield an optimum therapeutic response with minimum or no toxic effects in clinical settings. Encouraging results show that clinically approved small-molecule tyrosine kinase inhibitors have a favorable safety profile and can be combined with other forms of chemotherapy or radiation therapy [30]. Lapatinib/GW-2016 (**Figure 3**) is a reversible dual HER2 and -1 tyrosine kinase inhibitor [31-33]. Lapatinib also inhibits p95ErbB2 (truncated HER2 receptor) kinase activity *in vitro* and in tumor xenografts [34]. The combination of lapatinib with trastuzumab showed synergistic effects on HER2-expressing and trastuzumab-treated cancer cell lines [35]. The combination of lapatinib with trastuzumab enhances apoptosis in HER2-overexpressing breast cancer cell lines [36]. A recently completed Phase III clinical trial showed that lapatinib significantly improves disease progression-free survival in patients with HER2-positive advanced and metastatic breast cancers whose disease had progressed following treatment with trastuzumab and other cancer therapies [37]. Regulatory approval from the FDA for clinical use of lapatinib is awaited. This quinazoline derivative represents a first-generation HER2-targeted small-molecule anticancer agent. Canertinib/CI-1033 (**Figure 3**) is an irreversible pan-HER tyrosine

Copyright of Informa Li in a dis nu s ly prohibited

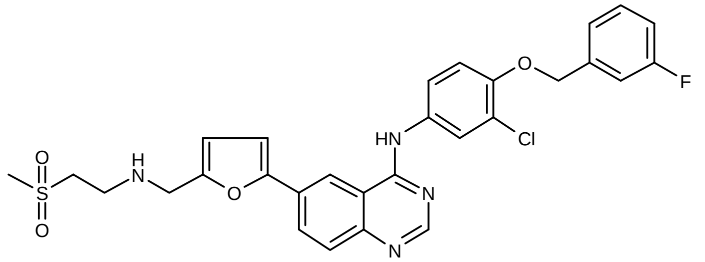

3 Lapatinib/Tykerb

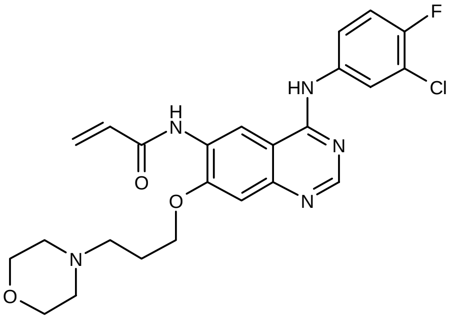

4 CI-1033

Figure 3. Structure of lapatinib and CI-1033, pan-HER tyrosine kinase inhibitors currently in clinical trials.

kinase inhibitor [38-41]. CI-1033 inhibits HER1, -2 and -4 kinase activities with similar potency. Phase II clinical trials of CI-1033 are under way. Recently, a number of small molecules with diverse structural scaffolds have been claimed as HER2 tyrosine kinase inhibitors in several patents. Recent advances in the design and discovery of small-molecule HER2 tyrosine kinase inhibitors are reviewed below.

2.2.1 *Quinazolines as HER tyrosine kinase inhibitors*

Quinazolines have been one of the most highly explored chemical classes in the discovery of HER tyrosine kinase inhibitors. Clinically used HER1 tyrosine kinase inhibitors gefitinib and erlotinib, and the most advanced HER2-targeted inhibitors, lapatinib and CI-1033, belong to the quinazoline class of compounds. These compounds have been designed to compete with ATP by binding at the ATP binding site on the HER tyrosine kinase domain. Several novel quinazoline HER tyrosine kinase inhibitors were disclosed in a recent patent [101]. Structures of some representative quinazolines are shown in **Figure 4**. Although the quinazoline core has been highly explored in the design of HER tyrosine kinase inhibitors, these novel compounds possess a unique hydrazinecarboximidamide substitution at the sixth position of the quinazoline core, thus making them different from previously reported quinazolines. These compounds inhibit HER1, -2 and -4 tyrosine kinase inhibitors [101]. They are also being claimed as serine, threonine and dual specific kinase inhibitors. However, details of receptor specific activities and *in vivo* anticancer activity profiles of compounds related to this patent are not described. Compounds presented in this patent are reported to inhibit HER tyrosine kinase activity with IC_{50} concentrations in the range of < 1 nM – 50 µM.

2.2.2 *Arylazole-based HER2 tyrosine kinase inhibitors*

Compounds containing an arylalkoxy oxazole or thiazole core are potent inhibitors of HER2 tyrosine kinase activity [102]. Structures of selected compounds along with their antiproliferative activities in A549 (human lung carcinoma) cells are given in **Table 1**. These compounds inhibited A549 cell proliferation at IC_{50} concentrations in the range of 7 – 70 nM. Compound **16** containing an arylalkoxy oxazole core inhibited cell growth at a concentration of 7 nM.

Several pentaflurosulfanyl derivatives of arylalkoxy oxazole core-containing compounds show significant inhibition of HER2 phosphorylation at a tested concentration of 1 µM [103]. The per cent inhibition of these compounds on HER2 phosphorylation is shown in **Table 2**. Arylazole (27) inhibited 97.5% of HER2 phosphorylation at a concentration of 1 µM, and is the most potent HER2 tyrosine kinase inhibitor from this series of compounds. Several structurally related compounds with the arylalkoxy oxazole core were also claimed as HER2 tyrosine kinase inhibitors [104]. These compounds show significant inhibition of HER2 phosphorylation in Calu3 tumor cells. Some of the selected compounds inhibited 70 – 86% of HER2 phosphorylation at 1 µM. Structures of representative compounds and their HER2 tyrosine kinase inhibitory activities are presented in **Table 3**.

Arylalkoxy oxazoles, in which a diazine moiety represents the aryl group, are also potent inhibitors of HER2 tyrosine kinase activity [105]. Structures of three representative compounds and their HER2 tyrosine kinase inhibitory activities are presented in **Table 4**. In addition, indole derivatives of arylazoles also inhibit HER tyrosine kinase and exhibit significant growth inhibition of HEK293 (human embryonic kidney) cells [106]. Structures of representative compounds and their anticancer activities are presented in **Table 5**. Furthermore, amide derivatives of arylazoles also inhibited HER2 phosphorylation at 1 µM and blocked HEK293 cell growth in the nanomolar range [107]. Structures of selected derivatives and their per cent inhibition of HER2 phosphorylation are presented in **Table 6**. Previously, several structurally similar arylalkoxy oxazoles were reported to show antidiabetic effects [42]. Some of these compounds show strong glucose lowering and lipid lowering effects in diabetic animal models. The antidiabetic effects of these compounds are shown to be connected to their potent agonistic activity on peroxisome proliferators-activated receptor-γ (PPARγ). Several structurally related arylalkoxy oxazoles containing a 2,4-thiazolidinedione or 2,4-oxazolidinedione ring substitution on the

Copyright of Informa UK Ltd. Printing and distributic ibited

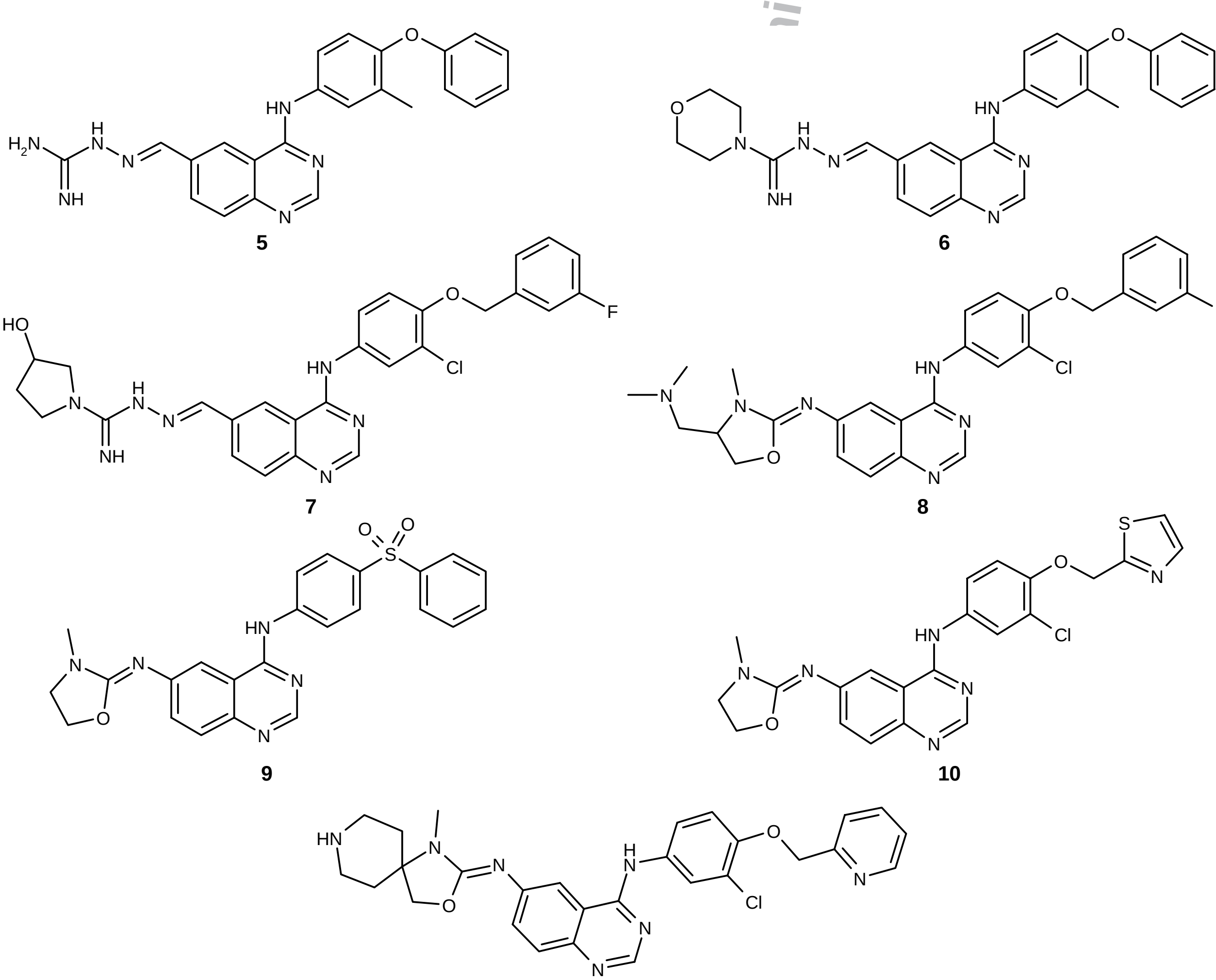

Figure 4. Representative quinazoline-based HER tyrosine kinase inhibitors.

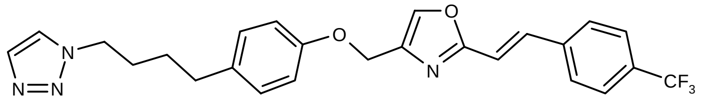

48 TAK 165

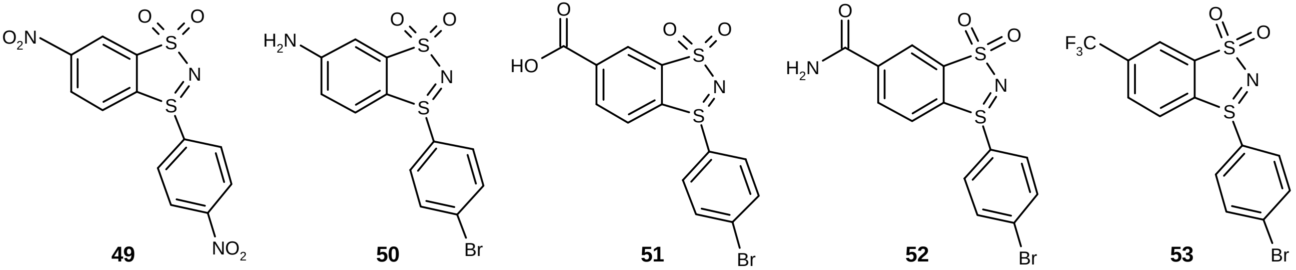

Figure 6. Representative benzodithiazole-based HER tyrosine kinase inhibitors.

Table 3. Inhibition of HER2 phosphorylation by representative arylazole-based HER2 tyrosine kinase inhibitors.

Compound	Structure	Percent inhibition of HER2 phosphorylation at 1 µM
29	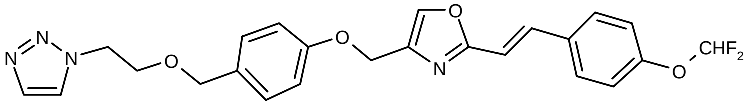	69.6
30	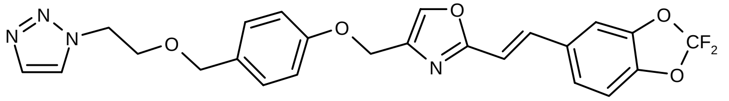	85.8
31	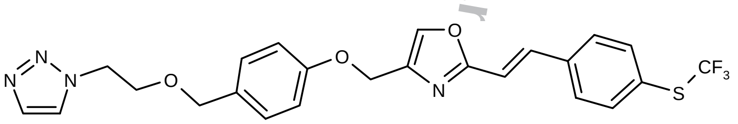	73.4
32	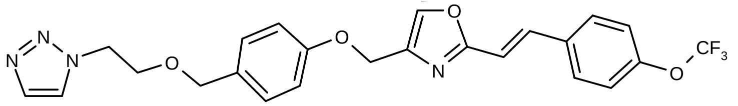	78.6

arylalkoxy group also show antidiabetic effects through their potent agonistic activity on PPARγ [43].

TAK-165 (**48**), an arylalkoxy oxazole-containing HER2 tyrosine kinase inhibitor, is presently under clinical studies (**Figure 5**). A Phase I study using a once-daily oral dosing regimen of TAK-165 in patients with advanced cancers that express HER2 has been completed [44]. TAK-165 selectively inhibits HER2 tyrosine kinase activity at an IC_{50} value of 6 nM and does not inhibit other types of tyrosine kinases up to 25,000 nM [45]. It was also shown to inhibit HER2 phosphorylation and its downstream PI3K and MAPK pathways *in vitro* in HER2-overexpressing BT474 breast cancer cells. TAK-165 also inhibited growth of HER2-expressing bladder, kidney and androgen-independent prostate cancers. This indicates a new hope for the possible therapeutic application of HER2 tyrosine kinase inhibitors in the treatment of cancers other than HER2-overexpressing breast cancers and, in particular, hormone-refractory prostate cancer. Details of the preclinical and clinical activity of the arylazole class of compounds are eagerly awaited. It is also interesting to note that TAK-165 inhibited HER2 phosphorylation in human rheumatoid synovial cells, indicating its therapeutic applications beyond cancer treatment [108].

2.2.3 *Benzo- and azabenzodithiazole-based HER tyrosine kinase inhibitors*

Several benzo- and azabenzodithiazoles were shown to inhibit HER1, -2 and -4 kinases with IC_{50} values of 0.001 – 25 µM [109]. However, details on receptor specific activity and anticancer properties of the claimed compounds are not disclosed. Structures of some representative compounds are shown in **Figure 6**. Previously, these compounds were not reported to show significant biological activity. However, compounds containing benzodithiazole were claimed as herbicides and plant growth regulators [110].

2.2.4 *Pyrrolopyridazine and pyrrolotriazine-based HER tyrosine kinase inhibitors*

Pyrrolopyridazine and pyrrolotriazine analogs are growing examples of HER tyrosine kinase inhibitors [111-117]. Selected compounds representing structural diversity are shown in **Figure 7** [111,112]. Pyrrolopyridazines are reported to inhibit HER tyrosine kinases with IC_{50} values of 0.001 – 25 µM. Some of these compounds are also shown to inhibit kinase activities of VEGF receptor (VEGFR)-2 and fibroblast growth factor receptor (FGFR)-1 receptors with IC_{50} values of ≤ 80 µM. Although several hundreds of compounds were claimed as HER tyrosine kinase inhibitors, details on receptor selective inhibitory activities and anticancer properties are not described. Apart from blocking phosphorylation activity of tyrosine kinase receptors, pyrrolopyridazines also inhibit activity of a variety of enzymes implicated in different disease conditions. For example, pyrrolopyridazine-containing compounds were reported to inhibit the activity of 15-lipoxygenase (15-LO) enzyme [46]. Considering the role of 15-LO in atherosclerosis, these compounds have potential therapeutic benefit in the treatment of atherosclerosis and other 15-LO-mediated disease conditions. Several pyrrolopyridazines are claimed as corticotropin-releasing factor (CRF) receptor antagonists [118,119]. These compounds are reported to possess therapeutic applications against CNS disorders such as anxiety and depression associated with deregulation or hypersecretion of the CRF receptor. Pyrrolopyridazine analogs also inhibit phosphodiesterase-4 (PDE-IV) and produc-

Copyright of Informa UK Ltd., Printing and distribution of this article is strictly prohibited

Table 4. Inhibition of HER2 phosphorylation by representative diazinealkoxy oxazole-based HER2 tyrosine kinase inhibitors.

Compound	Structure	Percent inhibition of HER2 phosphorylation at 1 μM
33	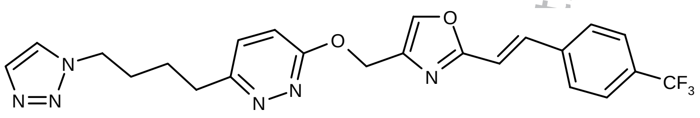	79.8
34	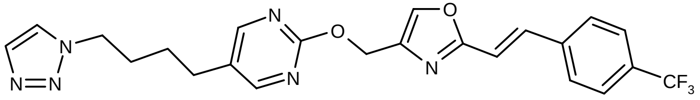	72.7
35	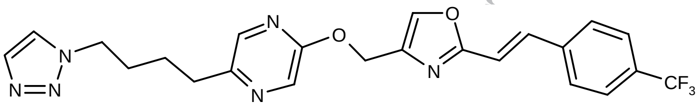	75.3

Table 5. Growth inhibitory activities of representative indole derivatives of arylazole-based HER2 tyrosine kinase inhibitors in HEK293 cells.

Compound	Structure	IC_{50} (nM)
36	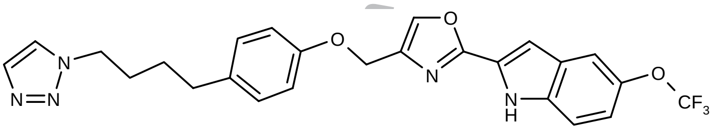	0.1
37	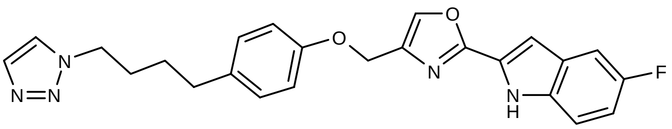	6.6
38	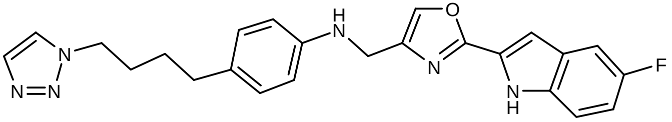	37
39	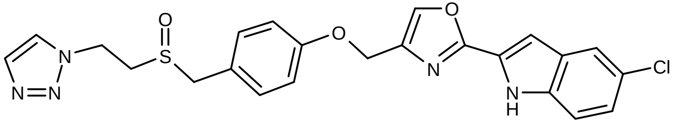	50
40	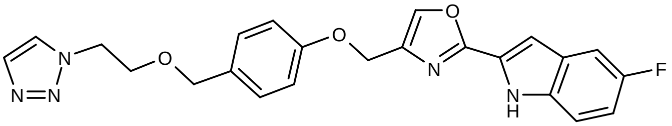	500

Table 6. Inhibition of HER2 phosphorylation by representative amide derivatives of arylazole-based HER2 tyrosine kinase inhibitors.

Compound	Structure	Percent inhibition of HER2 phosphorylation at 1 μM
41	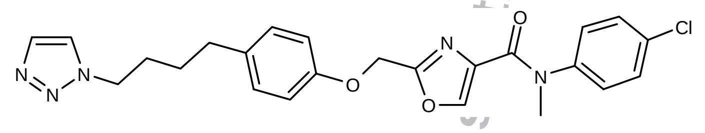	55 – 77
42	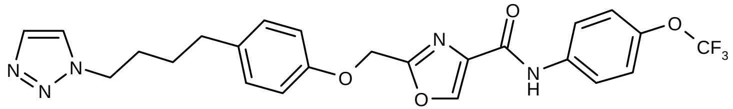	75
43	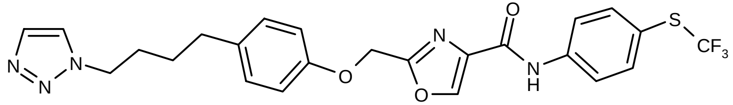	69
44	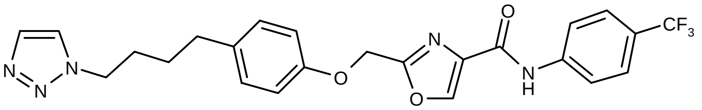	> 80
45	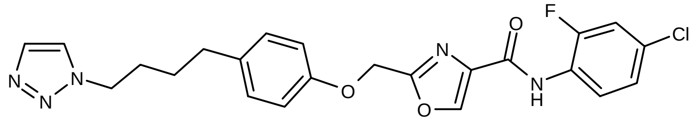	72
46	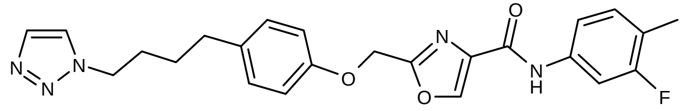	70
47	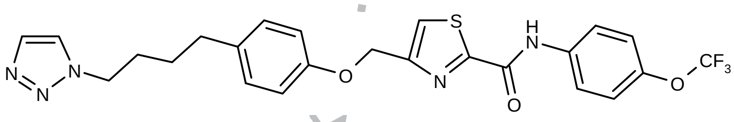	87

tion of TNF-α, which is important for the treatment of cancer, inflammatory and autoimmune diseases [120]. Recently, several pyrrolopyridazine core containing compounds were reported as MAPK/ERK (extracellular signal-regulated kinase) (MEK) inhibitors [47]. Some of the selected compounds inhibited MEK activity at < 1 μM and show cell growth inhibitory activity on human tumor cell lines HT29 and Colo205 at < 8 μM. In summary, the pyrrolopyridazine core is an excellent scaffold in designing of a variety of drugs, including inhibitors of HER family receptor tyrosine kinases.

The 4-aminopyrrolotriazine-containing compounds are interesting examples of HER family receptor tyrosine kinase inhibitors (**Figure 8**) [113]. Unfortunately, their HER tyrosine kinase inhibitory activities and anticancer properties have not been reported. The 4-aminopyrrolotriazine core has been considered as a novel template for the design of receptor tyrosine kinase inhibitors [48]. Several compounds containing the 4-aminopyrrolotriazine core have been reported as dual inhibitors of HER1 and -2 kinase inhibitors [49]. For example, BMS-599626 (72) is a potent inhibitor of HER1 and -2 kinase activity [50]. BMS-599626 also inhibited proliferation of a collection of diverse cancer cell lines that are dependent on signalling from either HER1 or -2. However, how BMS-599626 inhibits HER1 and -2 kinase activity and signalling, and the mechanism of binding to the receptors is not clearly understood. BMS-599626 acted as an ATP competitive inhibitor in HER1 inhibition. Interestingly, BMS-599626 inhibited HER2 with an ATP noncompetitive mechanism. Recently reported preclinical results project BMS-599626 as a promising candidate for further clinical development for cancers with HER1 and -2 overexpression.

ibited

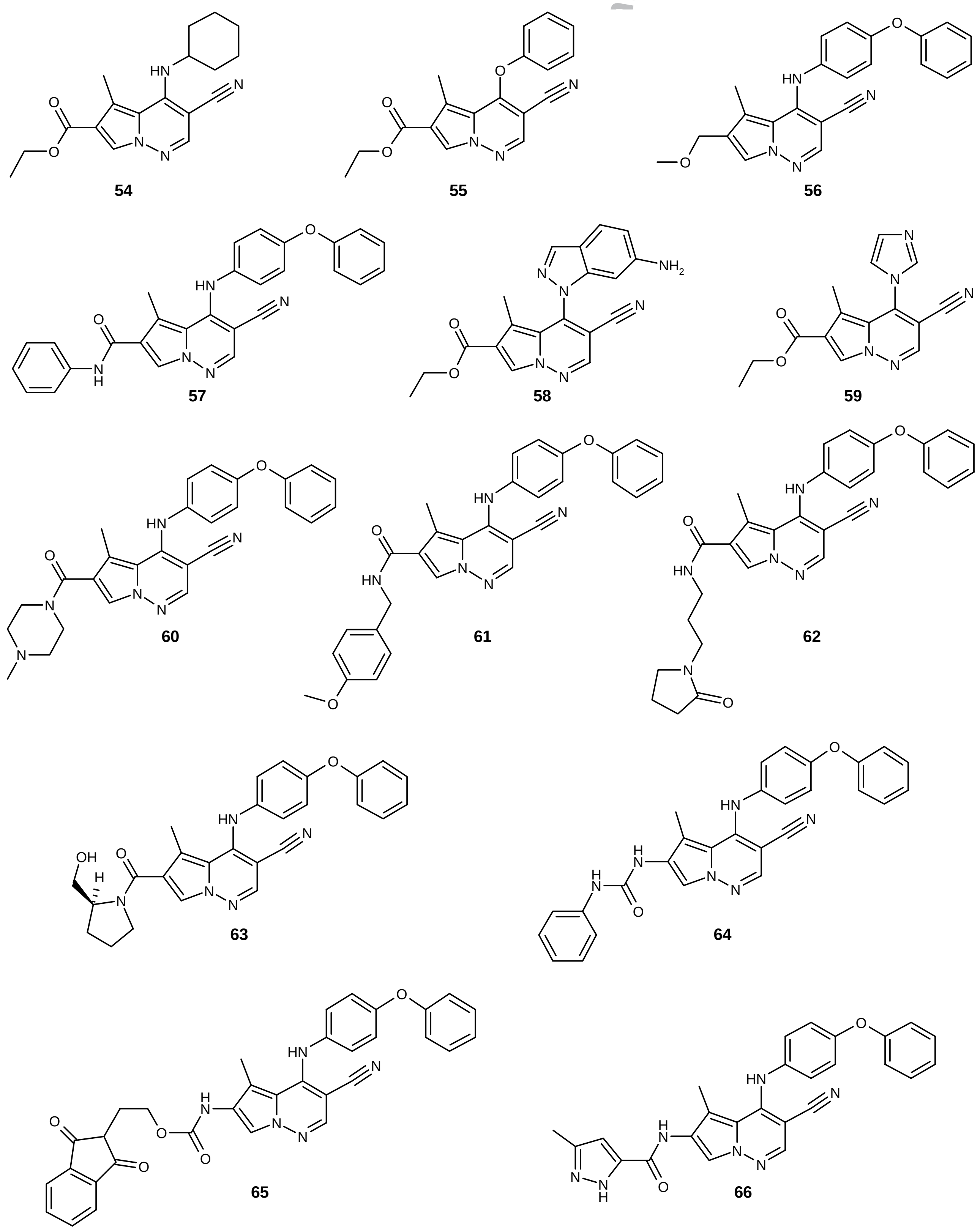
54
55
56
57
58
59
60
61
62
63
64
65
66

Copyr

Figure 7. Representative pyrrolopyridazine-based HER tyrosine kinase inhibitors.

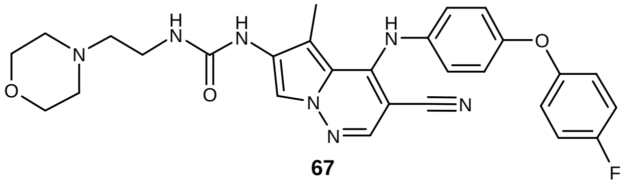

67

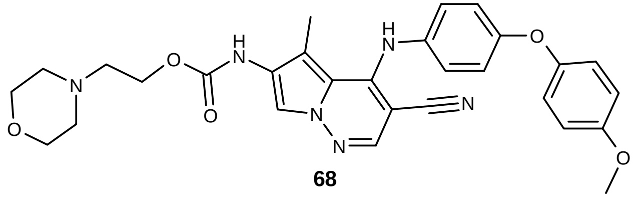

68

Figure 7. Representative pyrrolopyridazine-based HER tyrosine kinase inhibitors *(continued)*.

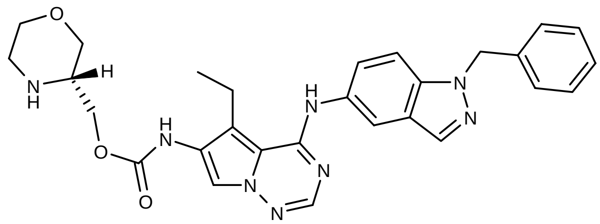

69

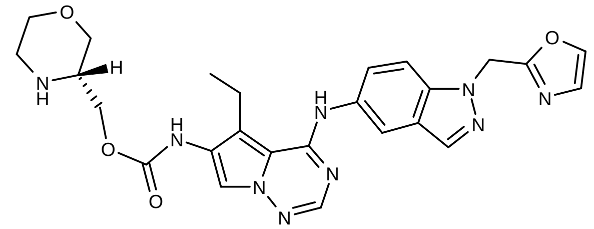

70

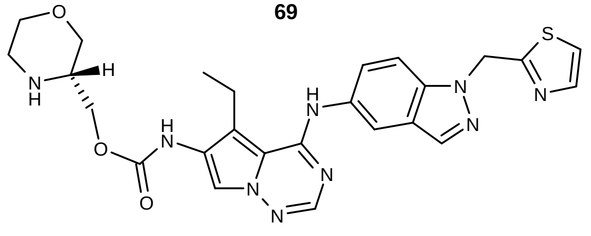

71

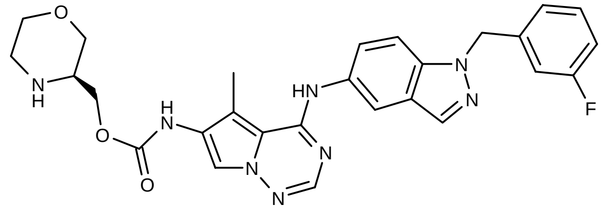

72 BMS-599626

Figure 8. Representative morpholinylmethyl ester darivatives of pyrrolotriazine-based HER tyrosine kinase inhibitors.

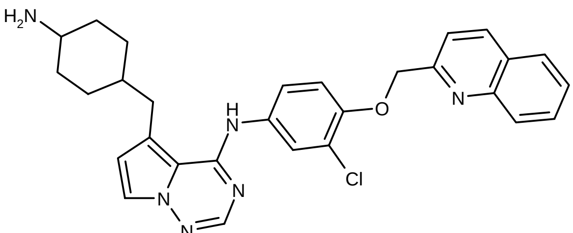

73

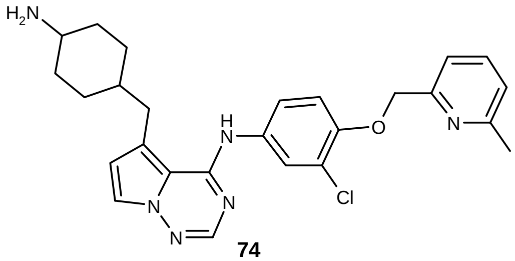

74

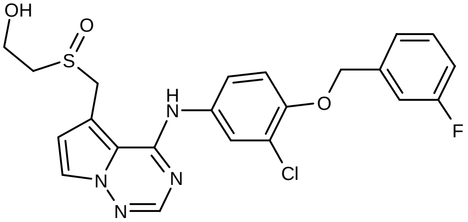

75

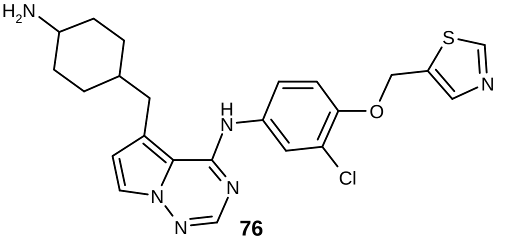

76

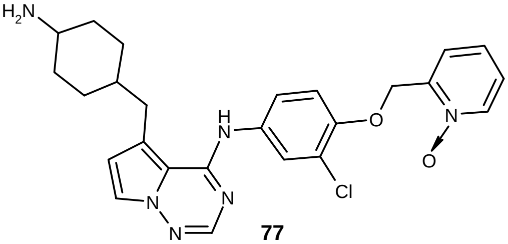

77

Figure 9. Substituted pyrrolotriazine-based HER tyrosine kinase inhibitors.

Selected structurally diverse 5-substituted 4-aminopyrrolotriazine HER tyrosine kinase inhibitors are shown in **Figure 9** [114]. Some of these compounds were reported to inhibit HER1, -2 and -4 kinases with IC_{50} values of 0.001 – 25 µM. Aminocyclohexyloxy derivatives of 4-aminopyrrolotriazines and other analogs are claimed as HER tyrosine kinase inhibitors [115,116]. Structures of representative aminocyclohexyloxy derivatives are shown in **Figure 10**. These compounds also inhibit receptor tyrosine kinases such as VEGFR2, FGFR1 and platelet-derived growth factor receptor in addition to HER family receptor kinases [116].

Several 5- and 6-substituted 4-aminopyrrolotriazine core-containing compounds are reported to inhibit VEGFR2 and FGFR1 kinases at < 100 nM [51,52]. Selected compounds show metabolic stability and acceptable pharmacokinetic profiles after oral administration in mice xenografts. Furthermore, some of these compounds are proposed to bind at the ATP binding site of VEGFR2 and form H-bonding interactions with amino acid residues from the hinge region. Several aminopiperidine and diazepan derivatives of 4-aminopyrrolotriazines are also reported as HER tyrosine kinase inhibitors. Three representative compounds are shown in **Figure 11**. As described above, 4-aminopyrrolotriazine analogs inhibit HER tyrosine kinases with IC_{50} values of 0.001 – 25 µM [117]. Moreover, the 4-aminopyrrolotriazine core is also considered as a lead template in the design of p38 kinase inhibitors for the treatment of inflammatory disorders and potentially other p38 kinase-mediated diseases [121].

2.2.5 *Pyrrolopyrimidine-based HER2 tyrosine kinase inhibitors*

Previously, pyrrolopyrimidine core-containing compounds were reported to inhibit HER tyrosine kinase activity [53,54]. Structures and HER2 tyrosine kinase inhibitory activities of some representative compounds are shown in **Figure 12** and **Table 7** [122]. Most of these compounds inhibited HER1 and -2 phosphorylation with IC_{50} values < 100 nM. In addition, several of these compounds also inhibit phosphorylation of VEGFR family members with IC_{50} values < 300 nM. Hence, they are considered as dual inhibitors of both HER and the VEGFR family of receptor tyrosine kinases. Additional analogs of pyrrolopyrimidines as inhibitors of HER, VEGFR, Bcr-Abl, c-Abl and c-Raf-1 kinases were also reported [123]. Three representative analogs are shown in **Figure 13**. Initially, pyrrolopyrimidines were developed as HER1 tyrosine kinase inhibitors. Nevertheless, now they are considered as dual HER1 and -2 inhibitors and also show considerable inhibition of phosphorylation of VEGFR and other kinases [54].

PK-I166 (**98**) is an example of the pyrrolopyrimidine HER tyrosine kinase inhibitors under advanced stages of clinical studies (**Figure 12**) [55]. PKI166 inhibits kinase activity of HER1 and -2 with IC_{50} values of 1 and 11 nM, respectively. PKI-166 inhibits EGF activated HER1 phosphorylation and activated HER1-mediated signalling with an IC_{50} value of 51 nM [54]. PKI-166 also inhibited HER2 autophosphorylation in two human breast cancer cell lines (SK-BR-3 and BT-474) with IC_{50} values of 0.1 – 1 µM. In cell-based assays, PKI-166 inhibited growth of HER1-overexpressing A431 and NCI-H596 cell lines and HER2-overexpresing SK-BR-3 and BT-474 cell lines. PKI-166 also blocks the growth of prostate cancer in mice in an androgen-dependent manner [56]. In nude mice implanted with human pancreatic carcinoma cells, PKI-166 treatment reduced tumor volume by 45%, and in combination with gemcitabine reduced tumor volume by 85%, whereas gemcitabine alone reduced tumor volume by only 59% [44]. In a recently completed Phase I study, PKI-166 was orally given to patients with advanced solid tumors. PKI-166 showed acceptable toxicity, safety and pharmacokinetic profiles. Dose-limiting transaminase elevations, diarrhea, skin rash, nausea and vomiting were the principal toxicities of PKI-166. Furthermore, the pharmacokinetic profile revealed that PKI-166 is orally bioavailable, quickly absorbed and showed a linear dose–response relationship without drug accumulation after multiple doses. Although there are no tumor responses observed with PKI-166 treatment, stable disease was observed in patients. Additional details on preclinical and clinical performance of PKI-166 are awaited.

2.3 Small-molecules targeting HER2 expression

HER2 receptor overexpression is associated with a variety of human cancers. HER2 overexpression is also connected to the aggressive nature of the disease and short survival times. Clinically approved HER2-specific anticancer therapeutics are targeted at elevated levels of the receptor. It seems that enhanced therapeutic benefits could be achieved through downregulation of HER2 by inhibiting HER2 gene expression in addition to targeting elevated levels of HER2 receptor that are already expressed. It has been demonstrated that HER2 overexpression is accomplished through gene duplication and increased transcription. Ets factor ESX (epithelial-restricted with serine box) is a transcription factor that activates the HER2 gene in breast cancers [57]. ESX is overexpressed in HER2-overexpressing breast cancers. It has been demonstrated that the interaction between ESX and another nuclear protein, Sur-2/DRIP130 (a Ras-linked subunit of the human mediator complex), is required for overexpression of HER2 in malignant breast cancers. Efficient inhibition of this interaction reduces HER2 expression. Recently, a number of adamanolol derivatives were claimed as inhibitors of Sur-2 [124,125]. Several representative analogs are shown in **Figure 14**. These peptidomimetic small molecules were claimed to inhibit expression of the HER2 receptor through disrupting ESX–Sur-2 interactions. Several of these compounds inhibited ESX–Sur-2 interactions at IC_{50} values in the range of 3 – 100 µM. Limited structure– activity relationships on some of the adamanolol analogs are also described.

2.4 Small-molecule inhibitors of HER2 shedding

HER2 undergoes a slow proteolytic shedding of its extracellular domain in cultured cells. The soluble HER2 extracellular

Printing and distribution strictly prohibited
Copyright of Informa UK Ltd.

ibited

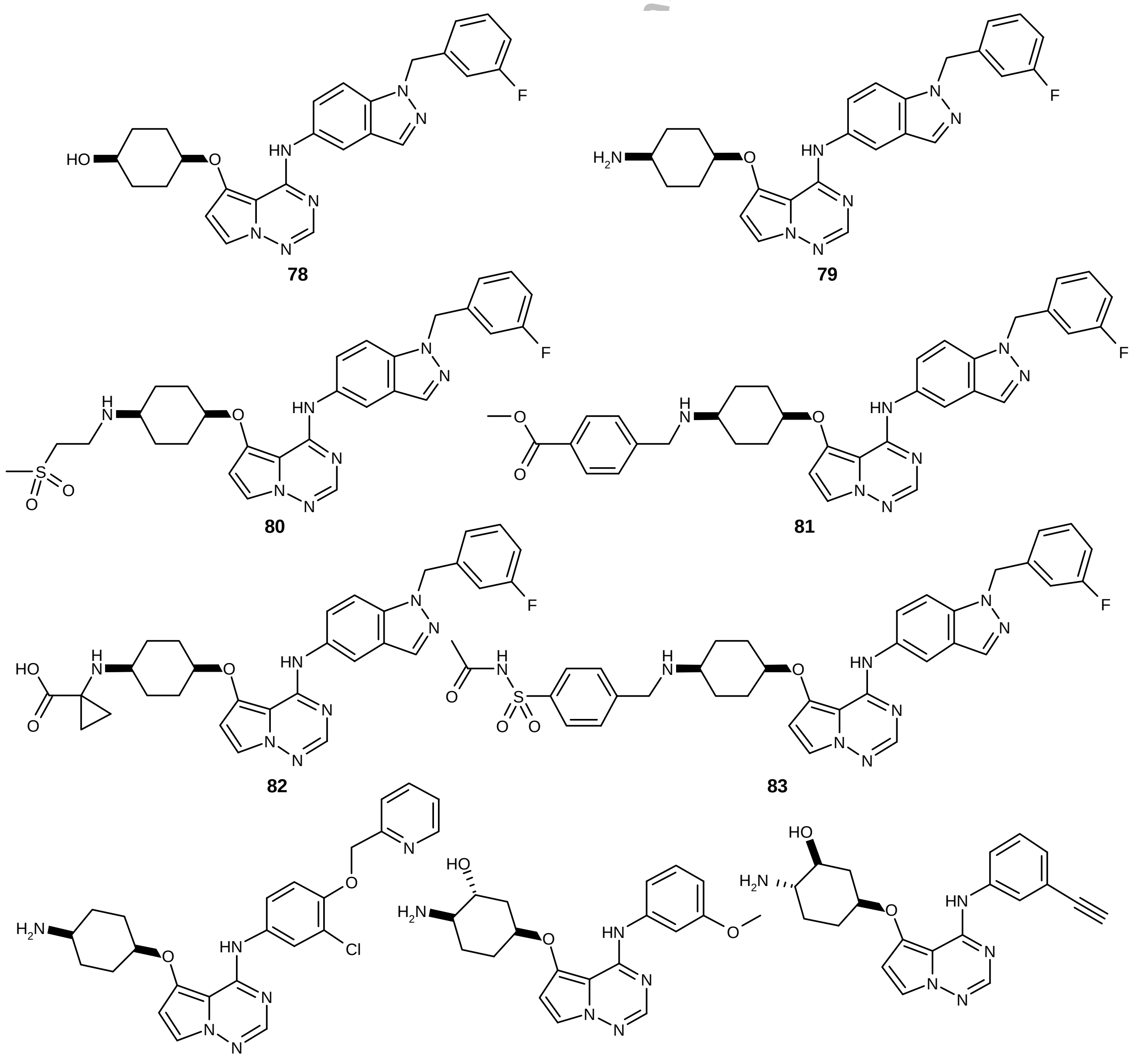

78

79

80

81

82

83

84

85

86

Figure 10. Representative aminocyclohexyloxy derivatives of pyrrolotriazine-based HER tyrosine kinase inhibitors.

orma

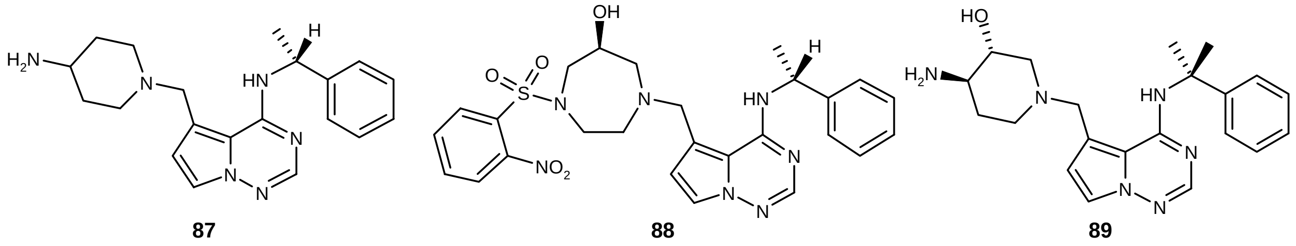

87

88

89

Figure 11. Representative aminopiperidine and diazepan derivatives of pyrrolotriazine-based HER tyrosine kinase inhibitors.

Copy

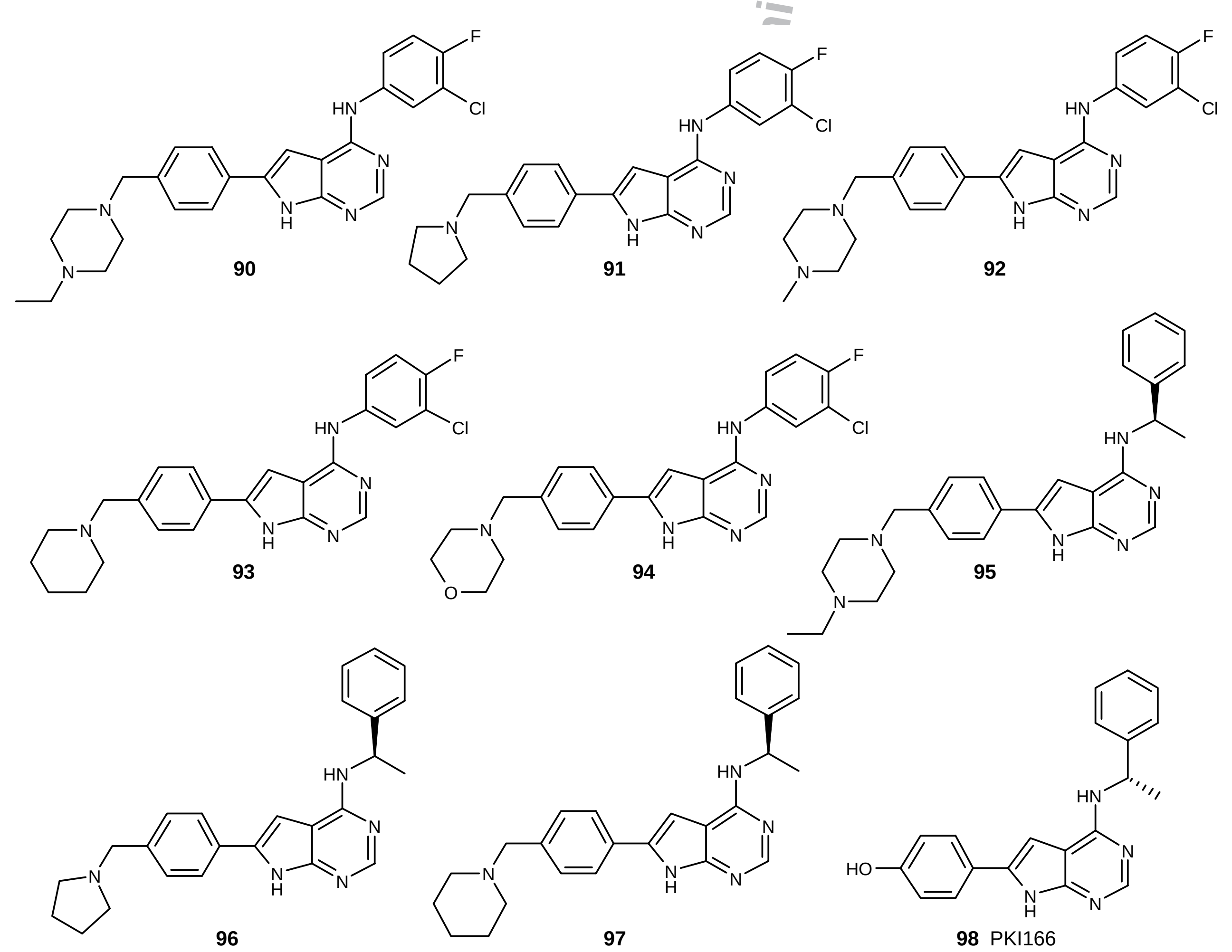

Figure 12. Representative pyrrolopyrimidine-based HER2 kinase inhibitors.

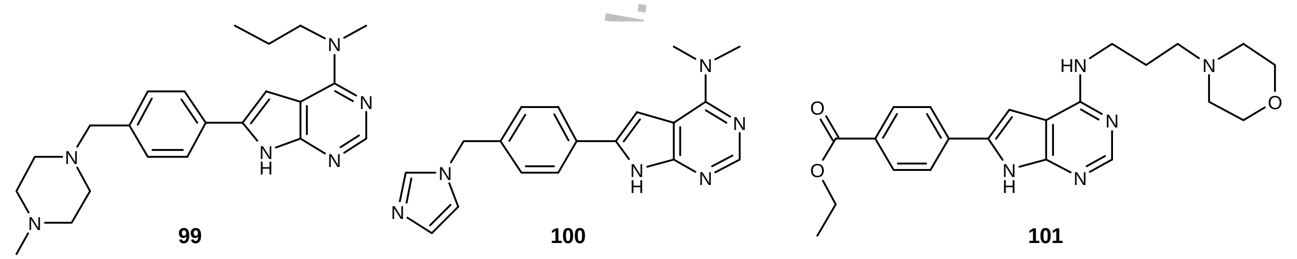

Figure 13. Representaive analogs of pyrrolopyrimidine-based HER2 kinase inhibitors.

domain was found in serum of patients with advanced breast cancer, where it correlates with a decreased response to therapy. In HER2-expressing clinically poor responsive cancers, the receptor is processed by an unknown matrix metalloprotease to yield a truncated membrane associated receptor (also known as p95HER2) and a soluble extracellular domain [58-60]. Interestingly, like other HER family receptors, particularly HER1, loss of the ligand binding extracellular domain renders the HER2 intracellular membrane associated domain a constitutively active tyrosine kinase. Furthermore, the increased level of p95HER2 in HER2-expressing breast cancers is correlated with a reduced responsiveness to treatment and a decreased overall clinical outcome [61]. On the basis of these observations it has been hypothesized that the processing of the HER2 extracelluar domain generates a constitutively active receptor kinase that can continuously deliver growth and survival signals to cancer cells. A method to disrupt shedding of HER2 extracellular domain using matrix metalloprotease antagonists has been claimed [126]. In a proof of concept study using GM-6001 (**107**), a

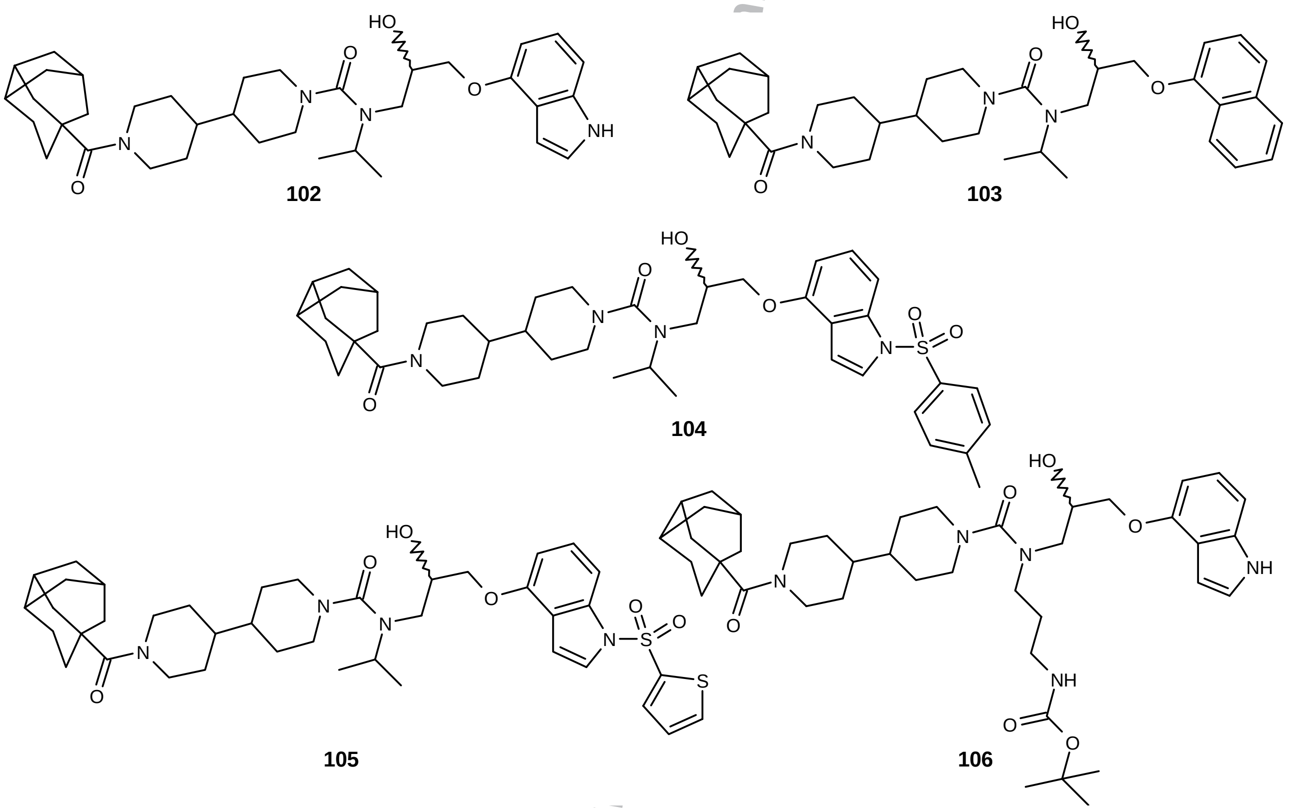

Figure 14. Reprsentative peptidomimetic small-molecule inhibitors of HER2 expression.

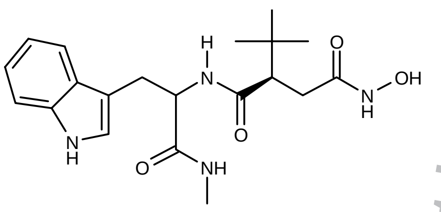

Figure 15. Structre of GM6001, a broad spectrum matrix metalloprotease antagonist that inhibits HER2 shedding.

Table 7. Inhibition of tyrosine kinase activity of HER2 and HER1 by the pyrrolopyrimidine analogs 90 – 97.

Compound	**IC$_{50}$ (µM)**	
	HER2	***HER1***
90	0.008	0.0031
91	0.0072	0.0031
92	0.0067	0.0031
93	0.005	0.007
94	0.0094	0.0024
95	0.005	0.0043
96	0.005	0.0047
97	0.0085	0.0063

matrix metalloprotease antagonist, particularly a MMP-15 antagonist, reduced shed HER2 extracellular domain serum levels (Figure 15). A diagnostic method to assess elevated level of MMP-15 in patients with HER2-expressing cancer is also claimed [126]. The elevated level of MMP-15 in HER2-expressing cancer indicates that the patient has an elevated p95HER2 or shed HER2 extracellular serum level or will have a poor clinical outcome. The small-molecule compounds that disrupt shedding of the HER2 extracellular domain and generation of a constitutively active intracellular receptor kinase represent a novel class of anticancer therapeutics targeting HER2-expressing cancers.

3. Expert opinion

The HER family of receptors are validated anticancer drug targets. Profound clinical performance of well-designed first-generation small-molecule and humanized mAb therapeutics signifies the rationale behind targeting the HER family of receptors. Several investigational drugs targeting members of the HER family are in various stages of clinical development. This indicates the intensiveness of drug discovery efforts targeting HER family receptors that mediate complex and vital signalling pathways. The long-term consequences of disruption of signalling pathways mediated by receptor tyrosine kinases using small-molecule or humanized mAbs have yet to be completely understood. For example, a recent report on cardiotoxic effects of imatinib mesylate,

Copyright of Informa UK Ltd. Print... ...ibited

the first Bcr-Abl kinase inhibitor to be approved for use in the clinic, highlight the surprising outcomes that may arise from disruption of kinase mediated signalling mechanisms [62]. Growing understanding of the structural details of HER family receptor kinase domains will allow the design of highly selective inhibitors targeting either active or inactive conformations of individual receptors. Finally, considering the prominent role of the HER2 signalling pathway in cancer, inhibitors of expression and shedding of HER2 will also provide an opportunity to study the consequences of selective inhibition of HER2.

Acknowledgements

This work was financially supported by funds from DOD Concept Award to Nouri Neamati

Copyright Informa UK Ltd. Printing and distribution strictly prohibited

Bibliography

1. SCHLESSINGER J: Cell signaling by receptor tyrosine kinases. *Cell* (2000) **103**(2):211-225.
2. WELLS A: EGF receptor. *Int. J. Biochem. Cell Biol.* (1999) **31**(6):637-643.
3. GUY PM, PLATKO JV, CANTLEY LC, CERIONE RA, CARRAWAY KL III: Insect cell-expressed p180erbB3 possesses an impaired tyrosine kinase activity. *Proc. Natl. Acad. Sci. USA* (1994) **91**(17):8132-8136.
4. JONES JT, AKITA RW, SLIWKOWSKI MX: Binding specificities and affinities of egf domains for ErbB receptors. *FEBS Lett.* (1999) **447**(2-3):227-231.
5. GULLICK WJ: The type 1 growth factor receptors and their ligands considered as a complex system. *Endocr. Relat. Cancer* (2001) **8**(2):75-82.
6. CHO HS, MASON K, RAMYAR KX *et al.*: Structure of the extracellular region of HER2 alone and in complex with the herceptin Fab. *Nature* (2003) **421**(6924):756-760.

•• **The first co-crystal structure of HER2 in complex with herceptin Fab.**

7. GARRETT TP, MCKERN NM, LOU M *et al.*: The crystal structure of a truncated ErbB2 ectodomain reveals an active conformation, poised to interact with other ErbB receptors. *Mol. Cell* (2003) **11**(2):495-505.

•• **The crystal structure reveals active conformation of HER2 extracellular domain.**

8. ALIMANDI M, ROMANO A, CURIA MC *et al.*: Cooperative signaling of ErbB3 and ErbB2 in neoplastic transformation and human mammary carcinomas. *Oncogene* (1995) **10**(9):1813-1821.
9. BLENIS J: Signal transduction via the MAP kinases: proceed at your own RSK. *Proc. Natl. Acad. Sci. USA* (1993) **90**(13):5889-5892.
10. BURGERING BM, COFFER PJ: Protein kinase B (c-Akt) in phosphatidylinositol-3-OH kinase signal transduction. *Nature* (1995) **376**(6541):599-602.
11. OLAYIOYE MA, NEVE RM, LANE HA, HYNES NE: The ErbB signaling network: receptor heterodimerization in development and cancer. *Embo. J.* (2000) **19**(13):3159-3167.
12. ZHANG W, LIU HT: MAPK signal pathways in the regulation of cell proliferation in mammalian cells. *Cell Res.* (2002) **12**(1):9-18.
13. CANTLEY LC: The phosphoinositide 3-kinase pathway. *Science* (2002) **296**(5573):1655-1657.
14. MOSCATELLO DK, HOLGADO-MADRUGA M, EMLET DR, MONTGOMERY RB, WONG AJ: Constitutive activation of phosphatidylinositol 3-kinase by a naturally occurring mutant epidermal growth factor receptor. *J. Biol. Chem.* (1998) **273**(1):200-206.
15. HYNES NE, LANE HA: ERBB receptors and cancer: the complexity of targeted inhibitors. *Nat. Rev. Cancer* (2005) **5**(5):341-354.

• **Details rationale and complexity of HER family of receptors as anticancer drug targets.**

16. SLAMON DJ, CLARK GM, WONG SG *et al.*: Human breast cancer: correlation of relapse and survival with amplification of the HER-2/neu oncogene. *Science* (1987) **235**(4785):177-182.
17. SLAMON DJ, GODOLPHIN W, JONES LA *et al.*: Studies of the HER-2/neu proto-oncogene in human breast and ovarian cancer. *Science* (1989) **244**(4905):707-712.
18. KAPITANOVIC S, RADOSEVIC S, KAPITANOVIC M *et al.*: The expression of p185(HER-2/neu) correlates with the stage of disease and survival in colorectal cancer. *Gastroenterology* (1997) **112**(4):1103-1113.
19. NAHTA R, ESTEVA FJ: HER-2-targeted therapy: lessons learned and future directions. *Clin. Cancer Res.* (2003) **9**(14):5078-5084.
20. SLIWKOWSKI MX, LOFGREN JA, LEWIS GD *et al.*: Nonclinical studies addressing the mechanism of action of trastuzumab (Herceptin). *Semin. Oncol.* (1999) **26**(4 Suppl. 12):60-70.
21. DREBIN JA, LINK VC, STERN DF, WEINBERG RA, GREENE MI: Down-modulation of an oncogene protein product and reversion of the transformed phenotype by mAbs. *Cell* (1985) **41**(3):697-706.
22. IZUMI Y, XU L, DI TOMASO E, FUKUMURA D, JAIN RK: Tumour biology: herceptin acts as an anti-angiogenic cocktail. *Nature* (2002) **416**(6878):279-280.
23. PICCART-GEBHART MJ, PROCTER M, LEYLAND-JONES B *et al.*: Trastuzumab after adjuvant chemotherapy in HER2-positive breast cancer. *N. Engl. J. Med.* (2005) **353**(16):1659-1672.

• **The first adjuvant clinical trials show that treatment with herceptin after adjuvant chemotherapy improves disease-free survival among women with HER2 positive breast cancer.**

24. AGUS DB, AKITA RW, FOX WD *et al.*: Targeting ligand-activated ErbB2 signaling inhibits breast and prostate tumor growth. *Cancer Cell* (2002) **2**(2):127-137.
25. FRANKLIN MC, CAREY KD, VAJDOS FF *et al.*: Insights into ErbB signaling from the structure of the ErbB2-pertuzumab complex. *Cancer Cell* (2004) **5**(4):317-328.

• **Co-crystal structure of HER2 in a complex with antigen binding fragment of pertuzumab.**

26. RABINDRAN SK: Antitumor activity of HER-2 inhibitors. *Cancer Lett.* (2005) **227**(1):9-23.

•• **Reviews progress of anticancer therapeutics under development targeting HER2 and other HER family of receptors.**

27. MOULDER SL, YAKES FM, MUTHUSWAMY SK *et al.*: Epidermal growth factor receptor (HER1) tyrosine kinase inhibitor ZD1839 (Iressa) inhibits HER2/neu (erbB2)-overexpressing breast cancer cells *in vitro* and *in vivo*. *Cancer Res.* (2001) **61**(24):8887-8895.

28. MOASSER MM, BASSO A, AVERBUCH SD, ROSEN N: The tyrosine kinase inhibitor ZD1839 ("Iressa") inhibits HER2-driven signaling and suppresses the growth of HER2-overexpressing tumor cells. *Cancer Res.* (2001) **61**(19):7184-7188.

29. ANDERSON NG, AHMAD T, CHAN K, DOBSON R, BUNDRED NJ: ZD1839 (Iressa), a novel epidermal growth factor receptor (EGFR) tyrosine kinase inhibitor, potently inhibits the growth of EGFR-positive cancer cell lines with or without ErbB2 overexpression. *Int. J. Cancer* (2001) **94**(6):774-782.

30. ARORA A, SCHOLAR EM: Role of tyrosine kinase inhibitors in cancer therapy. *J. Pharmacol. Exp. Ther.* (2005) **315**(3):971-979.

31. XIA W, MULLIN RJ, KEITH BR *et al.*: Anti-tumor activity of GW572016: a dual tyrosine kinase inhibitor blocks EGF activation of EGFR/ErbB2 and downstream Erk1/2 and AKT pathways. *Oncogene* (2002) **21**(41):6255-6263.

32. RUSNAK DW, LACKEY K, AFFLECK K *et al.*: The effects of the novel, reversible epidermal growth factor receptor/ErbB-2 tyrosine kinase inhibitor, GW2016, on the growth of human normal and tumor-derived cell lines *in vitro* and *in vivo*. *Mol. Cancer Ther.* (2001) **1**(2):85-94.

33. BENCE AK, ANDERSON EB, HALEPOTA MA *et al.*: Phase I pharmacokinetic studies evaluating single and multiple doses of oral GW572016, a dual EGFR-ErbB2 inhibitor, in healthy subjects. *Invest. New Drugs* (2005) **23**(1):39-49.

34. XIA W, LIU LH, HO P, SPECTOR NL: Truncated ErbB2 receptor (p95ErbB2) is regulated by heregulin through heterodimer formation with ErbB3 yet remains sensitive to the dual EGFR/ErbB2 kinase inhibitor GW572016. *Oncogene* (2004) **23**(3):646-653.

35. KONECNY GE, PEGRAM MD, VENKATESAN N *et al.*: Activity of the dual kinase inhibitor lapatinib (GW572016) against HER-2-overexpressing and trastuzumab-treated breast cancer cells. *Cancer Res.* (2006) **66**(3):1630-1639.

•• **Reports anticancer activity of lapatinib in HER2 expressing and herceptin-treated human breast cancer cells**

36. XIA W, GERARD CM, LIU L *et al.*: Combining lapatinib (GW572016), a small molecule inhibitor of ErbB1 and ErbB2 tyrosine kinases, with therapeutic anti-ErbB2 antibodies enhances apoptosis of ErbB2-overexpressing breast cancer cells. *Oncogene* (2005) **24**(41):6213-6221.

37. GEYER CE, CAMERON D, LINDQUIST D *et al.*: A Phase III randomized, open-label, international study comparing lapatinib and capecitabine vs capacitabine in women with refractory advanced or metastatic breast cancer (EGF100151). *2006 American Society of Clinical Oncology Annual Meeting.* Atlanta, Georgia (2006).

38. SMAILL JB, PALMER BD, REWCASTLE GW *et al.*: Tyrosine kinase inhibitors. 15. 4-(Phenylamino)quinazoline and 4-(phenylamino)pyrido[d]pyrimidine acrylamides as irreversible inhibitors of the ATP binding site of the epidermal growth factor receptor. *J. Med. Chem.* (1999) **42**(10):1803-1815.

39. FRY DW, BRIDGES AJ, DENNY WA *et al.*: Specific, irreversible inactivation of the epidermal growth factor receptor and ErbB2, by a new class of tyrosine kinase inhibitor. *Proc. Natl. Acad. Sci. USA* (1998) **95**(20):12022-12027.

40. SIMON GR, GARRETT CR, OLSON SC *et al.*: Increased bioavailability of intravenous versus oral CI-1033, a pan erbB tyrosine kinase inhibitor: results of a Phase I pharmacokinetic study. *Clin. Cancer Res.* (2006) **12**(15):4645-4651.

41. GARLAND LL, HIDALGO M, MENDELSON DS *et al.*: A Phase I clinical and pharmacokinetic study of oral CI-1033 in combination with docetaxel in patients with advanced solid tumors. *Clin. Cancer Res.* (2006) **12**(14 Pt 1):4274-4282.

42. MOMOSE Y, MAEKAWA T, ODAKA H, IKEDA H, SOHDA T: Novel 5-substituted-1*H*-tetrazole derivatives as potent glucose and lipid lowering agents. *Chem. Pharm. Bull.* (Tokyo) (2002) **50**(1):100-111.

43. MOMOSE Y, MAEKAWA T, YAMANO T *et al.*: Novel 5-substituted 2,4-thiazolidinedione and 2,4-oxazolidinedione derivatives as insulin sensitizers with antidiabetic activities. *J. Med. Chem.* (2002) **45**(7):1518-1534.

44. SRIDHAR SS, SEYMOUR L, SHEPHERD FA: Inhibitors of epidermal-growth-factor receptors: a review of clinical research with a focus on non-small-cell lung cancer. *Lancet Oncol.* (2003) **4**(7):397-406.

45. NAGASAWA J, MIZOKAMI A, KOSHIDA K *et al.*: Novel HER2 selective tyrosine kinase inhibitor, TAK-165, inhibits bladder, kidney and androgen-independent prostate cancer *in vitro* and *in vivo*. *Int. J. Urol.* (2006) **13**(5):587-592.

• **Preclinical evaluation of selective HER2 tyrosine kinase inhibitor.**

46. GUNDERSEN LL, MALTERUD KE, NEGUSSIE AH *et al.*: Indolizines as novel potent inhibitors of 15-lipoxygenase. *Bioorg. Med. Chem.* (2003) **11**(24):5409-5415.

47. CHEN Z, KIM SH, BARBOSA SA *et al.*: Pyrrolopyridazine MEK inhibitors. *Bioorg. Med. Chem. Lett* (2006) **16**(3):628-632.

48. HUNT JT, MITT T, BORZILLERI R *et al.*: Discovery of the pyrrolo[2,1-f][1,2,4] triazine nucleus as a new kinase inhibitor template. *J. Med. Chem.* (2004) **47**(16):4054-4059.

49. FINK BE, VITE GD, MASTALERZ H *et al.*: New dual inhibitors of EGFR and HER2 protein tyrosine kinases. *Bioorg. Med. Chem. Lett* (2005) **15**(21):4774-4779.

50. WONG TW, LEE FY, YU C *et al.*: Preclinical antitumor activity of BMS-599626, a pan-HER kinase inhibitor that inhibits HER1/HER2 homodimer and heterodimer signaling. *Clin. Cancer Res.* (2006) **12**(20 Pt 1):6186-6193.

51. BORZILLERI RM, ZHENG X, QIAN L *et al.*: Design, synthesis and evaluation of orally active 4-(2,4-difluoro-5-(methoxycarbamoyl)phenylamino)pyrrolo[2,1-f][1,2,4]triazines as dual vascular endothelial growth factor receptor-2 and fibroblast growth factor receptor-1 inhibitors. *J. Med. Chem.* (2005) **48**(12):3991-4008.

52. BORZILLERI RM, CAI ZW, ELLIS C *et al.*: Synthesis and SAR of 4-(3-hydroxyphenylamino)pyrrolo[2,1-f][1,2,4]triazine based VEGFR-2 kinase inhibitors. *Bioorg. Med. Chem. Lett.* (2005) **15**(5):1429-1433.

Copyright of Informa UK Ltd. - Printing and distribution strictly prohibited

53. TRAXLER PM, FURET P, METT H *et al.*: 4-(Phenylamino)pyrrolopyrimidines: potent and selective, ATP site directed inhibitors of the EGF-receptor protein tyrosine kinase. *J. Med. Chem.* (1996) **39**(12):2285-2292.
54. TRAXLER P, BOLD G, BUCHDUNGER E *et al.*: Tyrosine kinase inhibitors: from rational design to clinical trials. *Med. Res. Rev.* (2001) **21**(6):499-512.
55. HOEKSTRA R, DUMEZ H, ESKENS FA *et al.*: Phase I and pharmacologic study of PKI166, an epidermal growth factor receptor tyrosine kinase inhibitor, in patients with advanced solid malignancies. *Clin. Cancer Res.* (2005) **11**(19 Pt 1):6908-6915.
56. MELLINGHOFF IK, TRAN C, SAWYERS CL: Growth inhibitory effects of the dual ErbB1/ErbB2 tyrosine kinase inhibitor PKI-166 on human prostate cancer xenografts. *Cancer Res.* (2002) **62**(18):5254-5259.
57. CHANG CH, SCOTT GK, KUO WL *et al.*: ESX: a structurally unique Ets overexpressed early during human breast tumorigenesis. *Oncogene* (1997) **14**(13):1617-1622.
58. LIN YZ, CLINTON GM: A soluble protein related to the HER-2 proto-oncogene product is released from human breast carcinoma cells. *Oncogene* (1991) **6**(4):639-643.
59. PUPA SM, MENARD S, MORELLI D *et al.*: The extracellular domain of the c-erbB-2 oncoprotein is released from tumor cells by proteolytic cleavage. *Oncogene* (1993) **8**(11):2917-2923.
60. KANDL H, SEYMOUR L, BEZWODAW R: Soluble c-erbB-2 fragment in serum correlates with disease stage and predicts for shortened survival in patients with early-stage and advanced breast cancer. *Br. J. Cancer* (1994) **70**(4):739-742.
61. SAEZ R, MOLINA MA, RAMSEY EE *et al.*: p95HER-2 predicts worse outcome in patients with HER-2-positive breast cancer. *Clin. Cancer Res.* (2006) **12**(2):424-431.
62. KERKELA R, GRAZETTE L, YACOBI R *et al.*: Cardiotoxicity of the cancer therapeutic agent imatinib mesylate. *Nat. Med.* (2006) **12**(8):908-916.

•• **Reports cardiotoxicity of the first small-molecule tyrosine kinase inhibitor to be used in clinic.**

Patents

101. HOGAN & HARTSON LLP: US20050101616 (2005).
102. HOFFMANN-LA ROCHE, INC.: WO2005040158 (2005).
103. HOFFMANN-LA ROCHE, INC.: US20050197370 (2005).
104. HOFFMANN-LA ROCHE, INC.: US20050209290 (2005).
105. HOFFMANN-LA ROCHE, INC.: US20050222228 (2005).
106. HOFFMANN-LA ROCHE, INC.: US20060063812 (2006).
107. HOFFMANN-LA ROCHE, INC.: WO2006053778 (2006).
108. TAKEDA CHEMICAL INDUSTRIES LTD: JP2004161660 (2004).
109. BRISTAL-MYERS SQUIBB COMPANY: US20050101646 (2005).
110. DU PONT DE NEMOURS EI & CO., USA: US86868239 (1987).
111. BRISTAL-MYERS SQUIBB COMPANY: WO2003082208 (2003).
112. BRISTAL-MYERS SQUIBB COMPANY: US2004209886 (2004).
113. BRISTAL-MYERS SQUIBB COMPANY: WO2005058245 (2005).
114. BRISTAL-MYERS SQUIBB COMPANY: WO2005065266 (2005).
115. BRISTAL-MYERS SQUIBB COMPANY: WO2005066176 (2005).
116. BRISTAL-MYERS SQUIBB COMPANY: WO2006007468 (2006).
117. BRISTAL-MYERS SQUIBB COMPANY: US20060089358 (2006).
118. PFIZER INC., USA: US2004204414 (2004).
119. PHARMACIA & UPJOHN COMPANY, LLC, USA: WO2004099213 (2004).
120. ASTELLAS PHARMA, INC., JAPAN: WO2006004191 (2006).
121. BRISTAL-MYERS SQUIBB COMPANY: US2006019928 (2006).
122. NOVARTIS: US20040248911 (2004).
123. NOVARTIS: WO2005077951 (2005).
124. BAYLOR COLLEGE OF MEDICINE, USA: US20050283007 (2005).
125. BAYLOR COLLEGE OF MEDICINE, USA: WO2005074933 (2005).
126. GENENTECH, INC., USA: US20060177448.

Affiliation

Raveendra Dayam[2], Fedora Grande[2],
Laith Q Al-Mawsawi[2] & Nouri Neamati[†1]
[†]Author for correspondence
[1]Department of Pharmacology & Pharmaceutical Sciences, School of Pharmacy, University of Southern California, 1985 Zonal Avenue, PSC304A, Los Angeles, CA90089, USA
Tel: +1 323 442 2341; Fax: +1 323 442 1390;
E-mail: Neamati@usc.edu
[2]Department of Pharmacology & Pharmaceutical Sciences, School of Pharmacy, University of Southern California, 1985 Zonal Avenue, PSC304A, Los Angeles, CA90089, USA

Copyright of Informa UK Ltd. - Printing and distribution strictly prohibited

(Patent Application)

Novel Inhibitors of p53-MDM2 Interaction for the Treatment of Cancer

Nouri Neamati[*] and Jinxia Deng

Department of Pharmaceutical Sciences, School of Pharmacy, University of Southern California
1985 Zonal Avenue, PSC304A, Los Angeles, CA90089

[*]Corresponding Author:
Tel: 323-442-2341
Fax: 323-442-1390
Email: neamati@usc.edu

Running Title:
Pharmacophore model development in MDM2 Antagonists design

Abstract

Recent studies indicate that p53-MDM2 interactions can be successfully inhibited by small molecules or peptides. In this work, we performed pharmacophore model studies including the substructure concept and the explicit shape constrains to the active conformation of Nutlin or the p53 fragment that binds to the MDM2. Database screening using these models resulted in a series of structurally novel compounds. Eight eight representative hits were selected for initial cytotoxicity assay against HCT116 $p53^{+/+}$ and $p53^{-/-}$ cell lines. Eight of the compounds showed desirable activities in these cells as well two additional cell lines.

Keywords

P53-MDM2 inhibitor, MDM2 antagonist, MDM2, MDM2, anticancer drug, docking, pharmacophore model, drug design, active conformation

Introduction

Mouse double minute 2 (MDM2) is an oncogene that was originally isolated from a spontaneously transformed mouse fibroblast cell line.[1] Later this gene was rediscovered as a p53 binding protein in several rat fibroblast cell lines.[2] The human homologue has been shown to be over-expressed in 40-60% of human osteogenic sarcomas and about 30% of soft tissue sarcomas.[3,4] The human MDM2 gene encodes a 491 amino acid residues that includes a p53-binding domain, an acidic region, a zinc-finger, and a ring-finger domain (see Figure 1).[4]

p53 is a 393 amino acid residue transcription factor that up-regulates the expression of proteins that mediate distinct cellular responses such as apoptosis and cell growth arrest.[5,6] Over 50% of human tumors contain mutations in p53 that inactivate its transcription functions.[7] Most of the p53 mutations occur within the DNA-binding domain such that p53 is unable to act as a sequence-specific DNA binding transcription factor.[8] The fact that mutational inactivation of p53 was observed as one of the most common genetic events indicates that p53 plays a critical role in suppressing the tumor growth. Structural studies have shown that p53 is made up of at least four functional domains regulating its transcriptional activities (see Figure. 1): 1) an N-terminal trans-activation domain, which is prolin-rich and required for interaction with components of the transcriptional machinery, 2) a central conserved DNA-binding core domain, 3) a tetramerization domain that assists sequence-specific DNA binding, and 4) a C-terminial negative regulatory domain whose phosphorylation primes the latent sequence-specific DNA-binding function of p53 for activation.[4] The N-terminal transactivation domain contains the binding pocket of the most important negative cellular regulators of the p53, i.e. the product of the MDM2 oncogene.[9]

The MDM2 protein regulates the p53 protein activity in at least three different ways.[10] Briefly, 1) it binds to the p53 transactivation domain, blocking the transcriptional activity, 2) upon binding to p53, it induces nuclear export, and 3) it stimulates p53 degradation by catalyzing the ubiquitination of p53 through the uniquitin/proteasome pathway, as reviewed recently.[11,12] Transcription of the MDM2 gene itself is regulated by p53 in response to the cellular stress, indicating p53 and MDM2 form an autoregulartory feedback loop.[10] Therefore, as one of the approaches to stabilize the p53 level, MDM2 has been selected as a very attractive therapeutic cancer target. Efforts are underway to design peptides or small-molecule compounds to disrupt the p53-MDM2 interactions. Biological and functional studies have mapped the residues of 19-102 as the domain for p53 binding, while MDM2 binding domain of p53 was narrowed down to 15-residue peptide.[4] The first crystal complex of MDM2 with 15-mer wildtype p53 was resolved in 1996 and clearly revealed that MDM2 possesses a well-defined deep hydrophobic binding pocket efficiently occupied by the triad motif, i.e. F19, W23 and L26, of p53.[13] In addition to the H-bond interaction between N atom of W23 side chain of p53 and target MDM2, multiple van der Walls contacts were observed to stabilize the complex.

Most of the data on the inhibition of the p53-MDM2 interaction have been obtained with peptides. The initial work suggested that p53 peptide could be used as probes to investigate the interaction and confirmed the critical function of the triad motif as revealed from the resolved p53-MDM2 complex.[3,14,15] Subsequently, a potent 12-mer peptide was identified by screening phage peptide libraries.[16,17] Several shorter peptides showed tighter binding as observed from the kinetic and thermodynamic studies.[18]

Several small molecule inhibitors of the p53-MDM2 interactions including chalcones, chlorofusin, etc, have also been discovered recently.[19-24] A major development in the field was the discovery of Nutlin series of compounds and the determiniation of co-crystal structure at 2.3 Å resolution.[24] The Nutlin binding mode as revealed in the crystal structure mimics the interactions of the p53 peptide to a high degree. One bromophenyl moiety sitting deeply in the W23 pocket, the other bromophenyl group overlapping the L26 space, and the hydrophobic ethyl ether side chain directed toward the F19 pocket.[24]

Taken together, all these studies strongly prove that protein-protein interactions can be successfully manipulated with small molecules. Therefore, p53 pathway can be effectively targeted to develop novel anti-cancer drugs.

In this work, we carried out extensive pharmacophore model studies using the active conformations of imidazoline analogue (Nutlin) and the side-chain of P53 fragment which were resolved in the crystallographic structures of MDM2 complex. The derived models were applied to screen our in-house small molecule database and the representative compounds were tested in HCT116 p53$^{+/+}$ and HCT116 p53$^{-/-}$ cell-lines.

Computational Methods

Substructure Search. Initially, we applied a substructure concept to find a spiral compounds with extended arms, including Nutlin-like molecules. The Nutlin compound was built by Catalyst and converted to a hypothesis. Three additional structural motifs mimicking the Nutlin central bridge were designed, and these hypothesis were used as queries to search our database of small molecule compounds.

Functional Feature Pharmacophore Model. Functional feature pharmacophore model studies were extensively performed on both Nutlin and the p53 side chain of the conserved triad motif, i.e. F19, W23, L26 by Catalyst software package. The conformation of Nutlin or p53 was taken from the observation as resolved in the x-ray structures, as referred to as active conformation.[13,24] In light of Nutlin pharmacophore model development, we first mapped H-bond donor, H-bond acceptor, hydrophobic and aromatic ring features to the active conformation. We then assigned geometrical constraints to each feature, i.e., coordinate and size of the feature. Finally, all the selected features were merged into one pharmacophore model. Following the similar procedure, pharmacophore model of p53 triad motif, F19, W23, L26, was derived.

Shape-merged single compound pharmacophore query. The Catalyst was used to generate the explicit shape constraint of Nutlin or p53 side chain ligand. Fist, the active conformation of the template molecule (Nutlin or p53 fragment of amino acid residues from 19-26) was mapped to the corresponding feature model, respectively. Then the explicit shape constraint was generated. Finally, the shape was merged with the feature model as a single query in Catalyst, that we referred to as the shape-merged pharmacophore model. The similarity tolerance of shape is an important parameter to adjust the percentage of hits yielded from database screening. The values of 0.5-1was used as default value in the shape-merged p53 side chain model, but for the shape-merged Nutlin feature model, we relaxed the shape similarity to values of 0.45-1.

Docking studies. The docking studies were carried out by the GOLD (version 1.2 Genetic Optimization for Ligand Docking) software package[25] running on our multi-processor linux PC and a 24-processor Silicon Graphics Onyx workstation as described.[26] We used the crystal structure of Nutlin bound MDM2 complex (pdb code 1RV1)[24] as the template target, and the ligand, Nutlin, was subsequently removed to keep the binding pocket available. Hydrogen atoms were added to both protein and ligand according to the protonation state at pH 7.0 during the docking studies.

The docking area was defined as a sphere with the radius of 15 Å at the central coordinate position (47.47, 12.31, 35.24) of the Nutlin molecule as chrystallographically observed in the MDM2 binding pocket. The ligand was placed within the active site using a least-squares fitting procedure. All docking runs were performed using standard default settings with a population size of 100, a maximum number of 100,000 operations, a mutation and crossover rate of 95. The scoring function was contributed basically from H-bond interaction, van der Waals interactions within the complex, and the ligand internal energy which was summarized by ligand steric and torsional energies.[25] Explicit electrostatic interaction was ignored but was modeled into the H-bond interactions.

Database search. Substructure queries, and the shape-merged pharmacophore models derived from either the Nutlin or the side chain of p53 fragment in their active conformation, respectively, were applied to screen our in-house database by Catalyst.

Cell. Cancer cells (HCT116 $p53^{+/+}$, HCT116 $p53^{-/-}$) and human breast cancer cell MDA-MB-435 (p53 mutant) were obtained from Dr. Bert Vogelstein (Johns Hopkins). The human ovarian carcinoma cell line (HEY p53 wildtype) naturally resistant to cisplatin was kindly provided by Dr. Dubeau (University of Southern California Norris Cancer Center). Cells were maintained as monolayer cultures in RPM1 1640 supplemented with 10% fetal bovine serum (Gemini-Bioproducts, Woodland, CA) and 2 mmol/L L-glutamine at 37°C in a humidified atmosphere of 5% CO_2. To remove the adherent cells from the flask for passaging and counting, cells were washed with PBS without calcium or magnesium, incubated with a small volume of 0.25% trypsin-EDTA solution (Sigma-Aldrich, St. Louis, MO) for 5 to 10 minutes, and washed with culture medium and centrifuged. All experiments were carried out using cells in exponential cell growth.

Compounds. The selected compounds were prepared in 100% DMSO at a concentration of 10mM and stored at -20^oC. Further dilutions of each drug were freshly made in phosphate saline buffer to final concentration before use.

Cytotoxicity Assay. Cytotoxicity was assessed by a 3-(4,5-dimethylthiazol-2-yl)-2,5-diphenyltetrazolium bromide assay as previously described.[27]Briefly, cells were seeded in 96-well micro-titer plates (4,000 cells/well) and allowed to attach. Cells were subsequently treated with a continuous exposure to the corresponding drug for 72 hours. A 3-(4,5-dimethylthiazol-2-yl)-2,5-diphenyltetrazolium bromide solution (at a final concentration of 0.5 mg/ml) was added to each well and cells were inculated for 4 hours at 37 ^oC. After removal of the medium, DMSO was added and the absorbance was read at 570 nm. All assays were performed at least in triplicate. IC_{50} (dose of each drug that inhibits 50% of cell growth) was then determined from a plot of log (drug concentration) versus percentage of cell kill.

Results and Discussions

Substructure Query. Substructure query approach of active compounds is an easy first step to rapidly identify hits. The recent crystal structure (1RV1) revealed a deep substrate binding pocket, suggesting that a variety of compounds with a central cyclic structure and finger-like side chain substituents could occupy the cavity. Therefore, our first 5-memember ring hypothesis, sq1 (Table 1) contained the central core of Nutlin, while other three were conceptually bridge-like fragments functioning as searching queries (sq2-sq4, Table 1). The number of hits from two databases, Chembrdige and Chemdiv, against each substructure motif are listed in Table 1.

Pharmacophore Model Studies

Nutlin –based pharmacophore model. Referring to the interactions between Nutlin and the target protein, MDM2, determined in the X-ray structure(1RV1)[24], only hydrophobic features (P1-P6) were considered in the pharmacophore model (Figure 2a). The features P1, P2, and P4 were mapped by the benzene ring and P3 by aliphatic methane group which was observed to interact with MDM2 by its Van der Waals contacts. Additionally, P5 and P6 were recognized by the bromine substitutes. Shape-merged pharmacophore model was recently studied on several potent HIV-1 integrase inhibitors and successfully identify novel compounds to block the integrase activities. We applied the similar concept to generate the explicit shape of Nutline in its active orientation, as shown in Figure 2b. Apparently, both feature model (Figure 1a) and shape constraint itself (Figure 2b) can be used independently as searching query to screen small molecule database. In this work however, we combine the shape constraint onto the feature model to generated shape-merged pharmacophore model, labeled as SM1 (Figure 2b), in order to comprehensively extract the chemical characteristics of the potent imidazole antagonist. Consequently, the shaped-merged model, SM1, was applied to screen our in-house database, 705 compounds were identified. We selected the compounds with wide structure variant for cell line analysis. The structures and the predicted docking score are listed in Table 2 and some of cytotoxic measurement of the selected compounds are listed in Table 4.

p53 side chain –based pharmacophore model

Since the p53-MDM2 fragment was resolved by x-ray technique, a large number of peptide library was designed to compete the p53 binding. The first published putative p53-based pharmacophore model addressed the hydrophobic features recognized by the side chain of F19, W23 and L26, and H-bond donor mapped by the W23 indole side chain.[28] Its application to screen NCI database resulted series of non-peptide sulfonamide inhibitors.[29] In this work, however, we extended the pharmacophore studies by taking into account explicit shape of the active conformation of the p53 fragment, determined by the x-ray structure, therefore, two shape-merged pharmacophore models were systematically generated, as shown in Figure 3. Figure 3a shows the model with the consideration of only three hydrophobic features, but enhanced by shape constraint, referred to as SM2. Figure 3b shows the shape-merged model, referred to as SM3, that keeps additional hydrogen-bond feature. As consequence, SM2 and SM3 were treated as independent queries to virtually screen our in-house database. The structure and GOLD predicted docking scores of selected molecules identified by the pharmacophore models are listed in Table 3, and the cytotoxicity measurements are in Table 4.

Docking Studies

Docking simulations were performed on several potent inhibitors, to predict the binding mechanism (Figure 4)

Conclusions

References

(1) Cahilly-Snyder, L.; Yang-Feng, T.; Francke, U.; George, D. L. Molecular analysis and chromosomal mapping of amplified genes isolated from a transformed mouse 3T3 cell line. *Somat. Cell Mol. Genet.* **1987**, *13*, 235.

(2) Momand, J.; Zambetti, G. P.; Olson, D. C.; George, D.; Levine, A. J. The mdm-2 oncogene product forms a complex with the p53 protein and inhibits p53-mediated transactivation. *Cell* **1992**, *69*, 1237-1245.

(3) Oliner, J. D.; Kinzler, K. W.; Meltzer, P. S.; George, D. L.; Vogelstein, B. Amplification of a gene encoding a p53-associated protein in human sarcomas. *Nature* **1992**, *358*, 80-83.

(4) Zheleva, D. I.; Lane, D. P.; Fischer, P. M. The p53-MDM2 pathway: targets for the development of new anticancer therapeutics. *Mini Rev Med Chem* **2003**, *3*, 257-270.

(5) Woods, D. B.; Vousden, K. H. Regulation of p53 function. *Exp Cell Res* **2001**, *264*, 56-66.

(6) Malkin, D. The role of p53 in human cancer. *J Neurooncol* **2001**, *51*, 231-243.

(7) Hollstein, M.; Rice, K.; Greenblatt, M. S.; Soussi, T.; Fuchs, R. et al. Database of p53 gene somatic mutations in human tumors and cell lines. *Nucleic Acids Res* **1994**, *22*, 3551-3555.

(8) Harris, C. C. Structure and function of the p53 tumor suppressor gene: clues for rational cancer therapeutic strategies. *J Natl Cancer Inst* **1996**, *88*, 1442-1455.

(9) Momand, J.; Wu, H. H.; Dasgupta, G. MDM2--master regulator of the p53 tumor suppressor protein. *Gene* **2000**, *242*, 15-29.

(10) Freedman, D. A.; Wu, L.; Levine, A. J. Functions of the MDM2 oncoprotein. *Cell Mol Life Sci* **1999**, *55*, 96-107.

(11) Gottifredi, V.; Prives, C. Molecular biology. Getting p53 out of the nucleus. *Science* **2001**, *292*, 1851-1852.

(12) Chene, P.; Fuchs, J.; Carena, I.; Furet, P.; Garcia-Echeverria, C. Study of the cytotoxic effect of a peptidic inhibitor of the p53-MDM2 interaction in tumor cells. *FEBS Lett* **2002**, *529*, 293-297.

(13) Lin, J.; Chen, J.; Elenbaas, B.; Levine, A. J. Several hydrophobic amino acids in the p53 amino-terminal domain are required for transcriptional activation, binding to mdm-2 and the adenovirus 5 E1B 55-kD protein. *Genes Dev* **1994**, *8*, 1235-1246.

(14) Kussie, P. H.; Gorina, S.; Marechal, V.; Elenbaas, B.; Moreau, J. et al. Structure of the MDM2 oncoprotein bound to the p53 tumor suppressor transactivation domain. *Science* **1996**, *274*, 948-953.

(15) Picksley, S. M.; Vojtesek, B.; Sparks, A.; Lane, D. P. Immunochemical analysis of the interaction of p53 with MDM2;--fine mapping of the MDM2 binding site on p53 using synthetic peptides. *Oncogene* **1994**, *9*, 2523-2529.

(16) Bottger, A.; Bottger, V.; Garcia-Echeverria, C.; Chene, P.; Hochkeppel, H. K. et al. Molecular characterization of the MDM2-p53 interaction. *J Mol Biol* **1997**, *269*, 744-756.

(17) Bottger, V.; Bottger, A.; Howard, S. F.; Picksley, S. M.; Chene, P. et al. Identification of novel MDM2 binding peptides by phage display. *Oncogene* **1996**, *13*, 2141-2147.

(18) Chene, P. Inhibition of the p53-MDM2 interaction: targeting a protein-protein interface. *Mol Cancer Res* **2004**, *2*, 20-28.

(19) Schon, O.; Friedler, A.; Bycroft, M.; Freund, S. M.; Fersht, A. R. Molecular mechanism of the interaction between MDM2 and p53. *J Mol Biol* **2002**, *323*, 491-501.

(20) Massova, I.; Kollman, P. A. Computational alanine scanning to probe protein-protein interactions: a novel approach to evaluate binding free energiies. *J. Am. Chem. Soc.* **1999**, *2*, 8133-8143.

(21) Galatin, P. S.; Abraham, D. J. QSAR: hydropathic analysis of inhibitors of the p53-MDM2 interaction. *Proteins* **2001**, *45*, 169-175.

(22) Schon, O.; Friedler, A.; Freund, S.; Fersht, A. R. Binding of p53-derived ligands to MDM2 induces a variety of long range conformational changes. *J Mol Biol* **2004**, *336*, 197-202.

(23) Stoll, R.; Renner, C.; Hansen, S.; Palme, S.; Klein, C. et al. Chalcone derivatives antagonize interactions between the human oncoprotein MDM2 and p53. *Biochemistry* **2001**, *40*, 336-344.

(24) Duncan, S. J.; Gruschow, S.; Williams, D. H.; McNicholas, C.; Purewal, R. et al. Isolation and structure elucidation of Chlorofusin, a novel p53-MDM2 antagonist from a Fusarium sp. *J Am Chem Soc* **2001**, *123*, 554-560.

(25) Zhao, J.; Wang, M.; Chen, J.; Luo, A.; Wang, X. et al. The initial evaluation of non-peptidic small-molecule MDM2 inhibitors based on p53-MDM2 complex structure. *Cancer Lett* **2002**, *183*, 69-77.

(26) Kumar, S. K.; Hager, E.; Pettit, C.; Gurulingappa, H.; Davidson, N. E. et al. Design, synthesis, and evaluation of novel boronic-chalcone derivatives as antitumor agents. *J Med Chem* **2003**, *46*, 2813-2815.

(27) Vassilev, L. T.; Vu, B. T.; Graves, B.; Carvajal, D.; Podlaski, F. et al. In vivo activation of the p53 pathway by small-molecule antagonists of MDM2. *Science* **2004**, *303*, 844-848.

(28) Catalyst; 4.6 ed.; Accelrys Inc: San Diego, CA.

(29) Jones, G.; Willett, P.; Glen, R. C.; Leach, A. R.; Taylor, R. Development and validation of a genetic algorithm for flexible docking. *J Mol Biol* **1997**, *267*, 727-748.

(30) Long, Y. Q.; Jiang, X. H.; Dayam, R.; Sanchez, T.; Shoemaker, R. et al. Rational design and synthesis of novel dimeric diketoacid-containing inhibitors of HIV-1 integrase: implication for binding to two metal ions on the active site of integrase. *J Med Chem* **2004**, *47*, 2561-2573.

(31) Alley, M. C.; Scudiero, D. A.; Monks, A.; Hursey, M. L.; Czerwinski, M. J. et al. Feasibility of drug screening with panels of human tumor cell lines using a microculture tetrazolium assay. *Cancer Res* **1988**, *48*, 589-601.

(1) Cahilly-Snyder, L.; Yang-Feng, T.; Francke, U.; George, D. L. Molecular analysis and chromosomal mapping of amplified genes isolated from a transformed mouse 3T3 cell line. *Somat. Cell Mol. Genet.* **1987**, *13*, 235.

(2) Momand, J.; Zambetti, G. P.; Olson, D. C.; George, D.; Levine, A. J. The mdm-2 oncogene product forms a complex with the p53 protein and inhibits p53-mediated transactivation. *Cell* **1992**, *69*, 1237-1245.

(3) Oliner, J. D.; Kinzler, K. W.; Meltzer, P. S.; George, D. L.; Vogelstein, B. Amplification of a gene encoding a p53-associated protein in human sarcomas. *Nature* **1992**, *358*, 80-83.

(4) Zheleva, D. I.; Lane, D. P.; Fischer, P. M. The p53-Mdm2 pathway: targets for the development of new anticancer therapeutics. *Mini Rev Med Chem* **2003**, *3*, 257-270.

(5) Woods, D. B.; Vousden, K. H. Regulation of p53 function. *Exp Cell Res* **2001**, *264*, 56-66.

(6) Malkin, D. The role of p53 in human cancer. *J Neurooncol* **2001**, *51*, 231-243.

(7) Hollstein, M.; Rice, K.; Greenblatt, M. S.; Soussi, T.; Fuchs, R.; Sorlie, T.; Hovig, E.; Smith-Sorensen, B.; Montesano, R.; Harris, C. C. Database of p53 gene somatic mutations in human tumors and cell lines. *Nucleic Acids Res* **1994**, *22*, 3551-3555.

(8) Harris, C. C. Structure and function of the p53 tumor suppressor gene: clues for rational cancer therapeutic strategies. *J Natl Cancer Inst* **1996**, *88*, 1442-1455.

(9) Momand, J.; Wu, H. H.; Dasgupta, G. MDM2--master regulator of the p53 tumor suppressor protein. *Gene* **2000**, *242*, 15-29.

(10) Freedman, D. A.; Wu, L.; Levine, A. J. Functions of the MDM2 oncoprotein. *Cell Mol Life Sci* **1999**, *55*, 96-107.

(11) Gottifredi, V.; Prives, C. Molecular biology. Getting p53 out of the nucleus. *Science* **2001**, *292*, 1851-1852.

(12) Chene, P.; Fuchs, J.; Carena, I.; Furet, P.; Garcia-Echeverria, C. Study of the cytotoxic effect of a peptidic inhibitor of the p53-hdm2 interaction in tumor cells. *FEBS Lett* **2002**, *529*, 293-297.

(13) Kussie, P. H.; Gorina, S.; Marechal, V.; Elenbaas, B.; Moreau, J.; Levine, A. J.; Pavletich, N. P. Structure of the MDM2 oncoprotein bound to the p53 tumor suppressor transactivation domain. *Science* **1996**, *274*, 948-953.

(14) Picksley, S. M.; Vojtesek, B.; Sparks, A.; Lane, D. P. Immunochemical analysis of the interaction of p53 with MDM2;--fine mapping of the MDM2 binding site on p53 using synthetic peptides. *Oncogene* **1994**, *9*, 2523-2529.

(15) Bottger, A.; Bottger, V.; Garcia-Echeverria, C.; Chene, P.; Hochkeppel, H. K.; Sampson, W.; Ang, K.; Howard, S. F.; Picksley, S. M.; Lane, D. P. Molecular characterization of the hdm2-p53 interaction. *J Mol Biol* **1997**, *269*, 744-756.

(16) Bottger, V.; Bottger, A.; Howard, S. F.; Picksley, S. M.; Chene, P.; Garcia-Echeverria, C.; Hochkeppel, H. K.; Lane, D. P. Identification of novel mdm2 binding peptides by phage display. *Oncogene* **1996**, *13*, 2141-2147.

(17) Chene, P. Inhibition of the p53-MDM2 interaction: targeting a protein-protein interface. *Mol Cancer Res* **2004**, *2*, 20-28.

(18) Schon, O.; Friedler, A.; Freund, S.; Fersht, A. R. Binding of p53-derived ligands to MDM2 induces a variety of long range conformational changes. *J Mol Biol* **2004**, *336*, 197-202.

(19) Chen, L.; Yin, H.; Farooqi, B.; Sebti, S.; Hamilton, A. D.; Chen, J. p53 alpha-Helix mimetics antagonize p53/MDM2 interaction and activate p53. *Mol Cancer Ther* **2005**, *4*, 1019-1025.

(20) Stoll, R.; Renner, C.; Hansen, S.; Palme, S.; Klein, C.; Belling, A.; Zeslawski, W.; Kamionka, M.; Rehm, T.; Muhlhahn, P.; Schumacher, R.; Hesse, F.; Kaluza, B.; Voelter, W.; Engh, R. A.; Holak, T. A. Chalcone derivatives antagonize interactions between the human oncoprotein MDM2 and p53. *Biochemistry* **2001**, *40*, 336-344.

(21) Duncan, S. J.; Gruschow, S.; Williams, D. H.; McNicholas, C.; Purewal, R.; Hajek, M.; Gerlitz, M.; Martin, S.; Wrigley, S. K.; Moore, M. Isolation and structure elucidation of Chlorofusin, a novel p53-MDM2 antagonist from a Fusarium sp. *J Am Chem Soc* **2001**, *123*, 554-560.

(22) Zhao, J.; Wang, M.; Chen, J.; Luo, A.; Wang, X.; Wu, M.; Yin, D.; Liu, Z. The initial evaluation of non-peptidic small-molecule HDM2 inhibitors based on p53-HDM2 complex structure. *Cancer Lett* **2002**, *183*, 69-77.

(23) Kumar, S. K.; Hager, E.; Pettit, C.; Gurulingappa, H.; Davidson, N. E.; Khan, S. R. Design, synthesis, and evaluation of novel boronic-chalcone derivatives as antitumor agents. *J Med Chem* **2003**, *46*, 2813-2815.

(24) Vassilev, L. T.; Vu, B. T.; Graves, B.; Carvajal, D.; Podlaski, F.; Filipovic, Z.; Kong, N.; Kammlott, U.; Lukacs, C.; Klein, C.; Fotouhi, N.; Liu, E. A. In vivo activation of the p53 pathway by small-molecule antagonists of MDM2. *Science* **2004**, *303*, 844-848.

(25) Jones, G.; Willett, P.; Glen, R. C.; Leach, A. R.; Taylor, R. Development and validation of a genetic algorithm for flexible docking. *J Mol Biol* **1997**, *267*, 727-748.

(26) Dayam, R.; Sanchez, T.; Clement, O.; Shoemaker, R.; Sei, S.; Neamati, N. Beta-diketo acid pharmacophore hypothesis. 1. Discovery of a novel class of HIV-1 integrase inhibitors. *J Med Chem* **2005**, *48*, 111-120.

(27) Plasencia, C.; Dayam, R.; Wang, Q.; Pinski, J.; Burke, T. R., Jr.; Quinn, D. I.; Neamati, N. Discovery and preclinical evaluation of a novel class of small-molecule compounds in hormone-dependent and -independent cancer cell lines. *Mol Cancer Ther* **2005**, *4*, 1105-1113.

(28) Galatin, P. S.; Abraham, D. J. QSAR: hydropathic analysis of inhibitors of the p53-mdm2 interaction. *Proteins* **2001**, *45*, 169-175.

(29) Galatin, P. S.; Abraham, D. J. A nonpeptidic sulfonamide inhibits the p53-mdm2 interaction and activates p53-dependent transcription in mdm2-overexpressing cells. *J Med Chem* **2004**, *47*, 4163-4165.

Table 1 Substructure motif used as database searching query and the number of hits identified from two databases

	Sq1	Sq2	Sq3	Sq4
feature	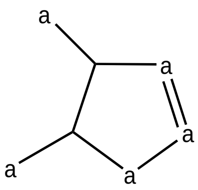 a = O, N, C	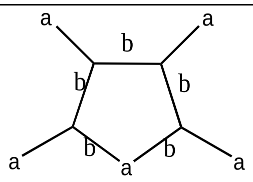 a = O, N, C b = single, or double bond	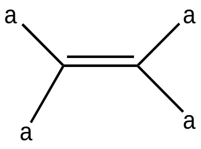 a = O, N, C	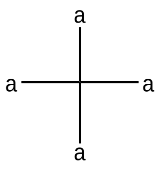 a = O, N, C
Hits from ChemDiv	245	4951	106	20
Selected for docking	100	60	5	2
Selected for testing	9	17	5	2
Hits from Chembridge	150	130	68	15
Selected for docking	33	20	6	15
Selected for testing	12	10	2	15

Table 2 Structures and GOLD docking scores of selected compounds identified from substructure queries.

Cpd	Structure	M..W.	GOLD Score	**Cpd**	Structure	M..W.	GOLD Score
mp1	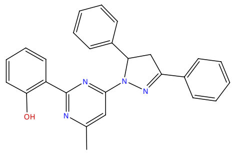	406.48	64.19	**mp2**	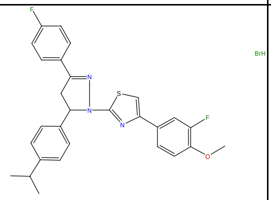	570.49	48.07
mp3	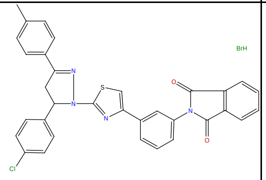	655.99	58.01	**mp4**	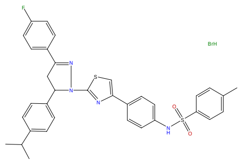	691.68	55.0
mp5	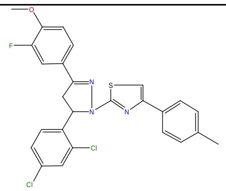	512.43	47.55	**mp6**	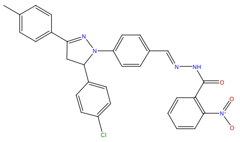	537.99	46.26
mp7	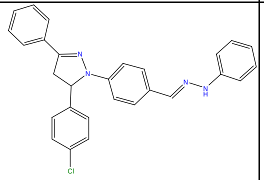	519.55	45.85	**mp8**	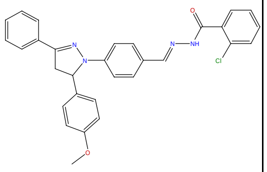	508.99	46.9
mp9	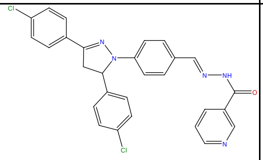	514.41	47.41	**mp10**	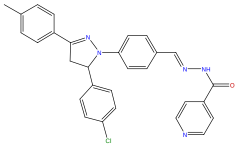	493.99	47.43
mp11	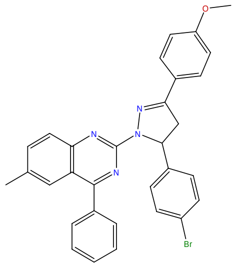	549.46	58.37	**mp12**	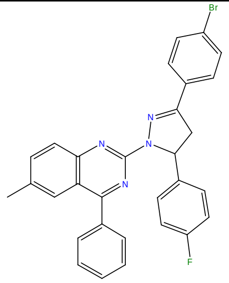	537.43	51.89

mp13	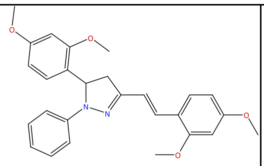	444.52	45.36	**mp14**	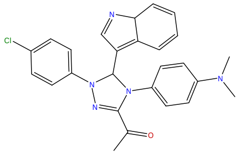	457.95	49.33
mp15	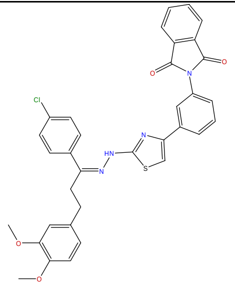	623.12	36.93	**mp16**	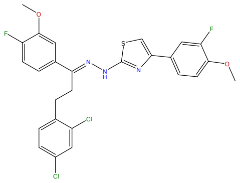	548.43	48.16
mp17	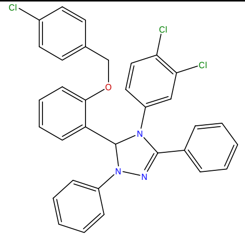	584.92	56.26	**mp18**	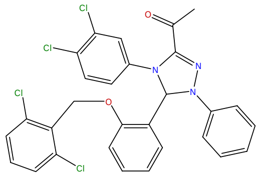	585.31	55.56
mp19	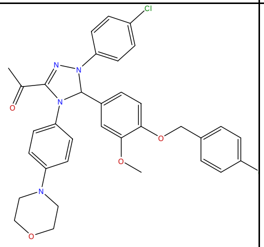	631.55	54.34	**mp20**	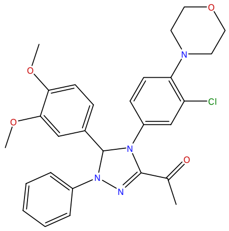	521.01	42.90
mp21	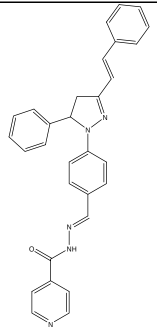	471.27	47.7	**MPS1**	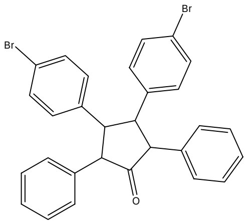	546.29	48.23
MPS2	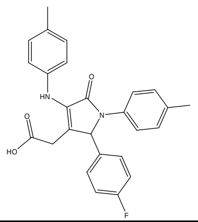	430.48		**MPS3**	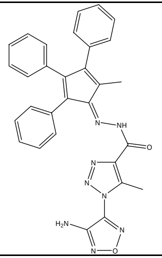		29.37

MPS4	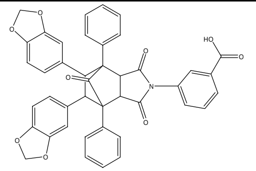	691.68	53.31	**MPS5**	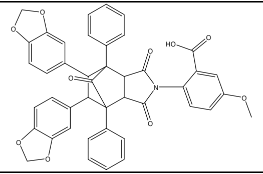	720.69	47.83
MPS6	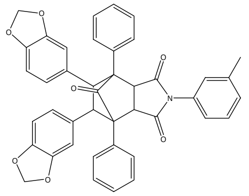	659.69	46.20	**MPS7**	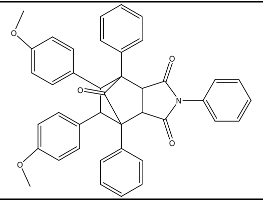	617.70	44.96
MPS8	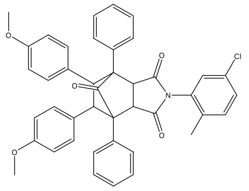	666.17	43.79	**MPS9**	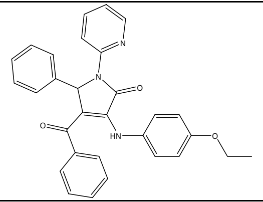	475.55	45.72
MPS10	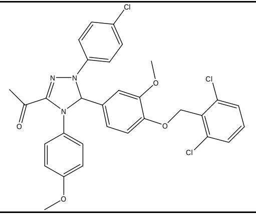	610.92	58.25	**MPS11**	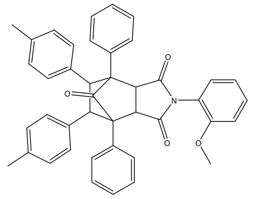	615.73	45.57
MPS12	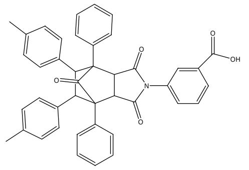	629.71	45.47	**MPS13**	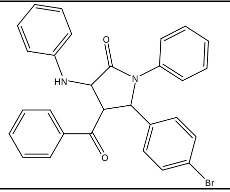	509.40	45.68
MPS14	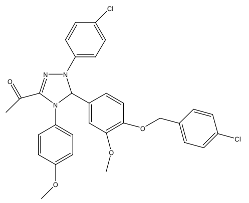	576.48	57.27	**MPS15**	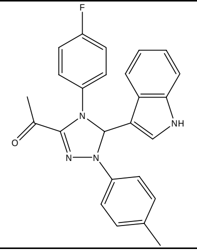	412.47	44.61

Table 3 Structures and GOLD docking scores of selected compounds identified from Nutlin and p53 side chain pharmacophore models

Cpd	Structure	M..W.	GOLD Score	**Cpd**	Structure	M..W.	GOLD Score
MP22	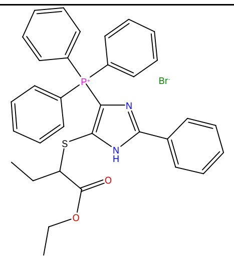	631.56	50.36	**MP23**	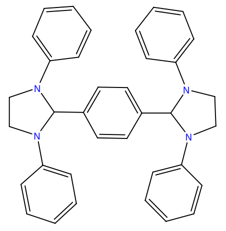	522.68	48.65
MP24	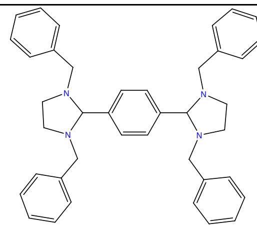	578.79	50.54	**MP25**	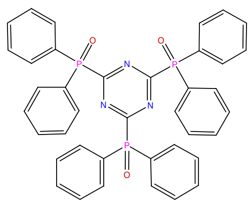	681.60	59.01
MP26	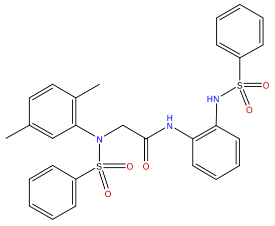	549.66	49.54	**MP27**	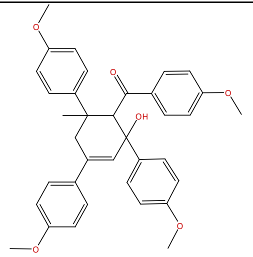	564.67	29.25
MP28	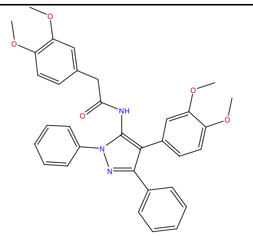	549.62	46.05	**MP29**	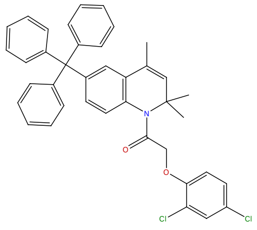	618.59	18.83
MP30	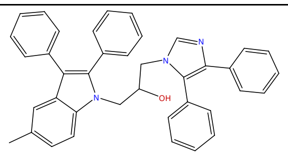	559.70	42.43	**MP31**	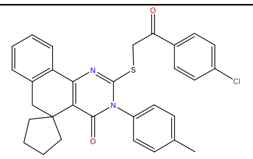	527.08	53.61

MP32	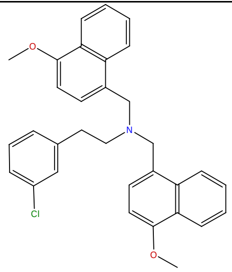	496.04	40.15	**MP33**	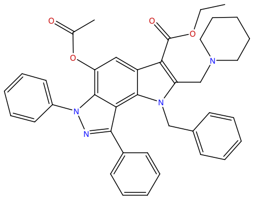	626.74	12.51
MP34	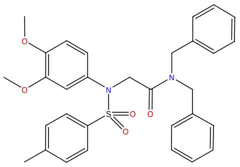	544.66	47.26	**MP35**	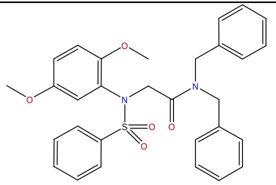	530.64	50.64
MP36	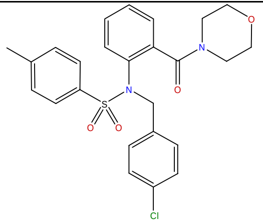	484.99	46.62	**MP37**	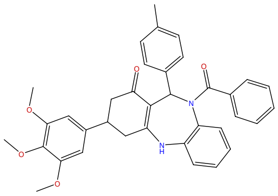	574.67	47.71
MP38	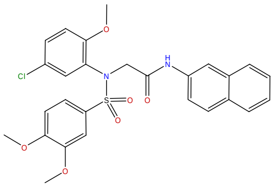	541.02	59.95	**MP39**	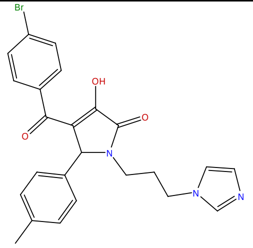	480.35	58.51
MP40	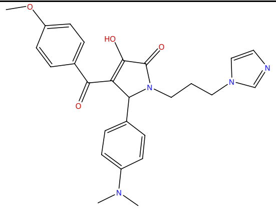	46053	42.01	**MP41**	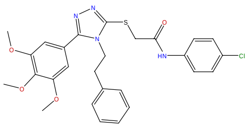	539.05	48.18
MPD1	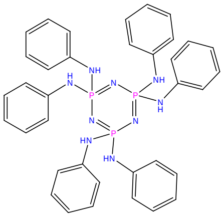	687.67	64.28	**MPD2**	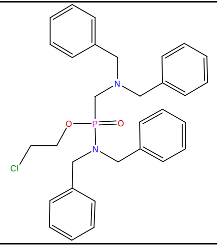	533.06	57.02

MPD3	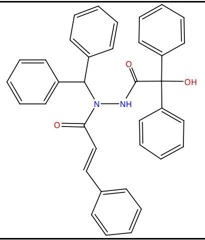	538.65	52.83	**MPD4**	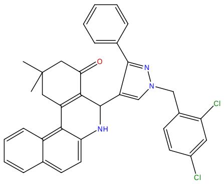	578.55	61.15
MPD5	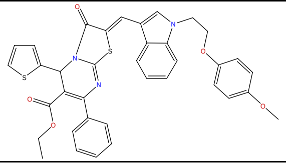	661.80	53.31	**MPD6**	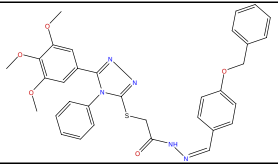	609.71	58.82
MPD7	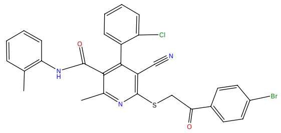	590.93	64.17	**MPD8**	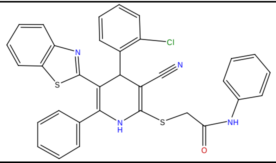	591.16	66.55
MPD9	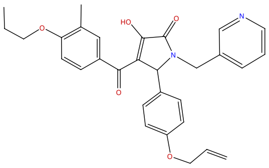	498.58	58.18	**MPD10**	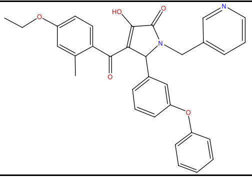	520.59	56.83
MPD11	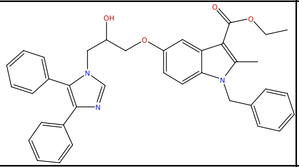	585.71	53.83	**MPD12**	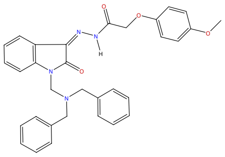	534.62	56.38
MPD13	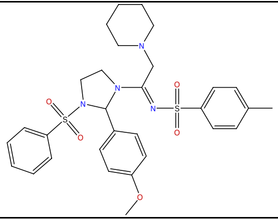	596.77	52.68	**MPD14**	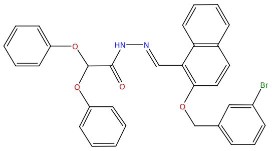	581.47	57.74
MPD15	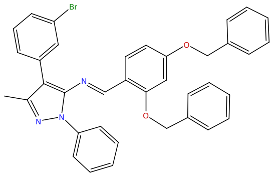	628.57	55.58	**MPD16**	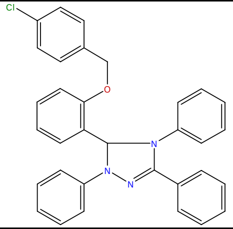	516.05	52.17
MPD17	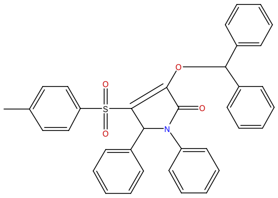	571.70	54.13	**MPD18**	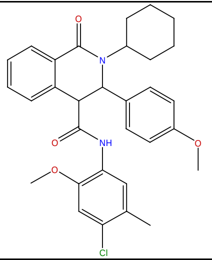	533.07	54.59

MPD19	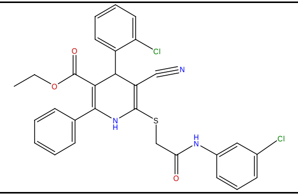	564.50	51.89	**MPD20**	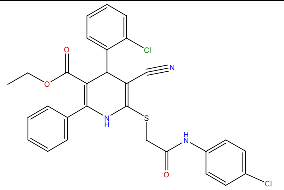	564.50	57.31
MPD21	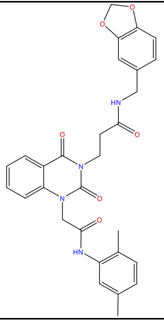	528.57	54.52	**MPD22**	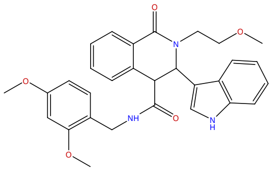	513.60	56.83
MPD23	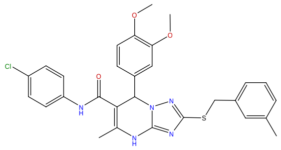	562.10	54.83	**MPS16**	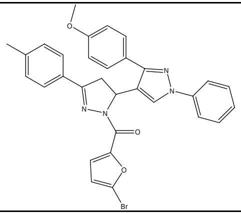	581.47	54.70
MPS17	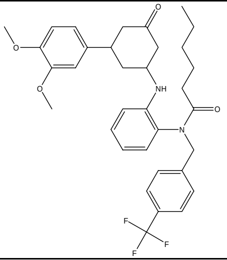	592.66	35.20	**MPS18**	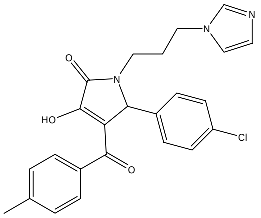	435.91	58.31
MPS19	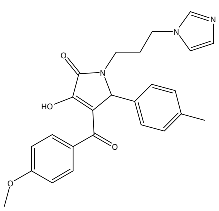	431.49	56.48	**MPS20**	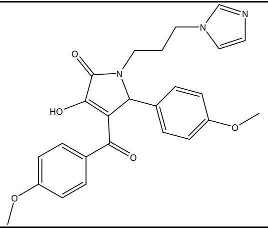	447.49	56.61
MPS21	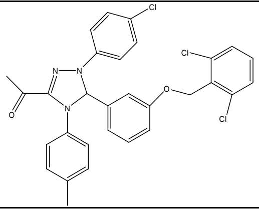	564.90	63.50	**MPS22**	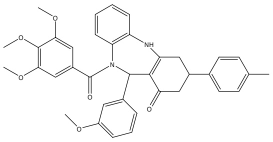	604.70	49.10
MPS23	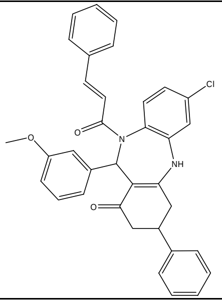	561.08	51.88	**MPS24**	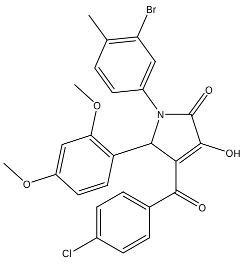	542.81	51.02

Table 4 Cytotoxicity assay of selected compounds in a panel of cancer cell lines

Cpds	IC_{50} HEY (µM)	IC_{50} 435 (µM)	IC_{50} HCT116 p53$^{+/+}$ (µM)	IC_{50} HCT116 p53$^{-/-}$ (µM)
MP16	38±7	> 20	> 20	> 20
MP17	> 20	25	18±7	22±6
MP18	> 20	> 40	> 20	> 20
MP22	14	11±1	6	9
MP24	>20	> 20	>20	> 40
MPD3	> 20	> 20	15±5	> 20
MPD5	13±5	> 20	10±6	16±5
MPD16	5.6±2	5±1.8	9±4	8±3

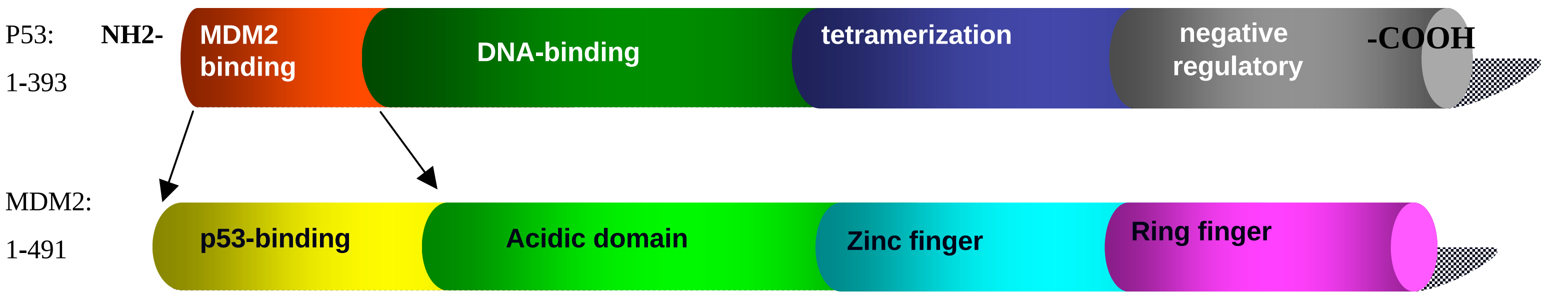
P53:
1-393
NH2-
MDM2 binding
DNA-binding
tetramerization
negative regulatory
-COOH
MDM2:
1-491
p53-binding
Acidic domain
Zinc finger
Ring finger

Figure 1. Schematic diagram showing the functional domains of p53 and MDM2.

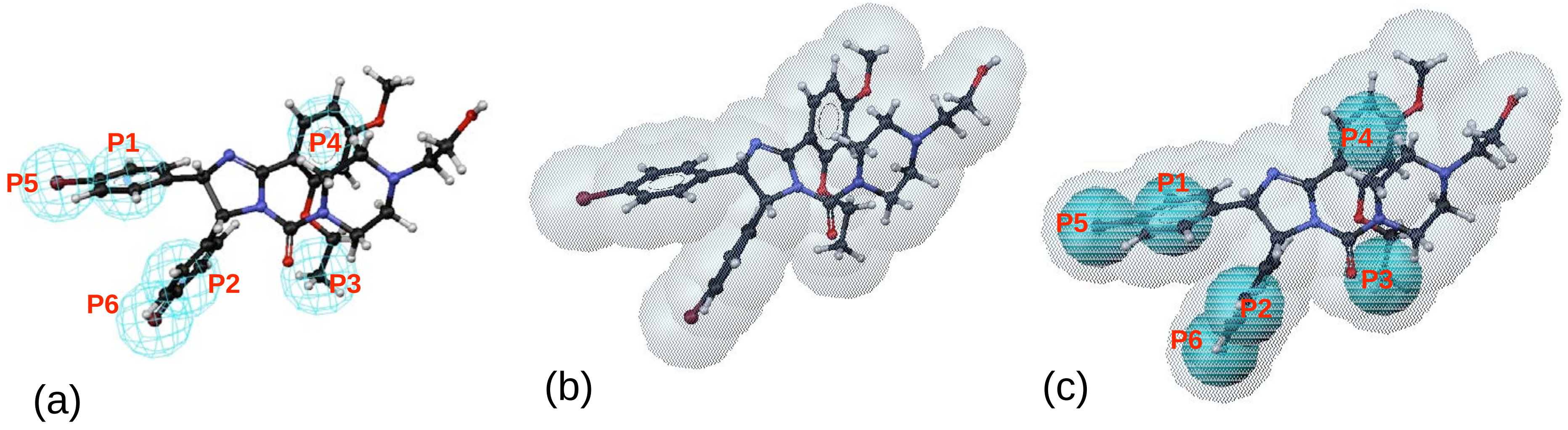
P1
P5
P4
P2
P6
P3
(a)
(b)
P1
P5
P4
P3
P2
P6
(c)

Figure 2. Pharmacophore models generated from active conformation of Nutlin. (a) Mapping Nutlin onto the feature pharmacophore model. (b) Mapping Nutlin to the shape-only query. (c) Mapping Nutlin onto shape-merged pharmacophore model.

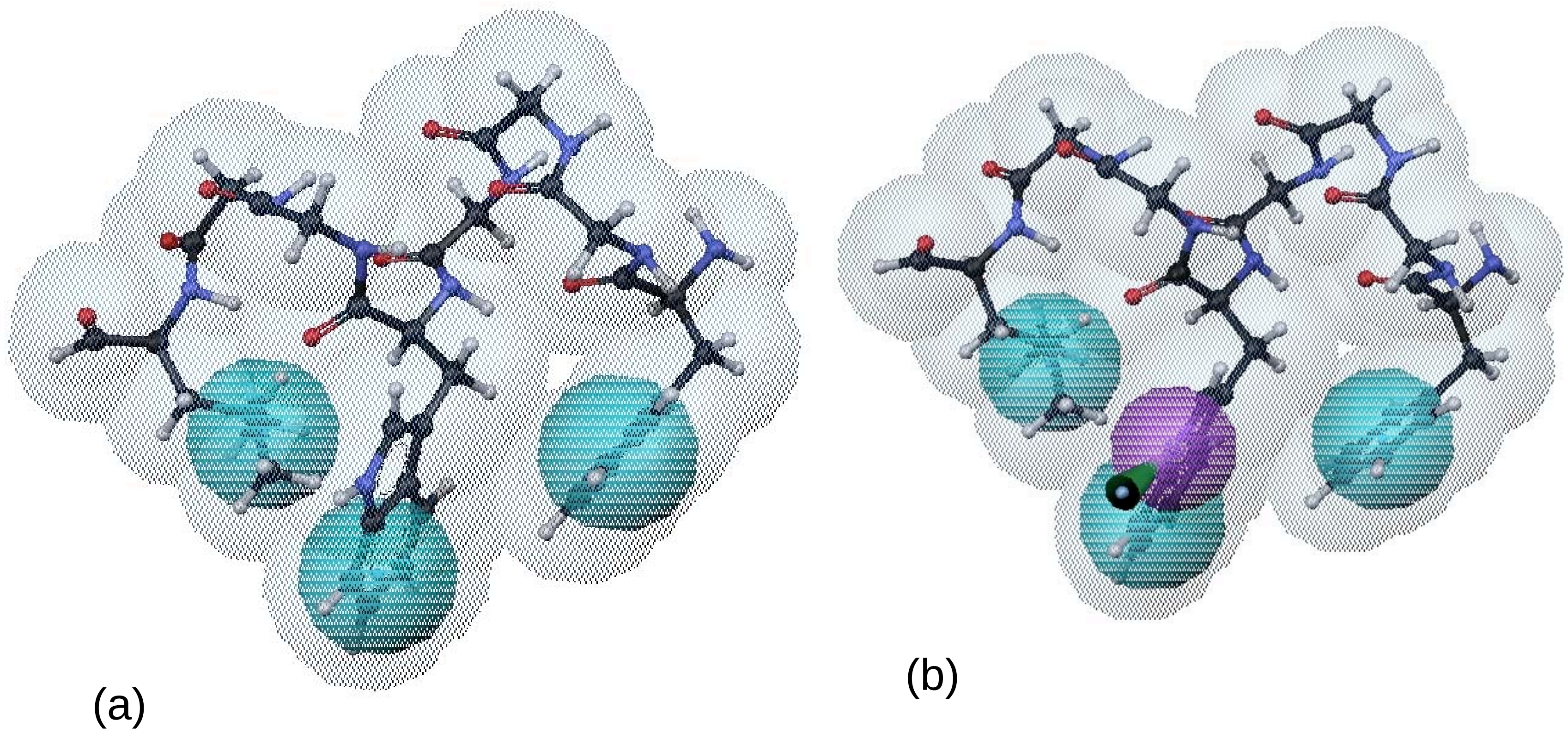

Figure 3. Pharmacophore models derived from the side chains of p53 fragment interacting with MDM2 p53 binding domain. (a) p53 fragment (amino acide residue 19-26) mapping onto the 3-hydrophobic feature pharmacophore model. (b) p53 fragment (amino acide residue 19-26) mapping onto the hetero-feature pharmacophore model.

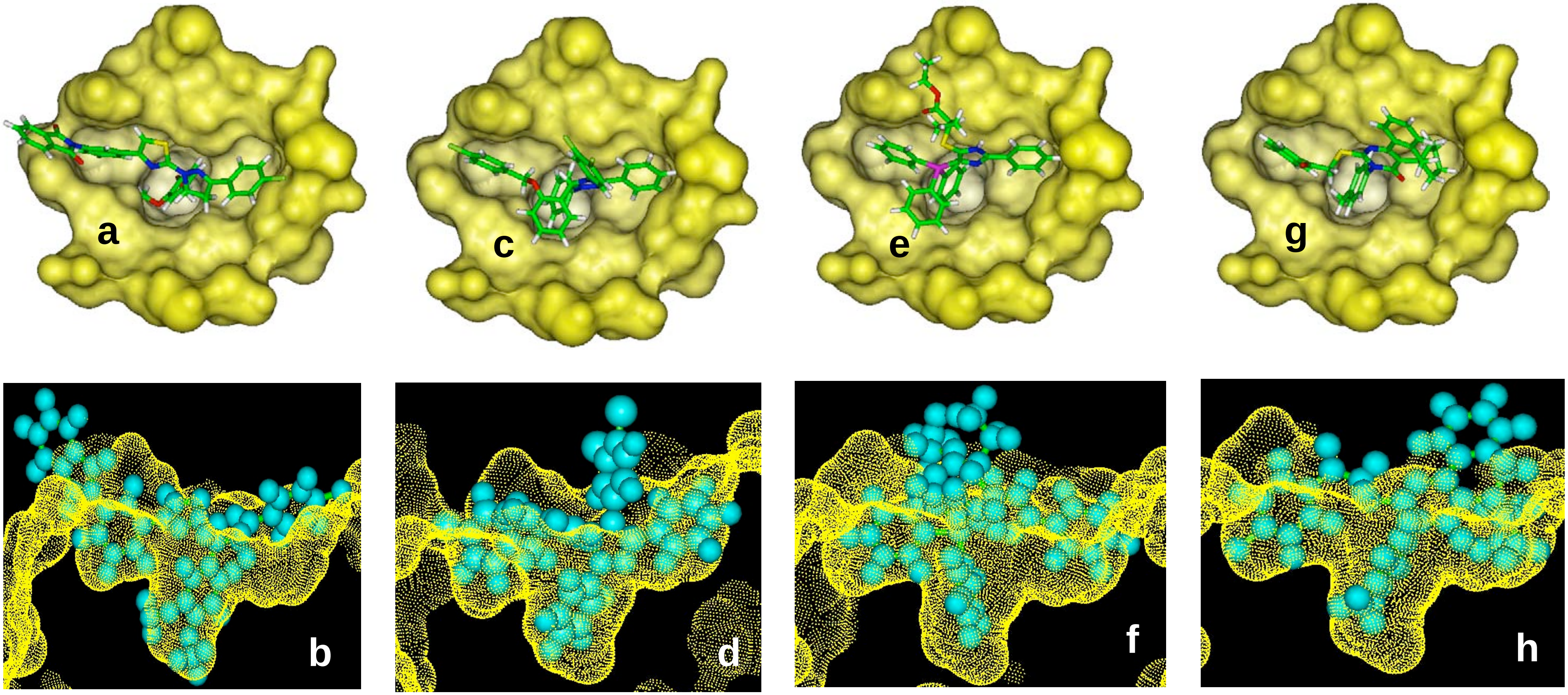

Cpds	MP15 (a)	MP17 (b)	MP22(c)	MP31(d)
Gold Score	36.93	56.26	50.36	53.61

Figure 4. Potent molecules binding mode analysis predicted from docking study. MDM2 binding surface is displayed in yellow (dot or solid) surface, and ligand is rendered as stick or ball-stick. (a) and (b) show the MP15 binding into the MDM2 pocket, (a is for top view and b for side view). (c) and (d) show the MP17 binding into the MDM2 pocket. (e) and (f) show the MP22 binding into the MDM2 pocket. (g) and (h) show the MP31 binding into the MDM2 pocket.

Discovery of Novel Small-Molecule Inhibitors of HER2/neu: Combined Ligand-Based and Target-Based Approach.

Rambabu Gundla,[a] Roza kazemi,[a] Ramadevi Sanam,[b] Ravikumar Muttineni,[b] Raveendra Dayam,[b] Sarma A R P Jagarlapudi,[b] Nouri Neamati[a,]*

[a]Department of Pharmaceutical Sciences, University of Southern California,
Los Angeles, CA-90033, USA.

[b]GVK Biosciences Pvt. Ltd. S-1, Phase-1, T.I.E. Balanagar, Hyderabad-500037, India.

Abstract

In an effort to develop a quantitative ligand-binding model for HER2 tyrosine kinase a combined virtual library screening models were developed to identify novel sets of molecules with activity in HER2 overexpressing cells. A search of a 3D database containing 350,000 small molecules using these consensus models yielded 57 compounds. Seven compounds inhibited the growth of SKBr3 cell lines with an IC_{50} value less than 10 µM.

*Corresponding Author:

Tel: 323-442-2341

Fax: 323-442-1390

Email: Neamati@usc.edu.

Introduction

The human epidermal growth factor receptor-2 (HER2) proto-oncogene encodes a 185-kDa glycoprotein that plays a key role in breast cancer. The HER tyrosine kinase receptor family comprises four homologous epidermal growth factor (EGF) receptors: EGFR/ErbB1/HER1, HER2/Neu/ErbB2, HER3/ErbB3, and HER4/ErbB4. The HER family receptors are among the most studied cell signaling families in cancer biology.[1] Each protein has an extracellular ligand-binding domain, a transmembrane region, and an intracellular cytoplasmic domain.[2] The extracellular domain is involved in recognizing and binding ligands that are able to activate receptor. The cytoplasmic domain contains a tyrosine kinase region and a carboxy terminal tail that harbors tyrosine autophosphorylation sites. The HER family receptors have similar structures and a high degree of homology in the tyrosine kinase region, although they possess diverse characteristics that determine their signaling specificity. The tyrosine kinase domains of HER2 and HER4 show approximately 80% homology to that of HER1, whereas HER3 lacks intrinsic tyrosine kinase activity.[3] Interestingly, the extracellular domains are less conserved among the four receptors, which is indicative of different specificity in ligand binding.

The HER receptors exist as inactive monomers. A variety of ligands can bind to extracellular domains of HER1, HER3 and HER4 and activate these receptors. These ligands have different specificities for each receptor, resulting in different cellular signaling effects.[4] There is no known ligand for HER2, rendering it as an orphan receptor. Upon binding to ligands, the extracellular domains of HER1, HER3, and HER4 receptors undergo conformational changes that allow activation of the receptors by either a homodimerization or a heterdimerization process, which is essential to stimulate the tyrosine kinase activity of the receptors for subsequent generation of an intracellular signal. The pairing of two receptors of the same type results in ‘homodimers’, whereas pairing of two different type of receptors produces ‘heterodimers’. Interestingly, constitutive conformation of the extracellular domain of HER2, an orphan receptor, resembles the conformation of ligand activated extracellular domains of the other HER receptors. This autoactivated conformation enables HER2 to perform as a preferred dimerization partner for all the other HER receptors.[5, 6]

In a variety of human cancer cells, aberrant signaling involving HER receptors stimulate pathways that activate many of the properties associated with cancer, including proliferation, migration, metastasis, angiogenesis, and resistance to apoptosis. Due to the high frequency of abnormalities in receptor signaling in human cancers, the HER family is an attractive target for therapeutic development. The frequently observed causes of signaling abnormalities in cancers involving HER receptors are overexpression of receptors, overproduction of growth factor ligands, and ligand-independent receptor activation. The HER receptors are overexpressed or deregulated in a wide variety of cancers including breast, colorectal, ovarian, prostate, and non-small cell lung cancers. Importantly, overexpression of HER receptors is associated with poor disease prognosis and reduced survival. Mounting pre-clinical and clinical evidence supports the rationale behind the HER family targeted anticancer therapeutic approaches. Although the complexities of the signaling pathways involving the HER family of receptors are not fully understood, several possible points within the pathways have been identified to be therapeutically advantageous if interrupted.[7] Drugs targeting HER family fall into three main categories depending on the receptor region targeted: extracellular, intracellular and nuclear. The most promising and advanced therapeutic strategies targeting HER receptors are monoclonal antibodies and small-molecule tyrosine kinase inhibitors. Intensive research over the last 20 years in these areas has yielded a number of promising anticancer therapeutics. Currently, five anticancer therapeutics targeting the HER receptor family have been approved. Two of them are humanized antibodies, trastuzumab (Herceptin) and cetuximab (Erbitux), targeted to the extracellular domains of HER2 and HER1, respectively. Remaining three of them are small-molecule tyrosine kinase inhibitors, Gefitinib **(1)**, and Erlotinib **(2),** targeted to the HER1 tyrosine kinase domain and GW2016/Tykerb/Lapatanib **(3)** targeted to the HER2 tyrosine kinase domain[8] **(Figure1).** Several small-molecule HER tyrosine kinase inhibitors are being investigated in various stages of clinical trials.[9,10] These compounds compete with ATP for binding to the ATP site on the receptor's intracellular tyrosine kinase domain. By binding to the ATP site and inhibiting catalytic activity, they block autophosphorylation of key tyrosine residues on the receptor kinase domain. This disrupts activation of the receptor mediated downstream signaling cascades. Considering the enormous research activity in the discovery of anticancer therapeutics targeting the HER receptor family and small molecule inhibitors that target the intracellular HER2 appear to be a very promising approach towards treating HER2 mediated cancers. These molecules act by binding either reversibly or irreversibly to the C-terminal tyrosine kinase domain of HER2, thereby inhibiting autophosphorylation of the receptor and therefore activation. Here, the study emphasis on HER2 targeted small-molecule therapeutics.

In the drug discovery process, computational methodologies are well-established useful tools. Other technologies, such as combinatorial chemistry and high throughput screening (HTS) can be used to synthesize and test thousands of compounds. A variety of computational techniques are currently available to rapidly screen the compound libraries. Virtual screening uses computational models to predict biological activity of compounds from existing databases or virtual libraries. This results in identification of molecules against a drug target of interest. There are two basic approaches in virtual screening depending on the availability of 3D structure of the drug target. If a 3D structure of the drug target is available, either from an experimental (X-ray, NMR) or theoretical (homology modeling) technique, structure-guided drug design procedures such as docking can be applied. Otherwise, ligand-based drug design methods for example QSAR and pharmacophore models can be used. The two screening approaches could be used separately or combined.[11] In this context, with an aim to discover small-molecule HER2 inhibitors, we employed a consensus model based on pharmacophore and docking simulations. In this study we also present novel HER2 inhibitors with activity in SKBr3 cells overexpressing HER2.

Materials and Methods

Database Mining and Ligand Preparation. Currently, there is only one FDA approved tyrosine kinase inhibitor (Tykerb/GW2016) **(3)** selectively targeting HER2 available for cancer treatment. Apart from this, there are two clinically approved HER1 specific tyrosine kinase inhibitors gefitinib **(1),** and erlotinib **(2)** also that inhibit HER2 phosphorylation and downstream signaling cascades in HER2/HER3 overexpressing cancer cells. It has been observed that most of the HER tyrosine kinase inhibitors in clinical development also show cross receptor activity. Tykerb (GW-2016) **(3)** is a reversible dual HER2 and HER1 tyrosine kinase inhibitor.[12] The quinazoline derivative represents a first generation HER2 targeted small-molecule anticancer agent.

Our in house HER database consists of 4500 HER2 antagonists collected from 250 references.[13] 1200 molecules have IC_{50} values for human HER2. In order to develop a virtual screening model targeting HER2 around 474 molecules were selected based on experimentally determined IC_{50} values, structural diversity and similar assay conditions.[14-41]

All ligand structures were built in Cerius2 and minimized using Open Force Field (OFF) methods with the steepest descent algorithm.[42] A gradient convergence value of 0.001 k.cal/mol was used. Partial atomic charges were calculated using the Gasteiger method. The resulting geometries with partial charges were used for docking calculations and the mol files of all molecules were exported and minimized using modified CHARMM force field in Catalyst software package.[43] Conformational analysis was carried out with Confirm module. Poling algorithm of Confirm module was used to generate 250 conformations for each molecule with in 20 k.cal/mol.[44]

Pharmacophore Model Generation and Validation. Pharmacophore modeling correlates activities with the spatial arrangement of various chemical features. A set of 474 HER2 inhibitors with activity data (IC_{50}) spanning over 5 orders of magnitude (pIC_{50} = 3-9) were selected. The data set were divided into training and test set. The training set was selected by considering both structural diversity and wide activity range. Highly active, moderately active and also inactive compounds were included in order to obtain critical information on pharmacophore requirements. This training set was used to generate quantitative pharmacophore models while some of the highly active molecules were used to generate qualitative pharmacophore models.

Comman feature hypotheses (qualitative models) were produced by comparing a set of conformational models and a number of 3D configurations of chemical features shared among the training set molecules. This results in a qualitative model wherein important chemical features can easily be identified. For chemically meaningful patterns it is important to identify such chemical features before proceeding to the quantitative model generation. In order to confirm essential features among HER2 inhibitors, 10 common feature hypotheses were generated using most active molecules **(3-9)** (Figure 2). In all these hypotheses hydrogen bond acceptors (HBA), hydrogen bond donor (HBD) and hydrophobic aromatic (HRA) groups are common features. However, these models cannot be directly used for prediction of biological activities for the compounds obtained from database. Therefore, we used quantitative model that can predict the biological activities of compounds.

In the quantitative model, the 22 compounds training set **(3, 7-27)** was selected with the above criteria (Figure 1, 2 and 3). A database of 452 known HER2 inhibitor was used as a test set to validate quality of the pharmacophore. Compounds were classified as: highly active (pIC_{50} >6.5) moderately active (pIC_{50} = 6.5-5) and inactive (pIC_{50} <5). While generating quantitative model, a minimum of 0 to a maximum of 5 features involving HBA, HBD and HRA features were selected and used to build a series of hypotheses using default uncertainty value of 3. In general, pharmacophore models should be statistically significant, predict activity of the molecules accurately and identify active compounds from a database. Therefore, the derived pharmacophore map was validated using cost analysis, test set prediction, enrichment factor, and goodness of hit.

Qualitative pharmacophore model and quantitative pharmacophore model were developed using HipHop and HypoGen modules respectively, implemented in the Catalyst software package.[43]

Modeling of Active and Inactive States of HER2 Structure. The HER receptors show close homology in their sequence and domain organization: they have a ~600-residue-long extracellular region with four domains responsible for ligand binding, a single transmembrane helix, and an ~500-residue long intracellular region with the most conserved tyrosine kinase domain, followed by a less conserved regulatory tail at the C-terminal end of the protein. To provide a molecular basis for understanding the role of HER2 in signalling and cancer, we tried to model active and inactive states of the receptor based on co-crystal structures of HER1 (1M17 PDB[45]and 1XKK PDB[46] bound to Erlotinib (OSI-774) (**2**) and Tykerb (GW572016) **(3)** respectively. The overall fold of these two crystal structures is similar, but there are significant differences in the orientation of the N and C-terminal lobes, the C-terminal tail, and helix. These orientations define the shape of the ATP binding pocket and conformation of the activation loop. The N and C-terminal lobes of kinases are connected by a flexible hinge region. The relative orientation of the two lobes with respect to each other influences the shape of the ATP binding cleft and is dependent on the activation state of the kinase and the presence of ligands. The ATP binding cleft in the HER1-Tykerb co-crystal structure is in a relatively closed conformation. The ATP binding cleft in the HER1-Erlotinib co-crystal structure is in a more open conformation. The N- terminal lobe in HER1-Tykerb complexed is rotated ~12° relative to its position in HER1-Erlotinib. The magnitude of the difference suggests that the two inhibitors target different forms of the enzyme, active and inactive. In HER1-Tykerb, residues 971 to 980 of the C- terminal tail form a short alpha-helix that packs along the hinge region connecting the N- and C-terminal lobes. This helix partially blocks the front of the ATP binding cleft. A second helical segment containing residues 983 to 990 extends along the NH2- terminal lobe of the protein. HER1-Erlotinib has active activation-loop conformations where as HER1-Tykerb has inactive activation-loop conformations.[47] Based on these two co-crystal structures, 1M17 and 1XKK, we tried to obtain the 3D model of HER2 in active and inactive states of HER2. The amino acid sequence of HER2 kinase domain was taken from Swissprot database (P04626). ClustalW program was used to identify the homologous regions between the two proteins. The catalytic domain of the EGFR and HER receptors is well conserved with 80% sequence identity (Figure 4). Amino acid residues Asp746 and Cys751 play a prominent role in ATP binding pocket and confer selectivity on EGFR and HER2 ligands.

Entire modeling was done using Insight II suite of softwares (Accelrys, Inc). Modeler algorithm was used to build both active and inactive-like conformations of HER2. Modeler is an automated comparative modeling program designed to find the most probable structure of a protein sequence, given its alignment with related structures. The model was obtained by the optimal satisfaction of spatial restraints derived from the alignment and was expressed as a probability density function for the features restrained. The optimization procedure is a variable target function method that applies conjugate gradients algorithm to position all non-hydrogen atoms. The structure has been further refined using molecular dynamics simulation in explicit water following standard procedure. Both the resultant models have the correct stereochemistry as judged by the Ramachandran plot and conserves the topological and active site features of the active and inactive-like conformations of HER1. The DFG motif of kinases is a part of the activation-loop and involved in coordination of ATP. The side chain conformations of these amino acids were checked and found to be in similar orientation as that of the template structures. The homology models of HER2 active and inactive states were built to explore whether inhibitors favorably bind to active or inactive states of HER2.

Moreover, we wanted to determine which state of HER2 (active or inactive) is suitable for docking simulations.

Docking Studies. Docking calculations were performed using GOLD, Glide, and eHITS as described below on the modeled active and inactive states of HER2. For each ligand, the best 20 scored poses were saved.

1. GOLD.[48] A collection of 474 minimized HER2 inhibitors were docked on to HER2 active and inactive state with the GOLD software in a 20Å radius surrounding the active site and ranked according to its score. Standard set parameters of GOLD were used through out simulations. For each of the 10 independent genetic algorithm runs, with a selection pressure 1.1, 100000 operations were performed on a set of 5 islands with a population size of 100 individuals. Default operator weights were used for crossover, mutation, and migration of 95, 95 and 10 respectively. Default cut-offs values of 2.5 Å for hydrogen bonds and 4.0 Å for van der Waals were employed. All other values were set to the default. Top 20 poses were saved for each ligand and best score values were taken to correlate with experimental data.

2. Glide.[49] Glide XP calculations were performed with Impact version 3.5. The protein charged groups that were not located in the binding pocket nor involved in salt bridges were neutralized. The center of the grid enclosing a box was defined by the center of the bound dummy ligand fragment at the hinge region of HER2 protein. The enclosing box and bounding box dimensions were fixed to 14 and 10 Å, respectively. No further modifications were applied to the default settings. A total of 20 poses were saved for each ligand and calculated Glide score for conformations of each molecule. High score value for each ligand was selected to correlate to its biological activity data.

3. eHITs.[50] Docking was performed for these 474 HER2 inhibitors on to HER2 active and inactive states by using the eHiTS docking program. eHITS evaluates all the possible protonation states for the receptor and ligands automatically for every receptor-ligand pair. The docking method systematically covers the part of the conformational and positional search space to avoid severe steric clashes. The top 20 conformations were saved and eHITs scores were calculated for each of the 20 saved ligand conformations. High score value of each ligand was selected to correlate to its biological activity.

Consensus Model Generation.[11] To generate a consensus model, a multiple regression analysis was carried out using pharmacophore predicted activity (Hypo-5) along with the three different scores from GOLD, Glide and eHITS as descriptors (X)) and experimental pIC_{50} as a dependant variable (Y). Of the 474 ligands, 158 were used in the training set and 316 in the test set. The combination of predicted activity from pharmacophore, GOLDscore, Glidescore and eHITSscore gave a better model than any other models with independent and/or combination of scores and predicted activity from pharmacophore (Hypo5 model).

Database Screening. The Hypo5 model was used to screen a database of 350,000 compounds. The search retrieved 961 hits. We selected 531 compounds with a predicted IC_{50} values <1 µM, for docking studies. GOLD, Glide and eHITs scores were calculated for all the 531 molecules using active and inactive state of HER2. All these values were then substituted in the Eq. 1 and Eq. 2 and calculated predicted activity value for each compound. Finally, 57 active hits with a predicted activity values of <100 µM were selected for in-vitro assay against human breast cancer cell line, SKBr3, which is known to overexpress HER2.[51-53]

Cell Culture. The human breast cancer cell line SKBr3 obtained from American Type Culture Collection (Manassas, VA) was used for the cytotoxicity assay. Cells were maintained as monolayer cultures in RPMI 1640 supplemented with 10% fetal bovine serum (Gemini-Bioproducts, Woodland, CA) and 2 mM L-glutamine at 37°C in a humidified atmosphere of 5% CO_2. To remove the adherent cells from the flask for pass aging and counting, cells were washed with PBS without calcium or magnesium, incubated with a small volume of 0.25% trypsin-EDTA solution (Sigma-Aldrich, St. Louis, MO) for 5 to 10 minutes, and washed with culture medium and centrifuged. All experiments were done using cells in exponential cell growth. A 10 mM stock solution of each compound was prepared in DMSO and stored at –80°C. Further dilutions were freshly made in media.

Cytotoxicity Assay. Cytotoxicity was measured using a 3-(4,5-dimethylthiazol-2-yl)-2,5-diphenyltetrazolium bromide (MTT) assay. Briefly, 8,000 cells were seeded in 96-well microtiter plates and allowed to attach over night. Cells were subsequently treated with a continuous exposure to the corresponding drugs for 72 hours. A MTT solution (at a final concentration of 0.3 mg/mL) was added to each well and cells were incubated for 4 hours at 37 °C. After removal of the medium, DMSO was added and the absorbance was read at

570 nm. The IC_{50} values were then determined for each drug from a plot of log value of drug concentration versus percentage inhibition of cells.

Results and Discussion

Pharmacophore Models. The best common feature pharmacophore model indicated the importance of HBA, HBD and HRA, which were further confirmed in the quantitative models. In the quantitative model, several hypotheses were generated using the most diverse training set **(3, 7 - 27)** along with experimental activities (Table1**)**. Top ten hypotheses were comprised of HBA, HBD, HRA features. The statistical values of the 10 hypotheses such as cost values, correlation (r) and root mean square deviations (RMSD) are given in Table 2. In addition to estimation of activity of training set molecules, the pharmacophore model should also estimate the activity of the test set compounds accurately. Two statistical methods were employed to rank the ten hypotheses. In the first method, all the 10 hypotheses were evaluated using a test set of 452 known HER2 inhibitors, which were not included in the training set. These molecules are covering a wide range of activities spanning from $pIC_{50} = 3$ to 9. Predicted activities of test set were calculated using all ten hypotheses and correlated with experimental activity. Out of 10 hypotheses, Hypo5 showed better correlation coefficient than other nine. A second statistical test, including calculation of false positives, false negatives, enrichment and goodness of hit were calculated to determine the robustness of the hypotheses. Under all validation conditions, Hypo5 showed better results than the other nine hypotheses.

On the basis of the Hypo5 model, predicted IC_{50} values for 22 training set compounds along with fitness score are presented in Table 1. In the training set, all six highly active compounds were correctly predicted as highly active. Of the seven moderately active compounds, six were predicted as moderately active, while one compound was predicted as highly active and all nine inactive compounds were predicted as inactive. From Table 1, it was also noticed that compounds were not only correctly predicted as high, moderate and low activity but also the fit values confer a good measure of how well the defined features of Hypo5 fit with the molecule. In the training set, it was observed that all features of Hypo5 (HBA, HBD and three HRA) were mapped on to the highly active compounds but in moderately active compounds, one or more features did not map well or were partially missing. In the inactive compounds set, one or more features were totally missing (Figure 5).

Database mining was performed using the BEST flexible searching technique. Hypo5 was used to screen a database of known HER2 inhibitors. Based on the data and considering a compound $pIC_{50} \geq 6.5$ as a highly active compound, number of parameters such as hit list (H_t), number of active percent of yields (%Y), percent ratio of actives in the hit list (%A), enrichment factor (E), false negatives, false positives and goodness of hit score (GH) were calculated (Table 3). From the table 3, 64 false positives and 55 false negatives were observed. An enrichment factor of 1.67 and a GH score of 0.536 indicate the quality of the model. Scatter plot of predicted activity obtained from Hypo5 against the experimental activity (pIC_{50}) of the training and test set is shown in Figure 6. From this plot it was noticed that the Hypo5 model has a greater tendency to show false positives. To avoid false positives and limit false negatives and also to understand the binding mechanism of inhibitors to HER2, we further extended this study to structure based ligand design.

Validation of HER2 Active and Inactive States and Docking Simulations. We constructed homology models for HER2 active and inactive state conformations to predict the correct binding mode. First, the 3D models of HER2 (active and inactive states) were validated by docking the Erlotinib (the bound ligand in co-crystal structure of active state of HER1 (1M17 PDB)) on to HER2 active state model and Tykerb (the bound ligand in co-crystal structure of inactive state of HER1 (1XKK PDB)) on to HER2 inactive model using GOLD. The ATP binding site was defined as the active site. Inspection of the binding modes of the two ligands inside the ATP binding site of HER2 models showed general agreement with the kinase family hinge region interactions and correlates with established pharmacophore model. To analyze the binding interactions of molecules with HER2 active and inactive states, known inhibitors were compared with crystal structures of HER1 active and inactive states (Figures 7 and 8). In the HER2 active state complexed with erlotinib, the N(1) of quinazoline ring accepts a N–H····N bond from the backbone N–H of Met801 (Figure 7). A strong C–H····O hydrogen bond is formed between the activated C(2)–H group and the backbone carbonyl oxygen of Glu799. The distance between the N3 atom of the quinoline and OH of Thr798 is 3.54 Å. Additionally, the 6- and 7-substituents project outside the active site (actually, in the cleft region between the C-terminal and N-terminal lobes). The meta-substituted 4-anilino group fits well in the hydrophobic pocket surrounded by amino acid residues Phe864, Asp863, Val797, Leu796, Met774, Ile752, Lys753, Phe731. In the complex of HER2 inactive state and Tykerb/GW2016 that the N1 atom of the quinoline is involved in a H-bond interaction with the backbone NH of Met801 at a distance of 2.04 Å. The distance between the N3 atom of the quinoline and OH of Thr798 is 3.39 Å. The aniline portion of the inhibitor is surrounded by residues Thr798, Lys753, Thr862, and Asp841. The pyridyl-methoxy group lies in a pocket surrounded by Val797, Met774, Arg784, Ser783, Phe864, Gly865 and Leu866 (Figure 8). It was observed from the docking studies that the overall interactions and the number of (C–H···O), (O–H···N) and (N–H···N) interactions of ligands that are forming with the two states of HER2 are nearly same. [54] A second type of analysis was carried out to verify goodness of these two models for our virtual screening study and to further discriminate the performance GOLD, Glide and eHITs programs. A diverse small set of molecules **(3, 7 -27)** was docked on to the active and inactive states of HER2. The individual scores of GOLD, Glide and eHITs of these twenty two compounds onto the HER2 active and inactive states were correlated with experimental activities (pIC_{50}) (Table 4). The docking results and the correlation of their scores with experimental activity further validated our models.

Next, we wanted to know which score correlates better with experimental activity of HER2 antagonists. In order to answer this question, the docking study with a database of 474 known HER2 inhibitors on HER2 active and inactive states were carried out. The individual scores of GOLD, Glide and eHITs were then used to correlate with experimental pIC_{50} values (Table 5). Overall we found that docking with GOLD, Glide and eHITs performed equally well. We also observed that docking study could limit false positives but showed more false negatives. To overcome the false positives and false negatives, we developed a combined model referred as a consensus model.

Consensus Model. As discussed above, no single scoring function and parmacophore prediction performed accurately enough for the 474 inhibitors for both active and inactive state of HER2. In principle, it should be possible to determine before hand which score is best suited in a given case and then to use this score to decide whether a docking result is likely to represent a hit or not. However, the complexity of the relationship between the performance of a given score and uniqueness of a given binding site and the docked compound complicates formulating explicit rules for such a relationship. Therefore, we chose to build a consensus model by taking predicted pharmacophore activity and docking scores from GOLD, Glide and eHITs obtained from active and inactive states of HER2 as descriptors.[54]

The final equations, Eq. 1 and Eq. 2 were generated for inactive and active states of HER2 using multiple linear regressions

$$\text{Pred\_activity } (pIC_{50}) = 0.233 + 0.7104 \times \text{"Pharma\_pIC}_{50}\text{"} - 0.063 \times \text{"Glide"} + 0.013 \times \text{"Gold"} - 0.159 \times \text{"eHITS"} \quad (1)$$

$n = 158$, $r^2 = 0.846$, $q^2 = 0.684$, $F = 90.12$, $PRESS = 32.691$ and $r^2_{pred} = 0.69$

$$\text{Pred\_Activity } (pIC_{50}) = 0.206 + 0.698 \times \text{"Pharma\_pIC}_{50}\text{"} - 0.096 \times \text{"Glide"} + 0.012 \times \text{"Gold"} - 0.127 \times \text{"eHITS"} \quad (2)$$

$n = 158$, $r^2 = 0.763$, $q^2 = 0.674$, $F = 88.50$, $PRESS = 33.691$ and $r^2_{pred} = 0.66$.

Eq. 1 confirms the predicted power of consensus model obtained with docking scores of HER2 inactive state along with pharmacophore predicted activity as proven by significant statistical parameters. Interestingly, Eq. 2 obtained with docking scores of HER2 active along with pharmacophore predicted activity afforded a very similar and good correlation with biological activity values (Figure 9). The scatter plot of Figure 11 shows remarkable correlation between predicted activity values from consensus models of both states versus experimental biological activity. Further, Eq. 1 and Eq. 2 were used to calculate a number of statistical parameters such as hit list (Ht), percent active (%Y), percent ratio of actives in the hit list (%A), enrichment factor of (E), false negatives, false positives, and goodness of hit score to cross validate the predicted power of the models (Table 6).

We noticed that the consensus models significantly reduced the false positives and false negatives (Figure 9 and Table 6). Equations Eq. 1 and Eq. 2 show similar statistical parameters and suggest that a good HER2 inhibitor would have to fit with the pharmacophore and have to successfully interact with both active and inactive states of HER2. Therefore, we used these two equations to screen the compounds against HER2.

Compound Selection and Cell Growth Inhibition Assay. The compound selection process that was implemented in the present study is shown as a flowchart in **Figure 10**. Finally, 57 compounds were selected for cytotoxicity assay in SKBr3 cell lines overexpressing HER2.[51-53] Tweleve compounds were cytotoxic with IC_{50} values ranging from 2 to 50 μM and are presented in this report (Table 7).

It is observed from the Table 7 that the tricyclic 4-anilino benzo[g]quinolines analogues **(1** and **2)** were found to be highly potent compounds among the tested compounds. The tricyclic 4-anilino benzo[g]quinoline compound **1** and **2** **i**nhibited the proliferation of SKBr3 cell lines, which highly overexpresses HER2, with IC_{50} value of 2.2 and 2.5µM, respectively. Compound **1** and **2** provide activity equivalent to that of the corresponding the tricyclic 3-cyanobenzo[g]quinoline with a 4-phenoxyanilino group at the 4-position, which were earlier reported as competitive inhibitors with ATP on a panel of kinase targets.[55,22] It is also observed that the potency of the compounds decreases with increasing aliphatic chain between benzo[g]quinolin-4-amine and phenyl group (**3). The** replacement of phenyl group of compound **3** with a 1,4-methylpiperazine led to compound **4** with decreased inhibitory activity. As envisaged by the pharmacophore model, most of the 2-methylquinoline or 2-methylquinazoline (**5 - 6**) exhibited enhanced inhibitory activity as compared to compound **1** against the proliferation of SKBr3 cell lines.[40] Partial mapping of the best pharmacophore model onto one of the tested compounds, a quinoline analogue (**7**), illustrates that two carbon linker between N and phenyl group of aniline is not required to enhance the activity of the compound. Compound **8**, containing 4-anilino thieno[2,3-d]pyrimidin core, showed with IC_{50} values of 9 µM. The two carbon linker containing thieno[2,3-d]pyrimidin analogue (compound **9)** inhibited the SKBr3 cell growth with IC_{50} value 14.10 µM, slightly higher than that of compound **8** (9.0 µM). Surprisingly, compound **10**, thieno[2,3-d]pyrimidine-4-thiol analogue, showed moderate activity with IC_{50} value of 16.5 µM. The [1,2,4]triazolo[1,5-a]pyrimidin-7-amine scaffold containing compounds (**11** and **12**) displayed moderate cytotoxic activity on the SKBr3 cell lines and the growth of the cell lines was inhibited with IC_{50} values of 9.0 and 4.8 μM, respectively. These results suggest that compound **1** with different C-6 and C-7 substituents on the tricyclic moiety warrants further modifications. Further structural optimization to enhance activity is in progress and the results will be described in the due course.

Conclusions

A set of novel cytotoxic compounds with diverse structural scaffolds were identified using two consensus models Eq. 1 and Eq. 2 that were generated on the basis of known HER2 inhibitors. Many of these compounds possess amenable chemical and structural features are useful potential leads for drug design strategies targeting HER2. Further structural optimization to enhance HER2 inhibitory activity is in progress and will be reported in due course.

Acknowledgment

This study was supported in part by DOD Concept Award to Nouri Neamati. Rambabu Gundla would like to thank Sunita Tajne, Jinxia Deng and Bikas Debnath for their technical support.

References

1. Schlessinger, J. Cell signaling by receptor tyrosine kinases. *Cell* **2000,** 103, 211-25.
2. Wells, A. EGF receptor. *Int J Biochem Cell Biol* **1999,** 31, 637-43.

3. Guy, P. M.; Platko, J. V.; Cantley, L. C.; Cerione, R. A.; Carraway, K. L., 3rd. Insect cell-expressed p180erbB3 possesses an impaired tyrosine kinase activity. *Proc Natl Acad Sci U S A* **1994,** 91, 8132-6.
4. Jones, J. T.; Akita, R. W.; Sliwkowski, M. X. Binding specificities and affinities of egf domains for ErbB receptors. *FEBS Lett* **1999,** 447, 227-31.
5. Cho, H. S.; Mason, K.; Ramyar, K. X.; Stanley, A. M.; Gabelli, S. B.; Denney, D. W., Jr.; Leahy, D. J. Structure of the extracellular region of HER2 alone and in complex with the Herceptin Fab. *Nature* **2003,** 421, 756-60.
6. Garrett, T. P.; McKern, N. M.; Lou, M.; Elleman, T. C.; Adams, T. E.; Lovrecz, G. O.; Kofler, M.; Jorissen, R. N.; Nice, E. C.; Burgess, A. W.; Ward, C. W. The crystal structure of a truncated ErbB2 ectodomain reveals an active conformation, poised to interact with other ErbB receptors. *Mol Cell* **2003,** 11, 495-505.
7. Hynes, N. E.; Lane, H. A. ERBB receptors and cancer: the complexity of targeted inhibitors. *Nat Rev Cancer* **2005,** 5, 341-54.
8. Moy, B.; Kirkpatrick, P.; Kar, S.; Goss, P. Lapatinib. *Nat Rev Drug Discov* **2007,** 6, 431-2.
9. Reid, A.; Vidal, L.; Shaw, H.; de Bono, J. Dual inhibition of ErbB1 (EGFR/HER1) and ErbB2 (HER2/neu). *Eur J Cancer* **2007,** 43, 481-9.
10. Spector, N.; Xia, W.; El-Hariry, I.; Yarden, Y.; Bacus, S. HER2 therapy. Small molecule HER-2 tyrosine kinase inhibitors. *Breast Cancer Res* **2007,** 9, 205.
11. Moro, S.; Bacilieri, M.; Deflorian, F. Combining ligand-based and structure-based drug design in the virtual screening arena. *Expert Opin. Drug Discov.* **2007,** 2, 37-49.
12. Feld, R.; Sridhar, S. S.; Shepherd, F. A.; Mackay, J. A.; Evans, W. K. Use of the epidermal growth factor receptor inhibitors gefitinib and erlotinib in the treatment of non-small cell lung cancer: a systematic review. *J Thorac Oncol* **2006,** 1, 367-76.
13. Kinase Database. Informatics, GVK Biosciences Pvt. Ltd, S-1, Phase-1, T.I.E. Balanagar, Hyderabad – 500 037, India.
14. Gazit, A.; Osherov, N.; Posner, I.; Yaish, P.; Poradosu, E.; Gilon, C.; Levitzki, A. Tyrphostins. 2. Heterocyclic and alpha-substituted benzylidenemalononitrile tyrphostins as potent inhibitors of EGF receptor and ErbB2/neu tyrosine kinases. *J Med Chem* **1991,** 34, 1896-907.
15. Singh, J.; Dobrusin, E. M.; Fry, D. W.; Haske, T.; Whitty, A.; McNamara, D. J. Structure-based design of a potent, selective, and irreversible inhibitor of the catalytic domain of the erbB receptor subfamily of protein tyrosine kinases. *J Med Chem* **1997,** 40, 1130-5.
16. Sun, L.; Tran, N.; Tang, F.; App, H.; Hirth, P.; McMahon, G.; Tang, C. Synthesis and biological evaluations of 3-substituted indolin-2-ones: a novel class of tyrosine kinase inhibitors that exhibit selectivity toward particular receptor tyrosine kinases. *J Med Chem* **1998,** 41, 2588-603.
17. Smaill, J. B.; Rewcastle, G. W.; Loo, J. A.; Greis, K. D.; Chan, O. H.; Reyner, E. L.; Lipka, E.; Showalter, H. D.; Vincent, P. W.; Elliott, W. L.; Denny, W. A. Tyrosine kinase inhibitors. 17. Irreversible inhibitors of the epidermal growth factor receptor: 4-(phenylamino)quinazoline- and 4-(phenylamino)pyrido[3,2-d]pyrimidine-6-acrylamides bearing additional solubilizing functions. *J Med Chem* **2000,** 43, 1380-97.

18. Wells, G.; Seaton, A.; Stevens, M. F. Structural studies on bioactive compounds. 32. Oxidation of tyrphostin protein tyrosine kinase inhibitors with hypervalent iodine reagents. *J Med Chem* **2000,** 43, 1550-62.

19. Tsou, H. R.; Mamuya, N.; Johnson, B. D.; Reich, M. F.; Gruber, B. C.; Ye, F.; Nilakantan, R.; Shen, R.; Discafani, C.; DeBlanc, R.; Davis, R.; Koehn, F. E.; Greenberger, L. M.; Wang, Y. F.; Wissner, A. 6-Substituted-4-(3-bromophenylamino)quinazolines as putative irreversible inhibitors of the epidermal growth factor receptor (EGFR) and human epidermal growth factor receptor (HER-2) tyrosine kinases with enhanced antitumor activity. *J Med Chem* **2001,** 44, 2719-34.

20. Smaill, J. B.; Showalter, H. D.; Zhou, H.; Bridges, A. J.; McNamara, D. J.; Fry, D. W.; Nelson, J. M.; Sherwood, V.; Vincent, P. W.; Roberts, B. J.; Elliott, W. L.; Denny, W. A. Tyrosine kinase inhibitors. 18. 6-Substituted 4-anilinoquinazolines and 4-anilinopyrido[3,4-d]pyrimidines as soluble, irreversible inhibitors of the epidermal growth factor receptor. *J Med Chem* **2001,** 44, 429-40.

21. Wissner, A.; Overbeek, E.; Reich, M. F.; Floyd, M. B.; Johnson, B. D.; Mamuya, N.; Rosfjord, E. C.; Discafani, C.; Davis, R.; Shi, X.; Rabindran, S. K.; Gruber, B. C.; Ye, F.; Hallett, W. A.; Nilakantan, R.; Shen, R.; Wang, Y. F.; Greenberger, L. M.; Tsou, H. R. Synthesis and structure-activity relationships of 6,7-disubstituted 4-anilinoquinoline-3-carbonitriles. The design of an orally active, irreversible inhibitor of the tyrosine kinase activity of the epidermal growth factor receptor (EGFR) and the human epidermal growth factor receptor-2 (HER-2). *J Med Chem* **2003,** 46, 49-63.

22. Tsou, H. R.; Overbeek-Klumpers, E. G.; Hallett, W. A.; Reich, M. F.; Floyd, M. B.; Johnson, B. D.; Michalak, R. S.; Nilakantan, R.; Discafani, C.; Golas, J.; Rabindran, S. K.; Shen, R.; Shi, X.; Wang, Y. F.; Upeslacis, J.; Wissner, A. Optimization of 6,7-disubstituted-4-(arylamino)quinoline-3-carbonitriles as orally active, irreversible inhibitors of human epidermal growth factor receptor-2 kinase activity. *J Med Chem* **2005,** 48, 1107-31.

23. Llauger, L.; He, H.; Kim, J.; Aguirre, J.; Rosen, N.; Peters, U.; Davies, P.; Chiosis, G. Evaluation of 8-arylsulfanyl, 8-arylsulfoxyl, and 8-arylsulfonyl adenine derivatives as inhibitors of the heat shock protein 90. *J Med Chem* **2005,** 48, 2892-905.

24. Borzilleri, R. M.; Zheng, X.; Qian, L.; Ellis, C.; Cai, Z. W.; Wautlet, B. S.; Mortillo, S.; Jeyaseelan, R., Sr.; Kukral, D. W.; Fura, A.; Kamath, A.; Vyas, V.; Tokarski, J. S.; Barrish, J. C.; Hunt, J. T.; Lombardo, L. J.; Fargnoli, J.; Bhide, R. S. Design, synthesis, and evaluation of orally active 4-(2,4-difluoro-5-(methoxycarbamoyl)phenylamino)pyrrolo[2,1-f][1,2,4]triaz ines as dual vascular endothelial growth factor receptor-2 and fibroblast growth factor receptor-1 inhibitors. *J Med Chem* **2005,** 48, 3991-4008.

25. Gaul, M. D.; Guo, Y.; Affleck, K.; Cockerill, G. S.; Gilmer, T. M.; Griffin, R. J.; Guntrip, S.; Keith, B. R.; Knight, W. B.; Mullin, R. J.; Murray, D. M.; Rusnak, D. W.; Smith, K.; Tadepalli, S.; Wood, E. R.; Lackey, K. Discovery and biological evaluation of potent dual ErbB-2/EGFR tyrosine kinase inhibitors: 6-thiazolylquinazolines. *Bioorg Med Chem Lett* **2003,** 13, 637-40.

26. Revesz, L.; Blum, E.; Di Padova, F. E.; Buhl, T.; Feifel, R.; Gram, H.; Hiestand, P.; Manning, U.; Rucklin, G. Novel p38 inhibitors with potent oral efficacy in several models of rheumatoid arthritis. *Bioorg Med Chem Lett* **2004,** 14, 3595-9.

27. Bridges, A. J. Chemical inhibitors of protein kinases. *Chem Rev* **2001,** 101, 2541-72.

28. Garcia-Echeverria, C.; Fabbro, D. Therapeutically targeted anticancer agents: inhibitors of receptor tyrosine kinases. *Mini Rev Med Chem* **2004,** 4, 273-83.

29. Stuart, C. G.; Clive, C. M.; Karl, M. S.; Sadie, V.; John, P. M.; Thomas, H. A.; Paul, B.; Witold, F. K. Preparation of heterocyclyl-substituted quinazolines as protein tyrosine kinase inhibitors. *WO 9703069 A1,* **1997**.

30. Stuart, C. G.; Clive, C. M.; Barry, G. S.; Jane, S. K. Preparation of bicyclic heteroaromatic compounds as protein tyrosine kinase inhibitors. *WO 9802437 A1,* **1998**.

31. Ronghui, L.; Peter, J. C.; Steven, W.; Shenlin, H.; Stuart, E.; Robert, G.; Steve, M. Preparation of 1,2,4-triazole-3,5-diamine derivatives as kinase inhibitors. *WO 2002057240 A1,* **2002**.

32. Peter, H. K.; Pruess, S. D.; Elaina, M.; Kay, S. L.; Gyorgi, K.; Istvan, S.; Tamas, B.; Janis, H.; Laszlo, O.; Alex, L.; Aviv, G.; Axel, U.; Reiner, L.; Fairooz, F. K.; Dennis, S.; Cho, T. P. Treatment of platelet derived growth factor-related disorders such as cancers. *US 5958959 A,* **1999**.

33. Chen, H.; Gazit, A.; Levitzki, A.; Hirth, K. P.; Mann, E.; Shawver, K. L.; Tsai, J.; Tang, P. C. Methods and compositions for inhibiting cell proliferative disorders. *US 20020068687 A1,* **2002**.

34. Yu, M.; Etsuya, M. Preparation of aralkylazoles as tyrosine kinase inhibitors useful as antitumor agents. *WO 9803505 A2,* **1998**.

35. Akihiro, T.; Takenori, H.; Etsuya, M. Preparation of 2-styryl-4-(phenoxymethyl)oxazole derivatives as tyrosine kinase inhibitors. *WO 2001077107 A1,* **2001**.

36. Hui, C.; Aviv, G.; Peter, K. H.; Elaina, M.; Laura, K. S.; Jianming, T.; Cho, P. T. Methods and compositions using receptor tyrosine kinase inhibitors for inhibiting cell proliferative disorders, and inhibitor preparation. *US 5789427 A,* **1998**.

37. Neal, R.; Scott, D. K.; Samuel, J. D.; Furzhong, F. Z.; Laura, S.; Ouathek, O. Methods and compositions using bifunctional hsp-binding derivatives for degradation and/or inhibition of HER-family tyrosine kinases and treatment of cancer. *WO 2000061578 A1,* **2000**.

38. Mien-Chie, H.; Lisha, Z. Emodin and related compounds for sensitization of HER2/neu over-expressing cancer cells to chemotherapeutic drugs. *WO 9727848 A1,* **1997**.

39. Stuart, G. C.; Clive, M. C.; Barry, S. G.; Jane, K. S. Preparation of azolylquinazolines and related compounds as protein tyrosine kinase inhibitors. *WO 9802434 A1,* **1998**.

40. Thomas, A. H.; Sadie, V.; Paul, B.; Karl Witold, F.; Stephen Carl, M.; P., M. J. Preparation of quinoline and quinazoline protein tyrosine kinase inhibitors. *WO 9609294 A1,* **1996**.

41. Hugh, R. B.; Grant, J. K.; Stewart, J. S.; Christophe, B. B. Preparation of 4-anilino-5-carbamoylmethoxyquinazolines as selective erbB2 receptor tyrosine kinase inhibitors for use against tumors. *WO 2005118572 A1,* **2005**.

42. Cerius2. 4.11; Accelrys Inc: San Diego, CA, USA, **2005**.

43. Catalyst. 4.11; Accelrys Inc: San Diego, CA, USA, **2005**.

44. Smellie, A. T., S. L.; Towbin, P. Polings-promoting conformational variation. *J. Comput. Chem* **1995,** 16, 171-187.

45. Stamos, J.; Sliwkowski, M. X.; Eigenbrot, C. Structure of the epidermal growth factor receptor kinase domain alone and in complex with a 4-anilinoquinazoline inhibitor. *J Biol Chem* **2002,** 277, 46265-72.

46. Wood, E. R.; Truesdale, A. T.; McDonald, O. B.; Yuan, D.; Hassell, A.; Dickerson, S. H.; Ellis, B.; Pennisi, C.; Horne, E.; Lackey, K.; Alligood, K. J.; Rusnak, D. W.; Gilmer, T. M.; Shewchuk, L. A unique structure for epidermal growth factor receptor bound to GW572016 (Lapatinib): relationships among protein conformation, inhibitor off-rate, and receptor activity in tumor cells. *Cancer Res* **2004,** 64, 6652-9.

47. Liao, J. J. Molecular recognition of protein kinase binding pockets for design of potent and selective kinase inhibitors. *J Med Chem* **2007,** 50, 409-24.

48. GOLD. 1.2; CCDC: Cambridge, UK, **2002**.

49. Friesner, R. A.; Murphy, R. B.; Repasky, M. P.; Frye, L. L.; Greenwood, J. R.; Halgren, T. A.; Sanschagrin, P. C.; Mainz, D. T. Extra precision glide: docking and scoring incorporating a model of hydrophobic enclosure for protein-ligand complexes. *J Med Chem* **2006,** 49, 6177-96.

50. Zsoldos, Z.; Reid, D.; Simon, A.; Sadjad, S. B.; Johnson, A. P. eHiTS: A new fast, exhaustive flexible ligand docking system. *J Mol Graph Model* **2007,** 26, 198-212.

51. Fantin, V. R.; Berardi, M. J.; Babbe, H.; Michelman, M. V.; Manning, C. M.; Leder, P. A bifunctional targeted peptide that blocks HER-2 tyrosine kinase and disables mitochondrial function in HER-2-positive carcinoma cells. *Cancer Res* **2005,** 65, 6891-900.

52. Gril, B.; Vidal, M.; Assayag, F.; Poupon, M. F.; Liu, W. Q.; Garbay, C. Grb2-SH3 ligand inhibits the growth of HER2+ cancer cells and has antitumor effects in human cancer xenografts alone and in combination with docetaxel. *Int J Cancer* **2007,** 121, 407-15.

53. Jin, Y.; Li, H. Y.; Lin, L. P.; Tan, J.; Ding, J.; Luo, X.; Long, Y. Q. Synthesis and antitumor evaluation of novel 5-substituted-4-hydroxy-8-nitroquinazolines as EGFR signaling-targeted inhibitors. *Bioorg Med Chem* **2005,** 13, 5613-22.

54. Aparna, V.; Rambabu, G.; Panigrahi, S. K.; Sarma, J. A.; Desiraju, G. R. Virtual screening of 4-anilinoquinazoline analogues as EGFR kinase inhibitors: importance of hydrogen bonds in the evaluation of poses and scoring functions. *J Chem Inf Model* **2005,** 45, 725-38.

55. Zhang, N.; Wu, B.; Wissner, A.; Powell, D. W.; Rabindran, S. K.; Kohler, C.; Boschelli, F. 4-Anilino-3-cyanobenzo[g]quinolines as kinase inhibitors. *Bioorg Med Chem Lett* **2002,** 12, 423-5.

Figure legends

Figure 1: Clinically used HER family targeted kinase inhibitors.

Figure 2: Training set compounds (**4 – 9**) used to generate qualitative pharmacophore models.

Figure 3: Training set compounds (**10 – 27**) used to generate quantitative pharmacophore models.

Figure4: ClustalW alignment of HER1 (EGFR) and HER2 with highlighted residues of Asp-746, Cys-751 and DFG motif.

Figure 5: A) The three dimensional arrangement of pharmacophoric features in the quantitative pharmacophore model (Hypo5). Green: hydrogen bond acceptor (HBA), blue: hydrophobic aromatics (HRA1- HRA3), magenta: hydrogen bond donor (HBD). B) Mapping of Hypo5 onto Tykerb (**3**). C) Mapping of Hypo5 onto compound **14** from the moderately active category, **D**) Mapping of Hypo5 onto compound **20** from the minimally active category.

Figure 6: Scatter plot of experimental vs predicted activities using pharmacophore model Hypo5.

Figure 7: A) HER1 active state conformation with Erlotinib, B) HER2 active state conformation with Erlotinib.

Figure 8: A) HER1 inactive state conformation with Tykerb/GW2016, B) HER2 inactive state conformation with Tykerb/GW2016.

Figure 9: **A**) Consensus model of HER2 inactive conformation with known HER2 inhibitors, **B**) Consensus model of HER2 active conformation with known HER2 inhibitors.

Figure 10: In silico screening protocol implemented in the discovery of HER2 inhibitors.

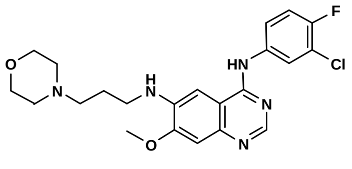

Gefitinib (**1**)

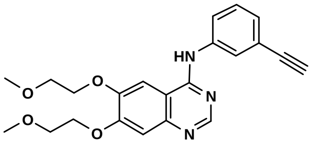

Erlotinib (**2**)

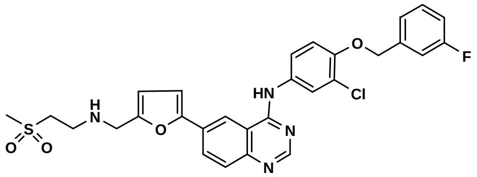

Tykerb (**3**)

Figure 1:

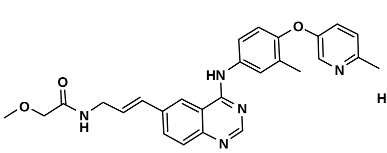

4

IC_{50} = 12 nM

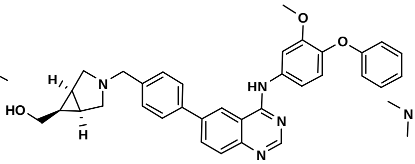

5

IC_{50} = 8 nM

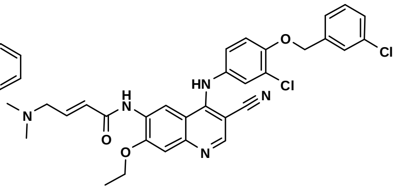

6

IC_{50} = 8 nM

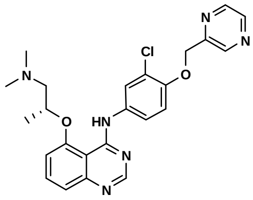

7

IC_{50} = 1 nM

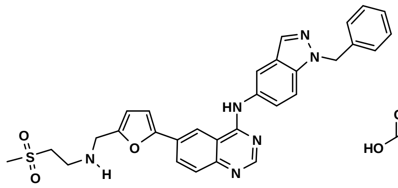

8

IC_{50} = 1 nM

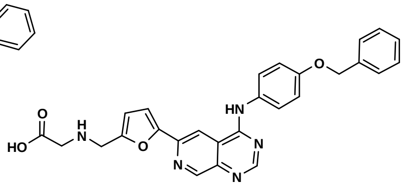

9

IC_{50} = 19 nM

Figure 2:

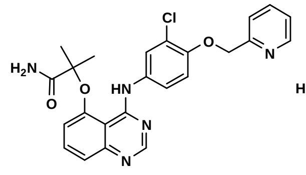

10
IC_{50} = 2 nM

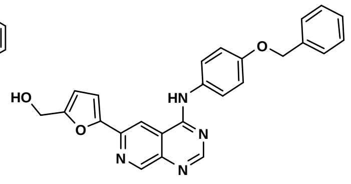

11
IC_{50} = 4 nM

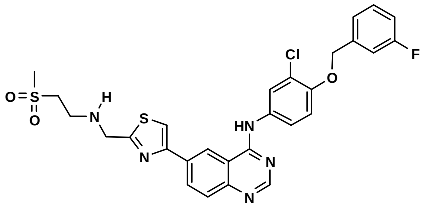

12
IC_{50} = 10 nM

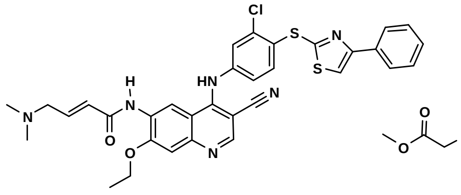

13
IC_{50} = 13 nM

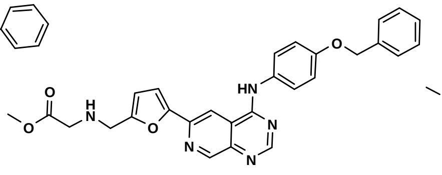

14
IC_{50} = 13 nM

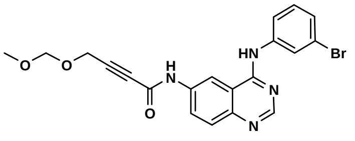

15
IC_{50} = 120 nM

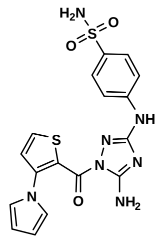

16
IC_{50} = 200 nM

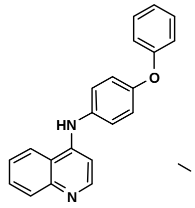

17
IC_{50} = 733 nM

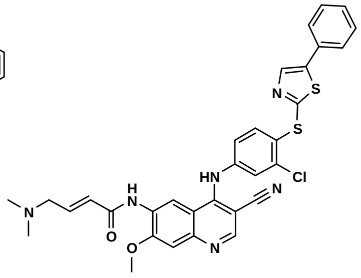

18
IC_{50} = 1000 nM

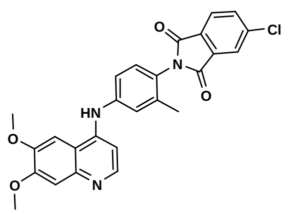

19
IC_{50} = 1700 nM

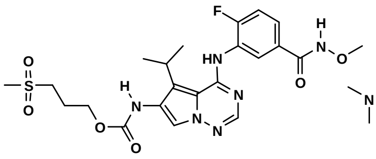

20
IC_{50} = 5300 nM

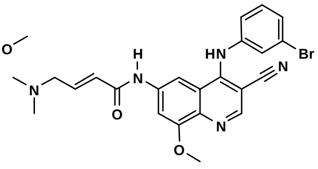

21
IC_{50} = 9300 nM

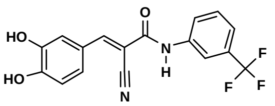

22
IC_{50} = 16000 nM

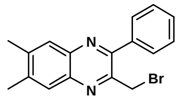

23
IC_{50} = 21000 nM

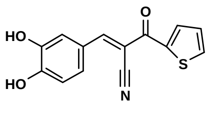

24
IC_{50} = 35000 nM

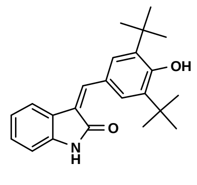

25
IC_{50} = 65000 nM

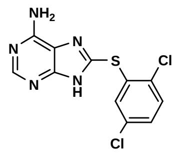

26
IC_{50} = 120000 nM

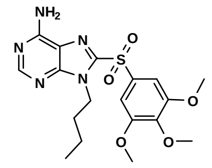

27
IC_{50} = 310000 nM

Figure 3:

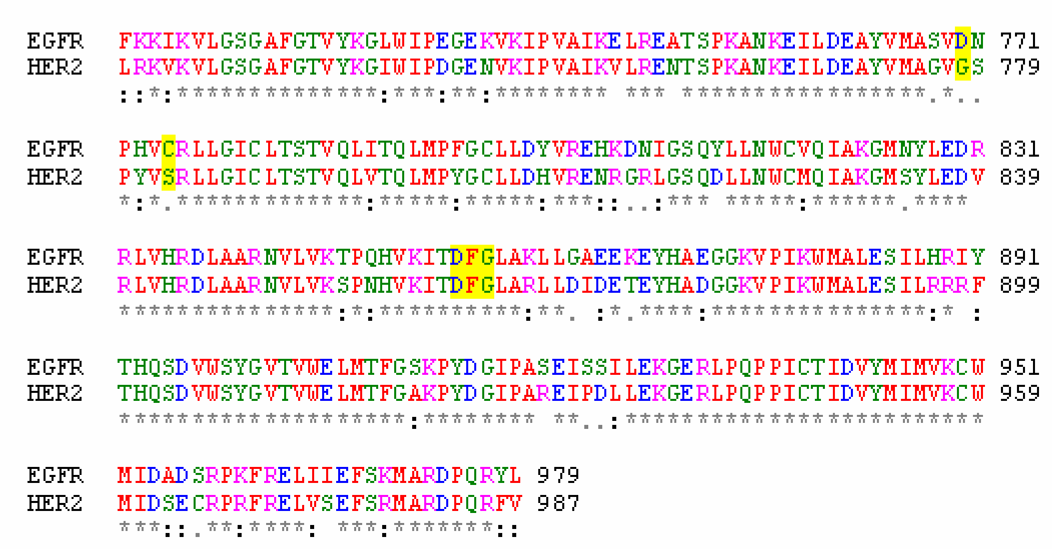

```
EGFR   FKKIKVLGSGAFGTVYKGLWIPEGEKVKIPVAIKELREATSPKANKEILDEAYVMASVDN 771
HER2   LRKVKVLGSGAFGTVYKGIWIPDGENVKIPVAIKVLRENTSPKANKEILDEAYVMAGVGS 779
       ::*:**************:***:**:******** *** *****************.*..

EGFR   PHVCRLLGICLTSTVQLITQLMPFGCLLDYVREHKDNIGSQYLLNWCVQIAKGMNYLEDR 831
HER2   PYVSRLLGICLTSTVQLVTQLMPYGCLLDHVRENRGRLGSQDLLNWCMQIAKGMSYLEDV 839
       *:*.*************:*****:*****:***::..:*** *****:******.****

EGFR   RLVHRDLAARNVLVKTPQHVKITDFGLAKLLGAEEKEYHAEGGKVPIKWMALESILHRIY 891
HER2   RLVHRDLAARNVLVKSPNHVKITDFGLARLLDIDETEYHADGGKVPIKWMALESILRRRF 899
       ***************:*:**********:**. :*.****:***************:* :

EGFR   THQSDVWSYGVTVWELMTFGSKPYDGIPASEISSILEKGERLPQPPICTIDVYMIMVKCW 951
HER2   THQSDVWSYGVTVWELMTFGAKPYDGIPAREIPDLLEKGERLPQPPICTIDVYMIMVKCW 959
       ********************:******** **..:*************************

EGFR   MIDADSRPKFRELIIEFSKMARDPQRYL 979
HER2   MIDSECRPRFRELVSEFSRMARDPQRFV 987
       ***::.**:****: ***:*******::
```

Figure4:

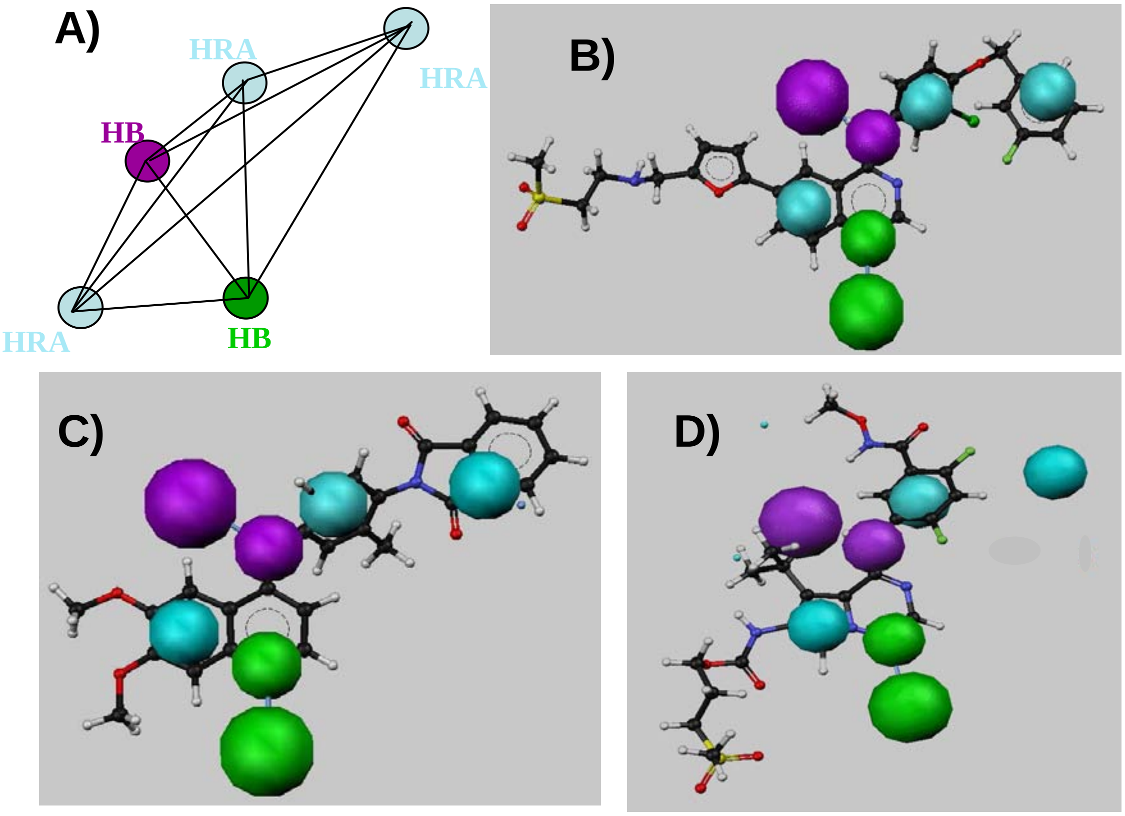
A)
HRA
HRA
HB
HRA
HB
HRA
B)
C)
D)

Figure 5:

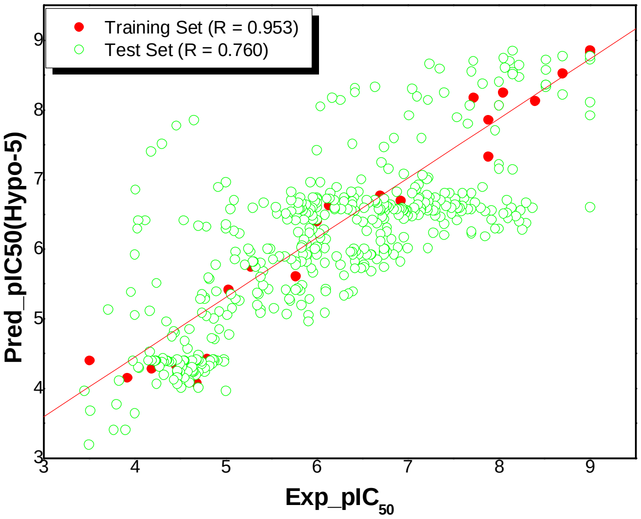

Figure 6:

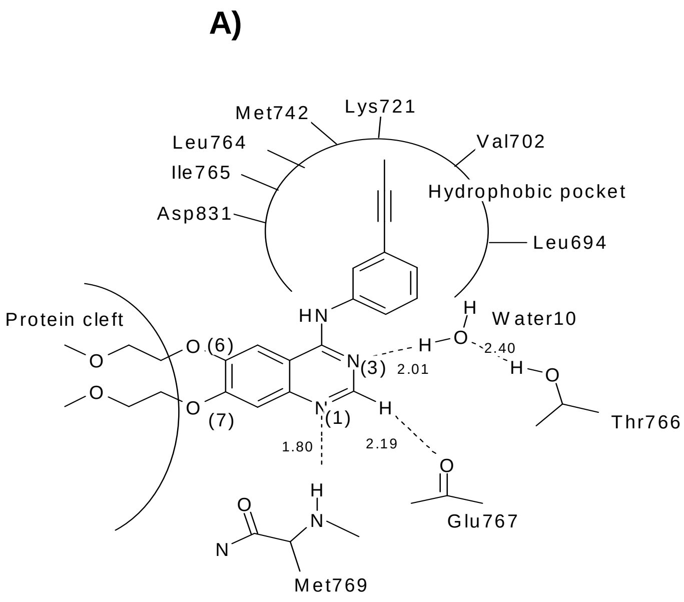
A)
B)
Met742
Lys721
Val702
Leu764
Ile765
Asp831
Hydrophobic pocket
Leu694
HN
H
Water10
Protein cleft
O
(6)
(7)
H
O
N(3)
2.01
2.40
H
O
Thr766
N(1)
H
1.80
2.19
O
Glu767
H
N
O
N
Met769
Leu 785
Ser 783
Met774
Leu 796
Glu 770
Val 797
Asp 863
Phe 864
Ile 752
Lys 753
Phe 731
Protein cleft
3.54
(3)
Thr 798
1.86
2.06
Glu 799
Met 801

Figure 7:

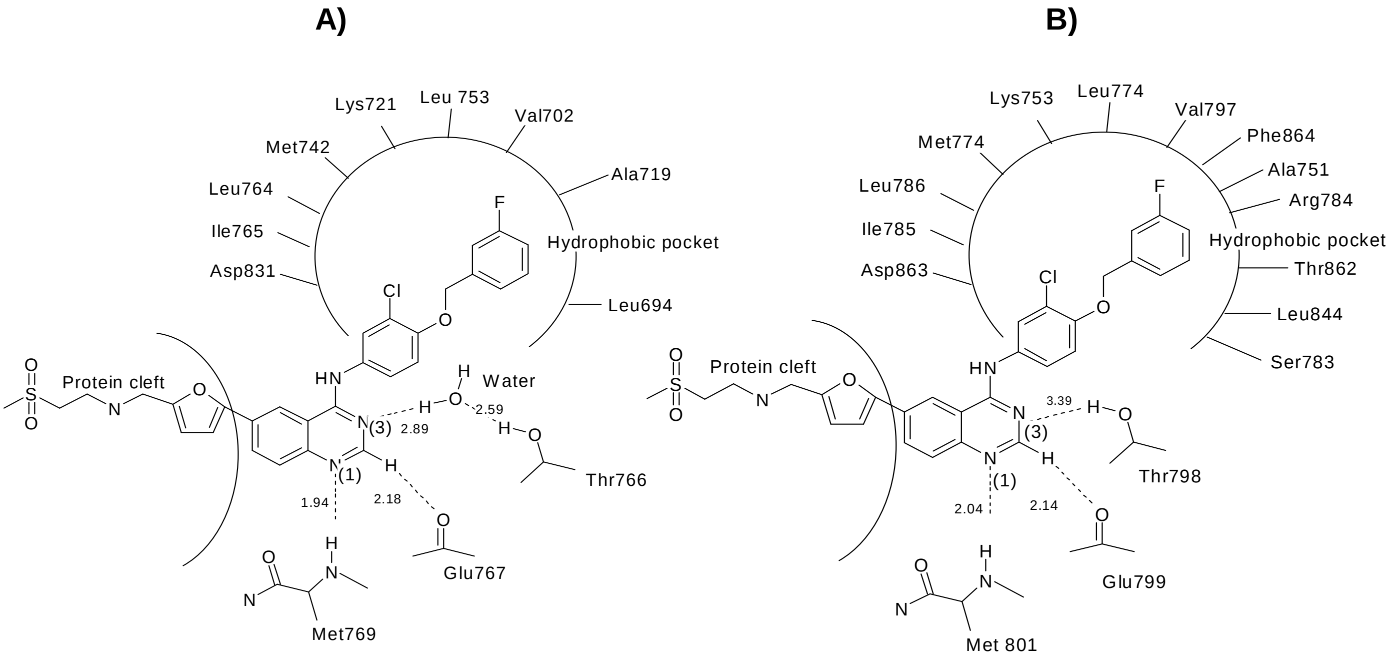
A)
B)
Lys721
Leu 753
Val702
Met742
Ala719
Leu764
Ile765
Asp831
F
Hydrophobic pocket
Cl
O
Leu694
Protein cleft
O
S
O
N
O
HN
Water
H
O
N(3)
2.89
2.59
H
O
Thr766
N(1)
H
1.94
2.18
O
Glu767
H
N
O
N
Met769
Lys753
Leu774
Val797
Met774
Phe864
Ala751
Leu786
Arg784
Ile785
Hydrophobic pocket
Asp863
Thr862
Leu844
Ser783
Protein cleft
3.39
(3)
Thr798
2.04
2.14
Glu799
Met 801

Figure 8:

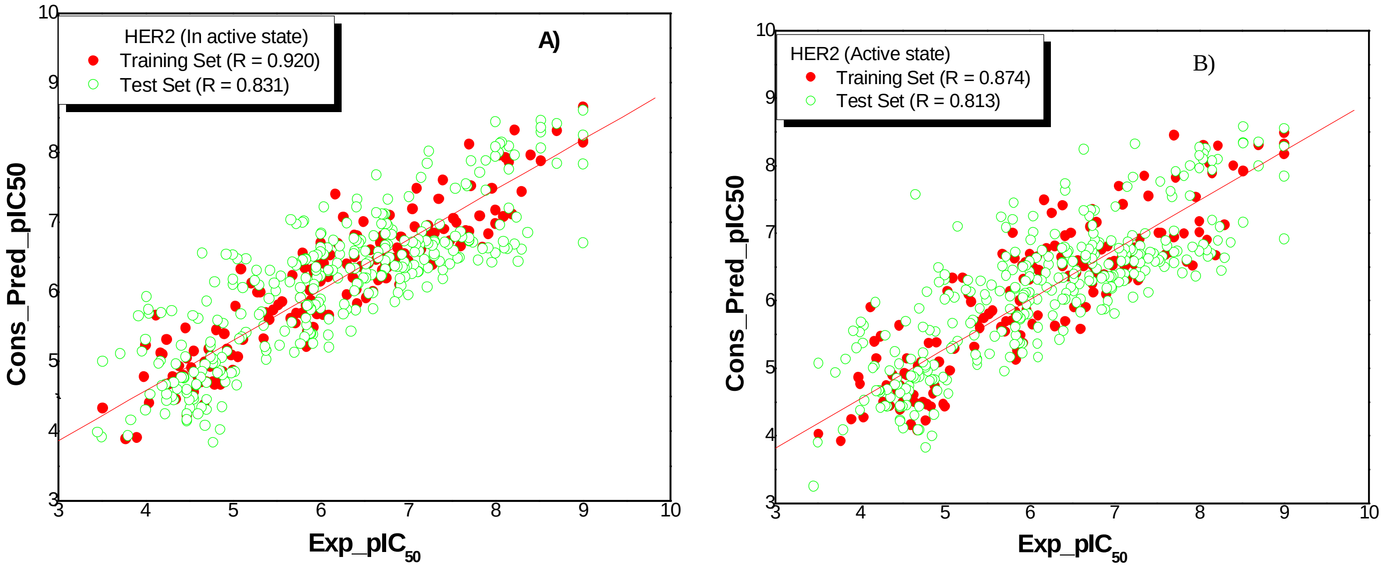

Figure 9:

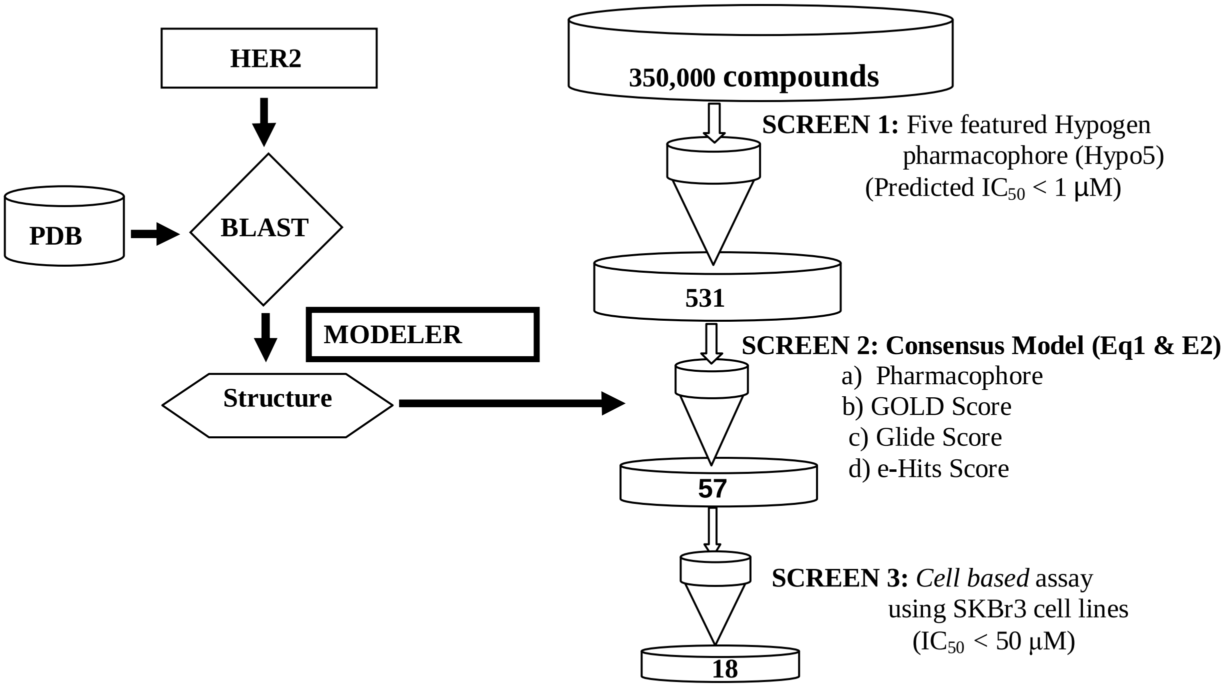
HER2
PDB
BLAST
MODELER
Structure
350,000 compounds
SCREEN 1: Five featured Hypogen pharmacophore (Hypo5)
(Predicted IC50 < 1 µM)
531
SCREEN 2: Consensus Model (Eq1 & E2)
a) Pharmacophore
b) GOLD Score
c) Glide Score
d) e-Hits Score
57
SCREEN 3: Cell based assay using SKBr3 cell lines
(IC50 < 50 µM)
18

Figure 10:

Table1. Experimental and Predicted IC_{50} Values of 22 Training Set compounds with Hypo5

Compound	Experimental IC_{50} (nM)	Predicted IC_{50} (nM)	Fit value
7	1	1.5	9.49
8	1	1.4	9.51
10	2	3	9.20
11	4	7.5	8.79
3	9	5.7	8.91
12	10	8.7	8.73
13	13	47	7.99
14	13	14	8.51
9	19	6.7	8.84
15	120	270	7.24
16	200	180	7.42
17	733	190	7.28
18	1000	380	7.09
19	1700	3990	6.69
20	5300	1800	6.40
21	9300	3900	6.08
22	16000	38000	5.09
23	21000	89000	4.72
24	35000	47000	5.00
25	65000	53000	4.95
26	120000	71000	4.82
27	310000	40000	5.06

Table 2. Statistical Parameters of Ten Pharmacophore Models Generated by the Hypogen Algorithm

Hypo No.	Total cost	Cost difference[a]	Error Cost	RMS deviation	Training set (r)	Features[b]
1	78.639	80.301	62.598	0.798	0.973	ADRR
2	79.722	79.218	63.796	0.882	0.967	ADRR
3	81.577	77.362	65.254	0.974	0.960	ADRR
4	81.636	77.303	66.339	1.037	0.953	ADRRR
5	**81.791**	**77.148**	**66.456**	**1.044**	**0.953**	**ADRRR**
6	81.874	77.065	64.108	0.902	0.966	ADRR
7	82.846	76.093	66.451	1.044	0.953	ADRR
8	83.890	75.049	67.846	1.120	0.946	ADRRR
9	85.148	73.791	69.858	1.221	0.935	ADRRR
10	86.974	71.965	68.504	1.154	0.944	ADRR

[a] (Null cost-Total cost), Null cost = 158.94, Fixed cost = 72.47,
For Hypo-5 Weight = 1.169, Configuration = 14.164.
[b] A- Hydrogen Bond Acceptor, D- Hydrogen Donor and R - Hydrophobic aromatic.

Table 3. Hypo5 Pharmacophore Model Validation with a Database of Known HER2 Inhibitors

No	Parameter	Value
1	Total compounds in database (D)	474
2	Total number of actives in database (A)	195
3	Total hits (Ht)	204
4	Active hits (Ha)	140
5	% Yield of actives	68.63
6	% Ratio of actives in the hit list	71.79
7	Enrichment factor or enhancement (E)	1.67
8	False negatives	55
9	False positives	64
10	GH score (Goodness of hit list)[a]	0.536

[a] (Ha/4HtA)(3A+Ht))x(1-((Ht-Ha)/(D-A))]; GH Score of 0.6 – 0.7 indicates a very good model.

Table 4. Correlation Coefficient Values of GOLD score, Glide score, eHITs score (HER2 Active and Inactive States) with Experimental pIC_{50} of Known 22 HER2 Inhibitors (table1)

	GOLD	Glide	eHITS
Inactive state[a]	0.844	-0.814	-0.695
Active state[a]	0.805	-0.704	-0.790

[a] HER2 conformation.

Table 5. Correlation Coefficient Values of GOLD Score, Glide score, eHITs score (HER2 Active and Inactive States) with Experimental pIC_{50} of Known 474 HER2 Inhibitors

	GOLD	Glide	eHITS
Inactive state[a]	0.551	-0.596	-0.549
Active state[a]	0.545	-0.589	-0.555

[a] HER2 conformation.

Table 6. A) Consensus Model of HER2 Inactive State Conformation and Validation with Known HER2 Inhibitors Database, B) Consensus Model of HER2 Active State Conformation and Validation with Known HER2 Inhibitors Database

A)

S. No	Parameter	Value
1	Total compounds in database (D)	474
2	Total number of actives in database (A)	195
3	Total hits (H_t)	193
4	Active hits (H_a)	156
5	% Yield of actives	81
6	% Ratio of actives in the hit list	80
7	Enrichment or Enhancement factor (E)	1.96
8	False negatives	39
9	False positives	37
10	GH score (Goodness of hit list)	0.699

B)

S. No	Parameter	Value
1	Total compounds in database (D)	474
2	Total number of actives in database (A)	195
3	Total hits (H_t)	197
4	Active hits (H_a)	154
5	% Yield of actives	78
6	% Ratio of actives in the hit list	79
7	Enrichment or Enhancement factor (E)	1.90
8	False negatives	41
9	False positives	43
10	GH score (Goodness of hit list)	0.663

[a] [(Ha/4HtA)(3A+Ht))x(1-((Ht-Ha)/(D-A))]; GH Score of 0.6 – 0.7 indicates a very good model.

Table 7. Cytotoxicity of Novel Compounds Against a SKBr3 Breast Cancer Cells Overexpressing HER2).

S.No	Structure	Predicted IC$_{50}$ (μM)		Experimental IC$_{50}$ (μM)
		Eq1	Eq2	SKBr3 cell lines
1	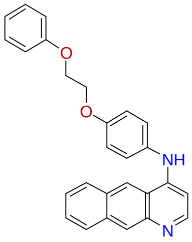	0.1	0.71	2.2 ± 0.2
2	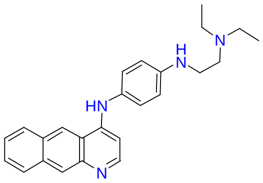	0.17	0.56	2.5 ± 0.2
3	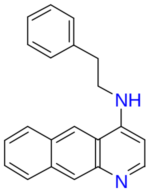	14.5	16.9	8.5 ± 0.3
4	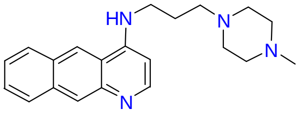	50.1	55.3	15.02 ± 0.4
5	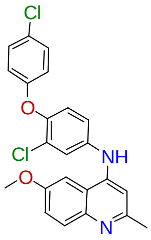	0.91	0.47	5.1 ± 0.1
6	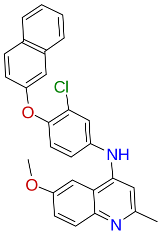	0.34	0.53	5 ± 0.2

7	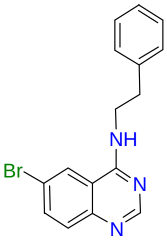	37.1	41.17	15.05 ± 0.5
8	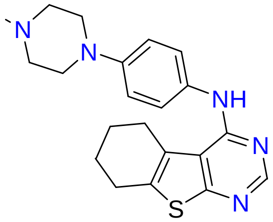	0.51	0.75	9 ± 0.5
9	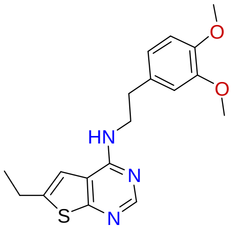	25.3	32.7	14.10 ± 0.5
10	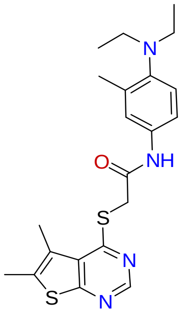	24.12	22.17	16.5 ± 0.3
11	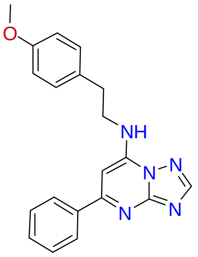	24.1	26.3	9 ± 0.5
12	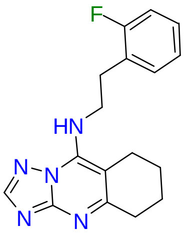	49.6	62.5	14.08 ± 0.4